Using Phase Response Curves to Optimize Deep Brain Stimulation

A DISSERTATION
SUBMITTED TO THE FACULTY OF
UNIVERSITY OF MINNESOTA
BY

Abbey Beuning Holt Becker

IN PARTIAL FULFILLMENT OF THE REQUIREMENTS

FOR THE DEGREE OF DOCTOR OF PHILOSOPHY

Theoden I. Netoff

April 2016

Acknowledgements

I would like to acknowledge the following individuals for their contributions and support:

Dr. Theoden Netoff: Thank you for the mentorship and support. Your enthusiasm and dedication to science always provided motivation, particularly during periods of time where nothing seemed to work. You created a truly collaborative and interdisciplinary environment, which allowed me to accomplish this work. Finally, lab would not have been nearly as entertaining without your Poi ball routines.

Past and present labmates in the Netoff lab: Vivek Nagaraj, Tyler Stigen, Jennifer Zick, Oscar Miranda-Dominguez, Bryce Beverlin II, Kenneth Louie, Logan Grado, and Max Shinn. Your support, collaboration, scientific feedback, and friendship were invaluable.

My classmates and friends, without whom graduate school would have been much less enjoyable.

My family, particularly my parents Sheila and Andy and my brother Paul, for providing me with love, support, and encouragement in everything I have done. You taught me to be independent, inquisitive, and hardworking.

My husband, Jordan, who has been through everything alongside me since Itasca. You have always been there to listen; encourage, support, and challenge me; and provide silliness and fun. I look forward to all our adventures yet to come.

Dedication

I would like to dedicate this to my parents, Andy and Sheila, and husband, Jordan, for their love and support.

Abstract

Deep brain stimulation (DBS) is a neuromodulation therapy effective at treating motor symptoms of patients with Parkinson's disease (PD). Currently, an open-loop approach is used to set stimulus parameters, where stimulation settings are programmed by a clinician using a time intensive trial-and-error process. There is a need for a systematic approach to tuning stimulation parameters based on a patient's physiology. An effective biomarker in the recorded neural signal is needed for this approach. It is hypothesized that DBS may work by disrupting enhanced oscillatory activity seen in PD. In this thesis I propose and provide evidence for using a simple measure, called a phase response curve, to systematically tune stimulation parameters and develop novel approaches to stimulation to suppress pathological oscillations. In this work I show that PRCs can be used to optimize stimulus frequency, waveform, and stimulus phase to disrupt a pathological oscillation in a computational model of Parkinson's disease and/or to disrupt entrainment of single neurons *in vitro*. This approach has the potential to improve efficacy and reduce post-operative programming time.

Table of Contents

Acknowledgements i
Dedication ii
Abstract iii
Table of Contents iv
List of Figures viii

Chapter 1 - Introduction 1
Parkinson's disease 2
History 2
The Basal Ganglia 3
Changes to the Basal Ganglia in Parkinson's disease 6
Treatment Options 10
Deep Brain Stimulation for Parkinson's disease 11
Mechanism of Action: Deep Brain Stimulation 11
Optimization Approaches 15
Using Phase Response Curves to Optimize DBS to Suppress Oscillatory Activity seen in PD 18
Conclusion 22

Chapter 2 - Computational Models of the Basal Ganglia 23
Introduction 24
Computational network models of deep brain stimulation 25
Abstract Network Models 26
Realistic Network Models 29
The Hahn and McIntyre Model (HM Model) 31
Generating Power Spectra 35
Pathological 34 Hz Oscillation 36

Limitations *39*
Conclusion 39

Chapter 3 - Origins of a Parkinsonian Oscillation in a Computational Model 41
Introduction 42
Mean field Modeling 43
Methods 44
Transfer Function Fits *47*
Generating the closed-loop system *51*
Results 53
34 Hz oscillation emerges from the STN-GPe feedback loop *54*
Comparing the output of the simplified mean field model and the HM model 58
Discussion 62

Chapter 4 - Optimizing Stimulus Frequency to Suppress a Parkinsonian Oscillation in a Computational Model of the Basal Ganglia 65
Introduction 66
Methods 68
Estimating the Phase and Phase Change from Spike Time Data *70*
Estimating the Phase Response Curve *71*
Using the PRC to Predict Effects of Stimulus Frequency on 34 Hz Oscillation *72*
Results 74
Discussion 76

Chapter 5 - Phasic Burst Stimulation: A Novel Approach to Optimizing Closed-Loop Deep Brain Stimulation 80
Introduction 81
Methods 84
Closed-loop Phasic Stimulation *85*
Phase Response Curve Theory *86*
Estimating the PRC *89*
Predicting Phase Dependent Modulation of 34 Hz Oscillation *89*
Results 90

Discussion 95
Advantages of closed-loop DBS *96*

Chapter 6 - Using the Phase Response Curve to Predict Entrainment of Single Neurons *in vitro* 100

Introduction 101
PRC theory *102*
Methods 103
Slice Preparation *103*
Electrophysiology Recording *104*
Frequency Protocol *105*
Phasic Burst Stimulation Protocol *107*
Estimating synchrony from experimental data *110*
Results 111
Effects of stimulus frequency *111*
Phasic burst stimulation *114*
Discussion 120

Chapter 7 - Testing Phase Response Curve Optimized Stimulus Waveforms *in vitro* 122

Introduction 123
Methods 124
Electrophysiology Recordings *124*
Estimating PRCs from single neurons *125*
Stimulus waveform *126*
Applying stimulus waveforms in vitro *130*
Entropy estimation *130*
Results 131
Discussion 136

Chapter 8 - Estimating Phase Response Curves from Local Field Potential Recordings in Non-Human Primates 139

Introduction 140

Methods 140
LFP Recordings *141*
Estimating the PRC *146*
Predicting the effects of stimulus frequency using the PRC *149*
Results 149
Conclusion 156

Chapter 9 - Conclusions & Future Directions 158
Summary and Significance of Results 159
Using PRCs to Optimize Stimulus Parameters for Open-Loop DBS *160*
Using PRCs to Optimize a Closed-Loop Approach to DBS *161*
Estimation of Phase Response Curves *162*
Clinical Limitations 163
Future Experiments 165
Conclusion 166
References 167

List of Figures

Figure 1. Circuit diagram of the basal ganglia thalamo-cortical network in heath and disease. 5

Figure 2. Enhanced oscillatory activity in the beta frequency range is seen in intraoperative neuronal and field recordings from the STN of a patient with Parkinson's disease. 9

Figure 3. Deep brain stimulation reduces enhanced beta oscillations seen in Parkinson's disease. 15

Figure 4. Using a phase response curve (PRC) to predict network synchrony..... 21

Figure 5. Connectivity and Output of Hahn and McIntyre Model.. 34

Figure 6. Parkinsonian 34 Hz oscillation present in power spectrum..... 38

Figure 7. Open-loop stimulation protocol for measuring neural responses to stimulation.. 46

Figure 8. Impulse responses and fits.. 50

Figure 9. Box diagram of the closed-loop systems-level model..... 52

Figure 10. The PZ plot shows the poles and zeroes of the transfer function of a dynamical system.. 55

Figure 11. The Parkinsonian closed loop STN-GPe system resonates better than the healthy system due STN and GPe resonating better with each other.. 57

Figure 12. Simulated cortical input used to drive the systems-level GPe-STN mean-field model produces spectral features similar to that seen in the Hahn and McIntyre model.. 59

Figure 13. Changes in the closed-loop STN-GPe transfer function model predict changes seen in the Hahn & McIntyre model.. 61

Figure 14. A phase response curve can be estimated from population local-field potential data.. 69

Figure 15. Predicting DBS frequencies to disrupt population oscillations using the Lyapunov exponent. 75

Figure 16. Phase response curves can be used to predict synchronization properties of a periodic stimulus. 88

Figure 17. Rastergrams from the external globus pallidus of the Hahn & McIntyre model..... 91

Figure 18. The phase response curve (PRC) can be used to predict the effects of phasic stimulation on the 34 Hz parkinsonian oscillation seen in the HM model. 93

Figure 19. Periodic forcing of a single neuron in the subthalamic nucleus (STN)..... 112

Figure 20. PRCs measured from single cells can be used to predict how stimulation frequency modulates entrainment. 113

Figure 21. Example from a Substantia nigra pars reticulata cell 115

Figure 22. Using phase response curves to predict entrainment of single cells in the substantia nigra pars reticulate to an oscillatory input. 117

Figure 23. Correlation between experimental and predicted synchrony across all cells 119

Figure 24. Four envelopes with separate optimal waveforms were used to determine which stimuli to use on a given cell. 129

Figure 25. Example cell using envelope 3.. 133

Figure 26. The PRC-optimized stimulus waveform is significantly better at entraining neurons to the stimulus across cells.. 135

Figure 27. 12.35 Hz oscillation present in the local field potential recordings of a naïve non-human primate. 143

Figure 28. 12.65 Hz oscillation present in the local field potential recordings of an MPTP-treated non-human primate. 145

Figure 29. Estimating instantaneous phase using the Hilbert Transform.. 148

Figure 30. Phase response curves estimated from local field potential recordings in the naïve NHP 151

Figure 31. Phase response curves estimated from local field potential recordings in the MPTP-treated NHP.. 153

Figure 32. Predicting the effects of stimulus frequency on the 12.35 Hz oscillation in the naïve non-human primate. 155

Chapter 1

Introduction

Parkinson's disease

History

Parkinson's disease (PD) is the second most common neurodegenerative disease, affecting an estimated four million people worldwide (Nolden, Tartavoulle, & Porche, 2014). The progressive disease was first described by James Parkinson as a "Shaking Palsy" in 1817 (Parkinson, 2002). Motor dysfunction, including bradykinesia, rigidity, and resting tremor, is the defining feature; however non-motor symptoms, such as sensory and cognitive deficits, are often present as well (Chaudhuri, Healy, Schapira, & Excellence, 2006).

Cell death and the accumulation of α-synuclein immunoreactive Lewy bodies in specific neuronal populations are histological markers of PD (Braak et al., 2003; Dauer & Przedborski, 2003; Polymeropoulos et al., 1997). The hallmark of the disease is the loss of dopaminergic neurons in the subatantia nigra pars compacta (SNc) (Carlsson, Lindqvist, Magnusson, & Waldeck, 1958; Ehringer & Hornykiewicz, 1960). Cell loss actually begins much earlier, first affecting the anterior olfactory nucleus and olfactory bulb and progressing to the brain stem, basal ganglia, and finally the neocortex (Braak et al., 2003). While pre-motor symptoms may accompany early lesions (Goldman & Postuma, 2014), the characteristic motor symptoms associated with PD arise due to the loss of dopaminergic neurons in the SNc. The SNc is a small group of neurons in the midbrain that release dopamine onto neurons in a distributed network of brain regions called the basal ganglia.

The loss of dopaminergic input leads to changes throughout the complex basal ganglia thalamo cortical network resulting in motor dysfunction.

The Basal Ganglia

The basal ganglia are made up of a number of subcortical nuclei strongly interconnected with the cerebral cortex, thalamus, and brainstem (Figure 1).

Information passes through the basal ganglia via multiple pathways: the direct, indirect, and hyperdirect pathway (Albin, Young, & Penney, 1989; M. R. DeLong, 1990; Nambu, Tokuno, & Takada, 2002). The cortex projects directly to the input nuclei of the basal ganglia: the striatum and subthalamic nucleus (STN). The striatum is the main input and sends inhibitory GABAergic connections directly to the output nucleus of the basal ganglia, the internal segments of the globus pallidus (GPi), constituting the direct pathway. The striatum also sends inhibitory projections to the external segment of the globus pallidus (GPe). The GPe then sends inhibitory projections to the sole excitatory nucleus in the network, the STN. Finally, the STN projects to the output nucleus, the GPi. This polysynaptic path through the basal ganglia constitutes the indirect pathway. Direct projections from the cortex to the STN constitute the hyperdirect pathway. The SNr is a second output nucleus of the basal ganglia, playing a similar structural and functional role to the GPi (Percheron, McKenzie, Férger, & International Basal Ganglia Society. Symposium, 1994). Often the GPi and SNr are generally considered part of the same complex, simply separated by white matter of the internal capsule (Franks, 1990).

Tonic levels of activity in the GPi/SNr result in inhibition of the thalamus, thereby preventing activation of the cortex and inhibiting movement (M.R. DeLong, Alexander, Miller, & Crutcher, 1992; Penney & Young, 1983). To initiate a movement output from the GPi/SNr must be decreased, thereby disinhibiting the thalamus. Activation of the direct pathway (striatum-GPi/SNr-thalamus) inhibits the tonic level of GPi/SNr activity, thereby leading to movement. The polysynaptic indirect pathway (striatum-GPe-STN-GPi/SNr) leads to excitation of the GPi/SNr, thereby inhibiting movement (Parent & Hazrati, 1995; Penney & Young, 1983). More recently, the hyperdirect pathway (cortex-STN) has been characterized (Nambu et al., 2000) and is thought to play a role in conflict resolution (Nambu et al., 2002).

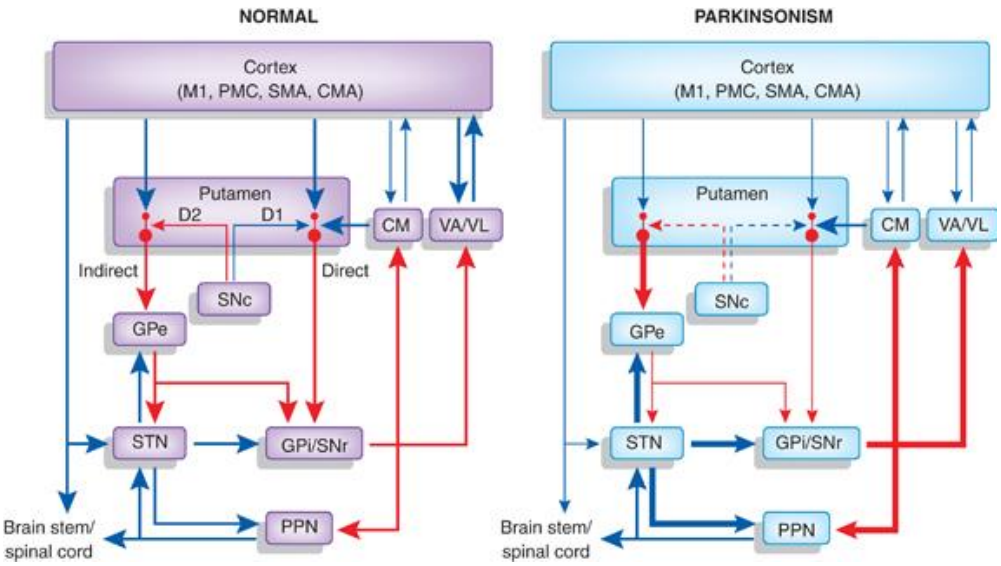

Figure 1. Circuit diagram of the basal ganglia thalamo-cortical network in heath and disease. (Smith, Wichmann, Factor, & DeLong, 2012). Left: Connectivity in the normal, healthy state. Right: Changes in connectivity seen in Parkinson's disease. Excitatory influences are shown in red; inhibitory in blue. The putamen is a part of the striatum. SNc: Substantia nigra pars compacta; GPe: external segment of the globus pallidus; internal segment of the globus pallidus; STN: subthalamic nucleus; SNr: substantia nigra pars reticulate; PPN: pedunculopontine nucleus; VA/VL: ventral anterior/lateral nuclei of the thalamus.

Changes to the Basal Ganglia in Parkinson's disease

In Parkinson's disease, the loss of dopaminergic input to the striatum from the SNc leads results in a cascade of changes throughout the basal ganglia thalamo-cortical network, ultimately leading to increased activity in the GPi/SNr (Obeso et al., 2008) (Figure 1).

Rate Theory

Classical theories of PD pathophysiology focused on changes in firing rate causing a failure of thalamo-cortical circuits to initiate movement (Albin et al., 1989; M. R. DeLong, 1990). The loss of dopaminergic input to the striatum leads to an increase in mean firing rates in the STN and SNr and a decrease in firing rates in the GPe. Overall this results in an increase in the firing rate of the GPi, thereby increasing inhibition to the thalamus and suppressing movement (Alexander, DeLong, & Strick, 1986; Bergman, Wichmann, Karmon, & DeLong, 1994). Supporting this hypothesis, lesioning overactive nuclei (the STN or GPi) leads to improvement in motor symptoms.

Dynamic Theory

The appropriate balance between input to the GPi/SNr via the direct and indirect pathway is necessary for proper motor control (Albin et al., 1989; M. R. DeLong, 1990). While the loss of dopaminergic input leads to an overall increase in activity in the striatum, these changes are not uniform (Obeso et al., 2008). Depending on the pathway they are a part of, striatal neurons differentially expresses dopamine receptors (Gerfen et al., 1990;

Gertler, Chan, & Surmeier, 2008). D1-receptors are expressed in neurons projecting to the direct pathway and are activated by dopaminergic input; while D2-receptors are expressed in neurons projecting to the indirect pathway and are inhibited by dopaminergic input. A desired motor program is selected and executed through the activation of the direct pathway and simultaneously inhibition of competing motor programs via activation of the indirect pathway (Mink, 2003; Nambu, 2008). Hypokinetic activity is thought to result from over-activation of the indirect pathway, thereby inhibiting movement; conversely, over-activation of the direct pathway is thought to result in hyperkinetic activity (Boraud, Bezard, Bioulac, & Gross, 2000; Chiken & Nambu, 2015; Leblois, Boraud, Meissner, Bergman, & Hansel, 2006). While this dichotomy has been questioned (Ariano, Larson, & Noblett, 1995), optogenetic probing of the network has led to evidence supporting the indirect/direct pathway hypothesis (Kravitz et al., 2010).

Synchronous Activity

Over the past 15 years it has been suggested that motor symptoms of PD arise due to the emergence of rhythmic synchronous neural activity within the basal ganglia network and its thalamo-cortical targets (P. Brown, 2007; P. Brown et al., 2001; Kühn et al., 2009; Little & Brown, 2014; Marsden, Limousin-Dowsey, Ashby, Pollak, & Brown, 2001). In particular, many patients display enhanced oscillatory neuronal activity in the beta range (12-30Hz) that can be detected in single basal ganglia neurons and local field potentials (LFPs) (Figure 2). The power of the beta oscillations is markedly reduced following dopamine replacement medication leading to improvement in motor symptoms. It has been

proposed that beta oscillations maintain the current motor program (Engel & Fries, 2010; Gilbertson et al., 2005). Thus, when abnormally sustained, as in PD, the ability to produce dynamic, healthy movement is impaired. While there is an increasing amount of evidence supporting the presence of enhanced synchrony in PD, the causal role remains controversial (Little & Brown, 2014). In fact, beta oscillations alone were not found to correlate well with disease severity in a progressive model of PD in a NHP (Connolly et al., 2015). Instead motor symptoms may arise due to increased coupling between beta and broadband frequency bands, known as phase amplitude coupling (de Hemptinne et al., 2013).

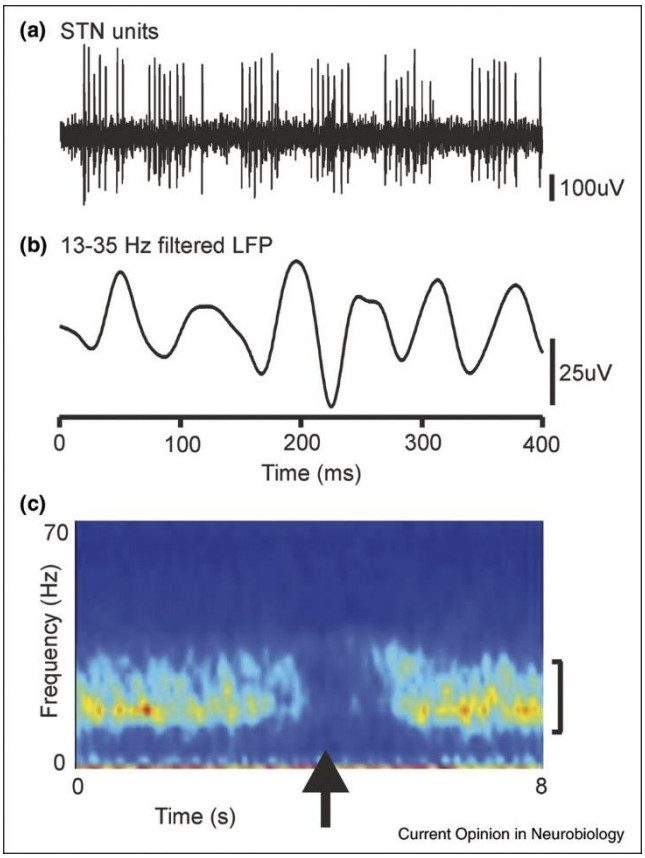

Figure 2. Enhanced oscillatory activity in the beta frequency range is seen in intraoperative neuronal and field recordings from the STN of a patient with Parkinson's disease. A) Neuronal spikes bursting at the beta frequency. B) Simultaneous local field potential recording showing the 15 Hz beta oscillation. C) Unit-LFP coherence over time. Arrow indicates onset of hand movement. Figure from (P. Brown, 2007).

Treatment Options

While there is no cure for Parkinson's disease, interventions such as medication (Barbeau, Sourkes, & Murphy, 1962), ablative surgery (Laitinen, Bergenheim, & Hariz, 1992), electrical stimulation (Limousin et al., 1995), or gene therapy (LeWitt et al., 2011) can be used to treat symptoms. Dopamine replacement medication is the primary therapy for treating motor symptoms. While this is extremely effective, after years of being on the medication patients begin to develop a tolerance for the drug as well as medication-induced dyskinesias (Cotzias, Papavasiliou, & Gellene, 1969). As a result, the therapeutic effectiveness decreases, while unwanted side-effects increase.

Ablative surgeries to lesion hyperactive nuclei in the basal ganglia offer another therapeutic option (Burchiel, 1995; Okun & Vitek, 2004). While lesions of the GPi (Hassler & Riechert, 1954; Lozano et al., 1995), thalamus (Burchiel, 1995), and the STN (Alvarez et al., 2001; Aziz, Peggs, Agarwal, Sambrook, & Crossman, 1992; Bergman, Wichmann, & DeLong, 1990) have all shown therapeutic benefit, the procedure is risky. Ablation surgeries permanently damage a portion of the brain; any resulting side effects from the therapy itself or incorrect targeting are irreversible (Alvarez et al., 2005; de Bie et al., 2002; Huss et al., 2015). The use of stimulation for targeting during ablation surgeries led to the discovery that high frequency electrical stimulation provides reversible therapeutic benefit (21); leading to the development of DBS (Guridi & Lozano, 1997). For patients with medication-induced side effects, deep brain stimulation offers the best therapeutic option to date.

Deep Brain Stimulation for Parkinson's disease

DBS was approved by the FDA in 1997 (Coffey, 2009). Since then more than 100,000 patients worldwide have received this therapy, clear evidence that DBS is a practical therapeutic approach. DBS for PD involves the chronic implantation of macro electrodes in one of two structures in the basal ganglia; the subthalamic nucleus (STN) or the globus pallidus internal segment (GPi). The leads are connected to an implantable pulse generator and electrical pulses, generally around 100-150 Hz, are delivered continuously to the target. DBS serves to provide a reversible replacement to permanent lesioning of the basal ganglia for the treatment of PD (Guridi & Lozano, 1997). While high frequency DBS (HF DBS) is effective at reducing motor symptoms in PD, the mechanism of action is a matter of debate.

Mechanism of Action: Deep Brain Stimulation

Many hypotheses have emerged to explain experimental findings related to the efficacy of DBS for PD. There are two main findings which mechanisms attempt to explain. First, HF DBS to the STN, GPi, and Vim nucleus of the thalamus produce similar benefits as lesioning each of the targets (Follett et al., 2010; Kleiner-Fisman, Saint-Cyr, Miyasaki, Lozano, & Lang, 2002). Second, stimulation frequency affects therapeutic outcome; high frequency stimulation improves motor symptoms, while low frequency stimulation does not provide therapeutic benefit, reportedly enhancing motor symptoms in certain cases (Chen et al., 2007; Moro et al., 2002). While DBS likely works through a

combination of mechanisms (Vitek, 2002; Vitek, Hashimoto, Peoples, DeLong, & Bakay, 2004), the following section will present major hypotheses that have been developed to explain the therapeutic effects of DBS.

Inhibition and Excitation Hypotheses

The therapeutic benefits of HF DBS are similar to those of ablations, leading to the thought that DBS works as a reversible lesion. A decrease in neural activity within or projecting from the stimulation target may occur through various mechanisms: 1) through the depolarization block of neurons surrounding the stimulation electrode (Beurrier, Bioulac, Audin, & Hammond, 2001), 2) through the activation of inhibitory synaptic afferents (J. O. Dostrovsky et al., 2000), 3) through the depletion of neurotransmitters (Urbano, Leznik, & Llinas, 2002), and/or 4) through the inhibition of excitatory synaptic afferents (T. R. Anderson, Hu, Iremonger, & Kiss, 2006). This hypothesis fits with the rate model and dynamic model of PD.

Supporting the inhibition hypothesis, neurons in the stimulation target show decreased firing (J. O. Dostrovsky et al., 2000; Filali, Hutchison, Palter, Lozano, & Dostrovsky, 2004; Meissner et al., 2005). However, downstream targets show changes in activity consistent with excitation of efferents of the stimulated nucleus, which is not explained by a functional lesion (M. E. Anderson, Postupna, & Ruffo, 2003; Hashimoto, Elder, Okun, Patrick, & Vitek, 2003; McIntyre, Grill, Sherman, & Thakor, 2004).

Furthermore, modeling studies suggest axons and dendrites have lower activation thresholds than the soma (McIntyre, Grill, et al., 2004).

This has led to the hypothesis that DBS works by activating efferent fibers nearby the stimulation target (Montgomery & Baker, 2000; Vitek, 2002). Simultaneous inhibition of neurons in the stimulation target and activation of downstream targets seen experimentally seemingly led to a paradox. Modeling studies have demonstrated (McIntyre, Grill, et al., 2004) that the effects of DBS can be different at the soma and axons of neurons within the stimulation target, resolving this paradox.

Informational Lesion

The informational lesion hypothesis suggests that DBS works by preventing the transmission of pathological activity through the basal ganglia thalmo-cortical network (Agnesi, Connolly, Baker, Vitek, & Johnson, 2013; Dorval et al., 2008; W. M. Grill, Snyder, & Miocinovic, 2004). High frequency stimulation drives high-frequency firing in the basal ganglia output nucleus, the GPi. While this high frequency firing is not a return to patterns of activity seen in the healthy state, it has little variability and is thought to be devoid of informational content. This theory explains why therapeutic efficacy depends on stimulation frequency, as low frequency stimulation does not induce the high frequency periodic firing locked to the stimulus necessary to produce the information lesion (Dorval, Kuncel, Birdno, Turner, & Grill, 2010).

DBS works by disrupting pathological synchrony

DBS has been found to disrupt enhanced pathological synchrony in a number of ways. 1) Therapeutic HF DBS reduces the power of the pathological beta oscillations seen in the basal ganglia in PD (Bronte-Stewart et al., 2009; Kuhn, Kupsch, Schneider, & Brown, 2006; Meissner et al., 2005) (Figure 3). Importantly, the magnitude of amplitude reduction predicts the level of symptom improvement (Little, Pogosyan, Kuhn, & Brown, 2012). Indeed, delivering high-frequency stimulation restricted to periods of enhanced beta oscillations produces a greater improvement in akinetic/rigid motor symptoms while using less battery power than continuous HF DBS (Little et al., 2013). 2) STN DBS has been shown to disrupt synchronous activity in the cortex through antidromic effects (Q. Li, Qian, Arbuthnott, Ke, & Yung, 2014). 3) DBS was found to reduce the enhanced interaction between the phase of beta oscillations and the amplitude of broadband activity (50-200 Hz) (de Hemptinne et al., 2015). Similar to the role of beta oscillations, phase amplitude coupling reduction is necessary to execute a movement. 4) DBS has been hypothesized to work through a mechanism termed "Chaotic Desynchronization" (C. J. Wilson, Beverlin, & Netoff, 2011). This approach suggests that subthreshold stimulus pulses can induce chaotic responses in periodic oscillators (in this case periodically firing neurons), thereby disrupting pathological synchrony. This approach will be investigated in depth throughout this thesis.

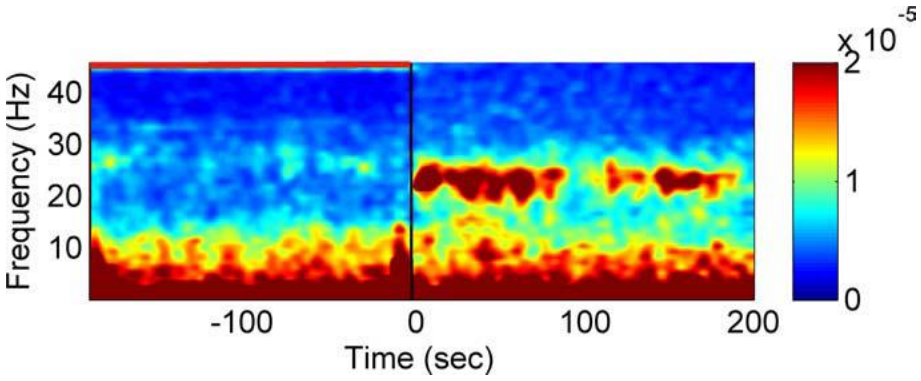

Figure 3. Deep brain stimulation reduces enhanced beta oscillations seen in Parkinson's disease. Spectrogram showing oscillatory activity at the beta frequency in a field recording from the internal segment of the globus pallidus of a patient with Parkinson's disease (right). High frequency DBS (time -200 to 0) reduces the pathological beta activity (left). Figure from (Kuhn et al., 2008) (Kühn et al., 2009).

Optimization Approaches

Many factors can affect the efficacy of DBS, including electrode placement, patient physiology, and stimulation parameters. Stereotaxic methods are used to accurately implant DBS leads. However, electrode placement is not always perfect, which can lead to negative side effects. Software, such as Cicerone (Miocinovic, Noecker, Maks, Butson, & McIntyre, 2007), is being developed to improve patient specific mapping to address this issue. Alternatively, postoperative approaches to steer the current to your desired target are being developed, a task made possible by high density electrode leads (Chaturvedi, Foutz, & McIntyre, 2012; Connolly et al., 2016; Contarino et al., 2014).

With the current implantable leads, stimulation parameters such as stimulation frequency, amplitude, polarity, pulse width, and electrode configuration can be tuned post-operatively (Volkmann, Moro, & Pahwa, 2006). Tuning of stimulation parameters is done by a clinician using a time-intensive trial-and-error process until maximum efficacy is achieved with minimal side effects (Hunka, Suchowersky, Wood, Derwent, & Kiss, 2005; Volkmann, Herzog, Kopper, & Deuschl, 2002). It is estimated that post-operative programming requires 30 hours of clinical time (Hunka et al., 2005). A systematic approach to tuning stimulation parameters based on objective measures from patient physiology has the potential to reduce tuning time and improve efficacy.

Optimization methods based on both kinematic data as well as neural recordings have been developed to improve post-operative programming (Mera, Vitek, Alberts, &

Giuffrida, 2011). Approaches utilizing kinematic data have involved capturing motion data with a device worn by the patient. The goal is to reduce/control behavioral markers of PD, such as tremor and bradykinesia (Malekmohammadi et al., 2016; Malekmohannadi et al., 2016; Mera et al., 2011). DBS hardware that can simultaneously stimulate and record the neural signal has recently been developed (Ryapolova-Webb et al., 2014), enabling new stimulus optimization approaches based on local field potential recordings. For approaches utilizing neural recordings, a biomarker representing the pathological state is needed for optimal control. Many groups have proposed using enhanced synchrony as a control signal (Cagnan et al., 2014; de Hemptinne et al., 2015; Little et al., 2013; P. A. Tass, 2002).

Future generations of devices may allow for optimization of novel parameters, such as stimulation pattern and waveform, to more efficiently and effectively target pathological neural activity. A significant number of patients experience detrimental side effects from DBS, including depression, psychosis, confusion, and impulse control disorders (Smith et al., 2012). Developing novel stimulation approaches has the potential to improve the quality of life for the patient by not only reducing negative side-effects, but also by decreasing power consumption and accounting for fluctuations in motor symptoms.

Open-loop approaches, which do not require a feedback signal, have been developed to optimally target enhanced synchronous activity. Coordinated Reset is an approach developed by Peter Tass which aims to desynchronize population synchrony by synchronizing multiple subpopulations of neurons to different stimulation electrodes (P. A. Tass et al., 2012). This approach has been shown to induce long-term effects even after

stimulation has been turned off (P. A. Tass et al., 2012). The temporal pattern of stimulation also affects efficacy of DBS (Dorval et al., 2010; Dorval et al., 2008). Warren Grill has developed an approach called Temporally Optimized Patterned Stimulation (TOPS), which uses a genetic algorithm to determine the optimal stimulus pattern for disrupting pathological synchrony in a computational model (Warren M. Grill & Dorval II, 2014).

Closed-loop approaches, which rely on a feedback control signal, have the added benefit of being able to adjust with fluctuating motor symptoms. Adaptive stimulation approaches, where stimulation is limited to times when pathological activity is high, is effective at improving motor symptoms while using less battery power (Little et al., 2013; Malekmohammadi et al., 2016).

The goal of this thesis is to investigate an optimization approach to suppress pathological oscillations based on patient-specific responses to stimulation. The underlying theory of this approach is that DBS works through a mechanism called "chaotic desynchronization," where certain stimulation parameters induce chaotic behavior in the neural population, thereby disrupting pathological oscillatory activity (C. J. Wilson et al., 2011). This approach can be used to both tune stimulus parameters in current devices, such as stimulus frequency and amplitude, and develop novel stimulus patterns and waveforms for use in future generations of devices.

Using Phase Response Curves to Optimize DBS to Suppress Oscillatory Activity seen in PD

We propose to use a simple measure called the phase response curve (PRC) to predict the optimal stimulus parameters to disrupt pathological beta oscillations seen in PD. Pulse coupled oscillator theory reduces the complex behavior of a periodically firing neuron to a simple input-output phase model, the PRC, that determines how the phase of an oscillation is changed given the phase of a subthreshold stimulus pulse (G. B. Ermentrout & Kopell, 1998; Winfree, 2001) (Figure 4).

Underlying this theory is the idea that the PRC can be used to predict when coupled oscillators, such as periodically firing neurons, will synchronize or desynchronize. Certain stimulus parameters will result in the oscillator becoming aperiodic or even chaotic (defined for our purposes as two neurons starting almost synchronously diverging in time until they are no longer related in phase). PRCs have been used to study synchrony in networks of heart cells (Guevara, Shrier, & Glass, 1986), fireflies (Mirollo & Strogatz, 1990), and networks of model neurons (E. Brown, Moehlis, & Holmes, 2004; Hoppensteadt & Izhikevich, 1996; Izhikevich, 2007; Kopell & Ermentrout, 2002; N. W. Schultheiss, Edgerton, & Jaeger, 2010; Smeal, Ermentrout, & White, 2010; Wu, Liu, & Chen, 2010).

The PRC can be used to optimize stimulus parameters to induce chaotic behavior, thereby desynchronizing neurons, through something called the PRC map. The distance between two neurons on the next cycle of the oscillation (ε_{i+1}) can be calculated given their distance on the current cycle (ε) using this map. Stimulating at phases where the slope of the PRC map is greater than one (slope of PRC is positive) will result in the neurons becoming

further apart on the next cycle, thereby desynchronizing over subsequent stimuli. Stimulating at phases where the slope of the PRC map is less than one (slope of PRC negative) will result in the neurons becoming closer together on the next cycle, thereby synchronizing over subsequent stimuli (Figure 4).

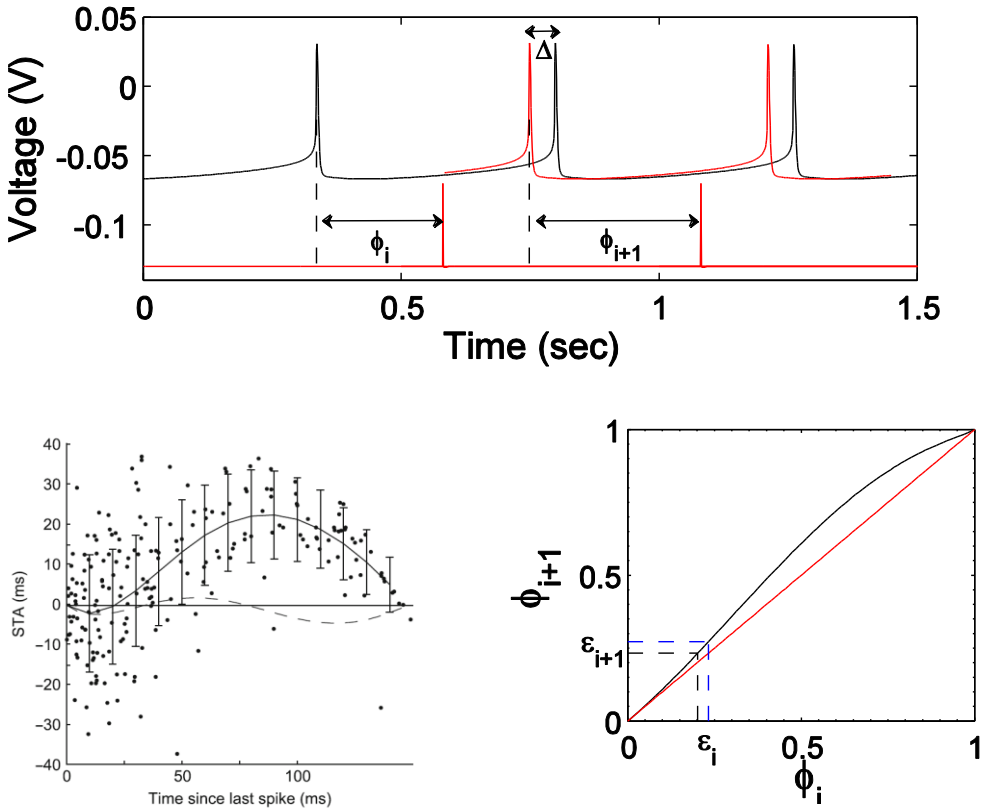

Figure 4. Using a phase response curve (PRC) to predict network synchrony. Top: A PRC can be estimated from the spike times of a periodically firing neuron (black). A current pulse is applied at some point in the phase (red/grey), which can result in a phase advance or phase delay (red compared to black). Bottom left: The spike time advance is plotted as a function of the stimulus time. A polynomial fit to the data represents the PRC (figure modified from (Netoff et al., 2005). Bottom right: The PRC map (stimulus phase on the next cycle as a function of the stimulus phase on the current cycle) can be used to predict synchronizing effects of the stimulus. The PRC (black) is added to the line of identity, which is used to predict the phase of the stimulus on the next cycle. Two neurons starting some distance, ε, apart will become further apart on the next cycle when the slope of the PRC is >1.

Conclusion

The overall goal of this thesis is to investigate the use of PRCs to predict stimulus parameters to optimally disrupt synchrony. This will be done by testing this approach in 1) a computational model of Parkinson's disease with an emergent pathological oscillation and 2) in periodically firing neurons in brain slices containing basal ganglia nuclei. A PRC-based optimization approach could be used to 1) systematically tune stimulus frequency and amplitude, potentially reducing time spent tuning stimulus parameters and improving efficacy, and 2) optimize stimulus waveforms and patterns, potentially improving battery life and improving efficacy. Importantly, this approach utilizes subthreshold stimulus pulses, much lower amplitudes than current stimulus protocols, which induce spiking. Using smaller amplitude stimulation has the potential to reduce unwanted side effects. Overall this framework offers insight into the underlying mechanism of DBS and provides a method for optimizing DBS parameters in a patient-specific manner.

Chapter 2

Computational Models of the Basal Ganglia

Part of the work presented in this chapter is from: Holt AB, Netoff TI (2014). Origins and suppression of oscillations in a computational model of Parkinson's disease. *J Comput Neurosci*, 37(3): 505-521.

Introduction

Computational modeling can be a powerful tool for an experimentalist, providing a rigorous mathematical model of a system valuable for testing hypotheses, explaining complex dynamics, and developing experimental protocols. Models have made important advancements in many fields. One famous example is Copernicus' mathematical model, which provided support of the heliocentric system (Copernicus, Herrmann, & Akademie der Wissenschaften der DDR., 1973). This simple model could explain many of the observed complex celestial patterns, such as planetary orbits. Further validation of the model occurred when Kepler, Galileo, Newton, and others collected novel data that the model was able to predict or that fit within the model. In this example a mathematical model was necessary, as technology did not allow for visualization of the entire system (Folkerts & Kühne, 2006; Westman, 1975). Similarly, mathematical models can be used to understand complex dynamical systems in the brain.

Even when an experiment can be done, modeling is a powerful approach for developing and designing experiments. We may have working mental models of how the brain works. However, making a computational model is a way to formalize this mental model, allowing us to systematically identify the necessary parameters and states of the nervous system to describe its behaviors. Computational models also offer advantages over a mental model. Computational models are portable, allowing others to easily reproduce your findings or test their hypotheses against yours without experimental confounds. Models allow you to perturb parameters, which might not be possible experimentally. They

also allow you to look at hidden states not observable experimentally and explicitly study interactions between different scales.

Much of my thesis work focuses on developing methods to optimize deep brain stimulation (DBS) in Parkinson's disease (PD). Due to the complexity of network interactions and the need to interpret complex experimental findings, many computational models of the basal ganglia and the effects of DBS have been developed. These models have been used to understand how information is processed within the network in heath and disease (Gillies & Arbuthnott, 2000; Gurney, Prescott, & Redgrave, 2001; Suri & Schultz, 1998), develop novel DBS algorithms (Santaniello, Fiengo, Glielmo, & Grill, 2011), move toward patient-specific approaches to DBS (Butson, Cooper, Henderson, & McIntyre, 2007; Holt & Netoff, 2014), and understand the mechanisms of DBS (Hahn & McIntyre, 2010; Humphries & Gurney, 2012; Rubin & Terman, 2004; Terman, Rubin, Yew, & Wilson, 2002; Thibeault & Srinivasa, 2013; C. J. Wilson et al., 2011).

Computational network models of deep brain stimulation

It is important to choose a model at the appropriate spatial scale and with the necessary level of complexity. Molecular and cellular level models may be useful in explaining how stimulation affects ionic currents or induces plasticity (Mahon, Deniau, Charpier, & Delord, 2000). However, when investigating DBS algorithms, a network model is likely the most appropriate as DBS induces network-wide effects (Alhourani et al., 2015; Humphries & Gurney, 2012). Network models can be used to understand

emergent behaviors that occur when large groups of neurons are coupled together. A number of different network models to explain DBS in the basal ganglia with various levels of abstractness have been developed over the last 20 years.

Abstract Network Models

The basal ganglia network is a complex non-linear system. Reducing the complexity of the system to a few abstract rules or equations to describe a given behavior makes it possible to determine parameter ranges over which the behavior of a network will change.

Oscillator Network Models

Networks of oscillators have been used to describe the dynamics of neuronal populations and investigate neural synchrony (G. Ermentrout & Kopell, 1991; Grannan, Kleinfeld, & Sompolinsky, 1993; Hansel, Mato, & Meunier, 1993; Kuramoto, 1984). A phase oscillator is defined by an eigen frequency, ω, and a phase, $\varphi(t)$, which varies from 0 to 2π according to:

$$\frac{\partial}{\partial t}\varphi(t) = -\omega$$

*N o*scillators can be coupled together using a sine function:

$$\frac{\partial}{\partial t}\varphi_i(t) = -\omega_i + \frac{K}{N}\sum_{i=j}^{N}\sin[\varphi_i(t) - \varphi_j(t)]$$

where K is the synaptic strength coefficient, and each oscillator *i* interacts with other oscillators *j*.

Peter Tass utilized phase oscillator models to investigate how DBS may be used to disrupt pathological synchrony seen in PD (P. A. Tass, 2001, 2002; Peter A. Tass, 2007). The effects of stimulation on coupled oscillators depend on the phase of the oscillator as well as the intensity of the stimulus. Tass used this approach to demonstrate how periodic stimulation can desynchronize and synchronize many independent neural oscillators. Importantly, Tass' work was used to design directed approaches to DBS, including the idea that neural synchrony could be used as a control signal to determine optimal stimulation.

The idea of phase oscillator models was then expanded to include a network of three oscillators, y_1, y_2, y_3, connected with excitatory and inhibitory sigmoidal coupling functions, f_E, f_I, in the Titcombe model (Titcombe, Glass, Guehl, & Beuter, 2001).

$$\frac{\partial y_1}{\partial t} = f_1(y_3) - y_1 \, , \frac{\partial y_i}{\partial t} = f_E(y_{i-1}) - y_i \, , i = 2,3$$

$$f_I = \frac{\theta^g}{y^g + \theta^g}, \quad f_E = \frac{y^g}{y^g + \theta^g}, \; \theta = 0.5,$$

Where θ is the threshold and g is the gain. Stimulation can be modeled by changing the gain on the coupling functions. The Titcombe model was used to show that stimulation may work by inducing a Hopf bifurcation, thereby disrupting the pathological oscillation by destabilizing the abnormal limit cycle associated with the oscillation (Titcombe et al., 2001).

Systems-level field models

Computational network models made up of individual neurons are limited to simulations of ~10,000 neurons generally; however, this does not yet approach the scale of complexity in the brain. Therefore, at some scale it is inevitable that more abstract models describing the population activity are used instead of models of individual neurons. Mean field models use simple equations to describe the average firing rates within a population of neurons (Beurle, 1956; Deco, Jirsa, Robinson, Breakspear, & Friston, 2008; Freeman, 1975; Lopes da Silva, Hoeks, Smits, & Zetterberg, 1973; Nunez, 1974). These models were first adapted to describe the cortex by Wilson and Cowan (H. R. Wilson & Cowan, 1972).

Mean field models have certain advantages over detailed models. First, parameters can be related to physiologically measurable local field potential data, an average of neural activity. Second, mean field models are well suited for bifurcation analysis, which describes how shifts in parameters may lead to different states/behaviors. Finally, as the role of the cortex becomes important in understanding the mechanisms of DBS (S. Li, Arbuthnott, Jutras, Goldberg, & Jaeger, 2007), mean field models offer a useful reduction approach to address the huge number of neurons.

Mean field models of the basal ganglia have been used to explain the emergence of pathological oscillations (van Albada, Gray, Drysdale, & Robinson, 2009; van Albada & Robinson, 2009). While these models have not been used to model DBS for PD to our knowledge, field models of the thalamocortical loop have been used to describe

mechanisms of DBS for epilepsy (Mina, Benquet, Pasnicu, Biraben, & Wendling, 2013). This approach could therefore be applied to field models of the basal ganglia.

Realistic Network Models

The abstract models described above lack biophysical details about ionic currents, different cell types, or individual synaptic input. Realistic network models can be used to understand molecular, cellular, and biophysical properties of networks. This can be important for modeling DBS, where changes in firing rates, bursting properties of single cells, and ionic currents have all been proposed to play a role in the mechanism of action (McIntyre, Savasta, Kerkerian-Le Goff, & Vitek, 2004; McIntyre, Savasta, Walter, & Vitek, 2004).

Spiking Network Models

Spiking network models utilize synaptically coupled biophysical representations of neurons, such as conductance-based neuron models (Hodgkin & Huxley, 1952a, 1952b):

$$C_m \frac{d}{dt} v(t) = -I_{Na} - I_K - I_L - I_x$$

Here the membrane voltage is modeled as a function of the membrane capacitance, C_m, and ionic currents affecting the cell, such as the sodium current, I_{Na}, potassium current, I_K, and leak current, I_L. Different cell types can be modeled using various currents, I_X.

The Rubin-Terman (RT) model was the first and arguably most famous spiking network model of DBS to the subthalamopallidal network (Rubin & Terman, 2004; Terman

et al., 2002). The model contains single-compartment conductance based neuron models of four different cell types, STN, GPe, GPi, and thalamocortical, which are synaptically coupled based on anatomy. The parkinsonian state is created by altering the synaptic weights between different populations, resulting in the emergence of a pathological oscillation at the tremor frequency (5-8 Hz). The RT model was initially used to show DBS regularizes firing in the STN by driving spiking, thereby reestablishing the ability of thalamic neurons to relay information to the cortex.

While the RT model has been a popular choice for investigating cellular effects of DBS (Feng, Shea-Brown, Greenwald, Kosut, & Rabitz, 2007; Guo, Rubin, McIntyre, Vitek, & Terman, 2008; Pirini, Rocchi, Sensi, & Chiari, 2009; Schiff, 2010), it does not adequately replicate frequency dependent effects of DBS and is not robust to relatively small variations in parameters (J Modolo, Edwards, Campagnaud, Bhattacharya, & Beuter, 2010). More robust and physiologically realistic models of the effects of DBS on the basal ganglia network have since been developed and used to investigate mechanisms related to changes in firing rates (Humphries & Gurney, 2012; Moroney, Heida, & Geelen, 2008), changes in the burstiness of cells (Hahn & McIntyre, 2010; J. Modolo, Henry, & Beuter, 2008), the effects of DBS on action-selection (Thibeault & Srinivasa, 2013), and regularization of neural firing (Dorval, Panjwani, Qi, & Grill, 2009; Santaniello et al., 2015; So, Kent, & Grill, 2012).

Electric Field Models

Many computational models of DBS have focused on realistically modeling the effects of voltage distribution produced by extracellular stimulation (Butson et al., 2007; Butson & McIntyre, 2008; Chaturvedi et al., 2012; Martens et al., 2011; Zitella et al., 2015). Models of the electric field can range in complexity, from simple point source models to finite element models incorporating topography, composition of the surrounding tissue, and electrode geometry (McIntyre & Foutz, 2013). Generally finite element modeling is used to model the effects of DBS (Aström, Lemaire, & Wårdell, 2012; Lempka & McIntyre, 2013). These models have been used to explain how stimulation differentially affects the soma and axon of the same neuron (Miocinovic et al., 2007); to design patient specific models of tissue activation (Butson et al., 2007; Hemm et al., 2005; McIntyre, Mori, Sherman, Thakor, & Vitek, 2004); and to optimize target selection, current steering, electrode configuration, and electrode design (Butson & McIntyre, 2006; Connolly et al., 2016; McIntyre & Foutz, 2013; Willsie & Dorval, 2015; Xiao, Pena, & Johnson, 2016).

The Hahn and McIntyre Model (HM Model)

The focus of this thesis is on developing optimization approaches for stimulation parameters, specifically using pathological oscillations as a biomarker. These approaches were developed and tested in the Hahn and McIntyre model (HM Model), a spiking network model of the subthalamopallidal network with STN DBS (Hahn & McIntyre, 2010). The HM model was chosen for a number of reasons. 1) The model is more physiologically realistic than many, containing conductance-based neuron models

synaptically coupled in a somewhat physiologically realistic manner. 2) There is a healthy and parkinsonian state, both of which were fit using non-human primate data. This allows me to investigate emergent pathological activity. 3) There is an emergent pathological oscillation not specified in the equations for the model. This was necessary to test optimization approaches targeting this activity. 4) The model and emergent oscillation are robust to changes in various parameters. 5) The effects of DBS are modeled both through activation of efferent activity and through antidromic effects on neurons within the stimulation; this is more physiologically realistic than many models. 6) The model's spiking output can be directly compared to physiological recordings and thus can be used to design future non-human primate experiments. The model can be downloaded at http://senselab.med.yale.edu/modeldb and is run in NEURON (Hines & Carnevale, 1997, 2001).

The HM model contains 500 single-compartment conductance-based neurons: 100 STN neurons, 100 globus pallidus internal (GPi), and 300 globus pallidus external (GPe) neurons. Excitatory cortical synaptic drive to the STN is simulated as a 16 Hz stochastic bursting input. We added a standard deviation of 5 msec to the period of the 16 Hz cortical input to widen the distribution of the cortical drive and significantly decreased the harmonics of the 16 Hz signal. Inhibitory striatal synaptic drive is delivered to the GPi and GPe. Neurons are synaptically coupled in a physiologically realistic way, illustrated in Figure 5**.** (Hahn & McIntyre, 2010).

Parameters for the parkinsonian state were fit using *in vivo* microelectrode recordings from non-human primates (Hahn et al., 2008; Hashimoto et al., 2003; Wichmann & Soares, 2006). The model was tuned to replicate the mean firing rates and bursting rate within each population (STN, GPe, and GPi) as well as their shifts in the parkinsonian state using a least squares error optimization.

While there are many effects of STN DBS on the neural tissue, the focus of the HM model is on targeting efferent activity. In the model, DBS is simulated by activating neurons in the efferent target. To model antidromic effects of the axonally generated action potentials, a subthreshold current injection is applied to the STN neurons.

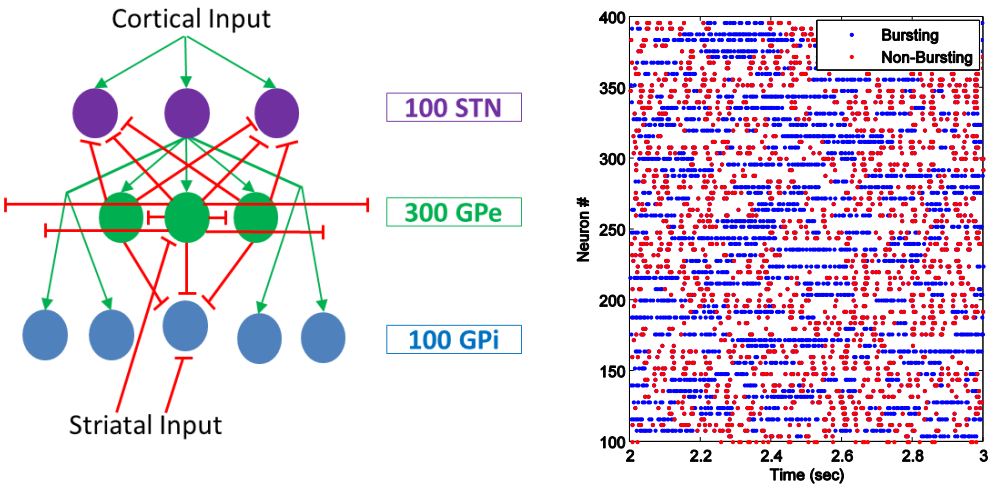

Figure 5. Connectivity and Output of Hahn and McIntyre Model. Computational model of the basal ganglia fit to non-human primate data developed by Hahn and McIntyre. A: Connectivity diagram of the Hodgkin-Huxley neurons making up the network. B: The output of the computational model is spike times. A rastergram of Globus Pallidus external neurons over a small window of time are shown here where the y-axis is neuron number, and the x-axis is time (seconds). Neurons exhibit a bursting and non-bursting phase classified by the spiking rate.

Generating Power Spectra

The original Hahn and McIntyre paper focused on the bursting rates of different populations. However, we were interested in the emergence of pathological oscillations. To detect pathological oscillations from the spike times of the neurons in the HM model, we looked for peaks in the power spectrum.

There are multiple ways to calculate the power spectrum from spike time data. One approach is to calculate the power spectrum by Fourier transforming the autocorrelation spike density. However, in this approach, the instantaneous phase of the oscillation at a particular time cannot be calculated. Another approach is to use a truncated point process Fourier transform of the spikes. The spike train can be represented as the sum of delta functions, $s(t) = \sum_{i=1}^{N} \delta(t - k_i)$, where k_i represents the time of the ith spike in the network. The Fourier transform of the spike train can be calculated as $S(\omega) = \int_0^\infty s(t)e^{-j\omega t}dt$, where $j = \sqrt{-1}$ and $\omega = 2\pi f$ and f is the frequency at which the spike train is Fourier transformed. However, because $s(t)$ is zero, except at the spike times, this can also be calculated as $S(\omega) = \sum_{i=0}^{N} e^{-j\omega k_i}$. The truncated Fourier transform was calculated over a range of 0-100 Hz. From the Fourier transform it is then possible to estimate the instantaneous phase and amplitude of the population oscillation at any given time from the spikes of the individual neurons.

Pathological 34 Hz Oscillation

Spectral analysis of the spike times of the GPe neurons revealed an emergent 34 Hz oscillation in the HM model (Figure 6). This 34 Hz oscillation is not seen in the healthy state and is reduced with 136 Hz DBS-like stimulation to the STN (Figure 6).

Synaptic drive from the cortex is patterned onto the STN at 16Hz, raising the concern that the 34 Hz oscillation is simply a harmonic. However, the 16 Hz stimulation remained consistent throughout all conditions, while the 34 Hz oscillation was modulated by the state of the model as well as by stimulation. Furthermore, changing the frequency of the cortical input, for example from 16 Hz to 10 Hz, results in a shift of the 16 Hz peak but not the 34 Hz peak (data not shown). Removing the 16Hz drive causes the 34 Hz oscillation to disappear, presumably due to a decrease in excitability of the STN neurons. This fits with the hypothesis that both internal and external drive is needed to generate the pathological oscillations (Bevan & Wilson, 1999).

The oscillatory activity is generated by neurons during the non-bursting phase. Neurons were classified as bursting if their firing rate was above a selected threshold. The threshold was set by convolving the spike times with a Gaussian kernel 4 ms wide (all spikes above a threshold of 4 were classified as bursting). A periodicity to the firing in the non-bursting phase, which is not present in the bursting phase, can be seen in the rastergram (Figure 5B). When the bursting phase is removed to calculate the power spectrum, the peak

at 34 Hz oscillation remains (Figure 6), indicating that the 34 Hz oscillation is generated by neurons in the non-bursting phase.

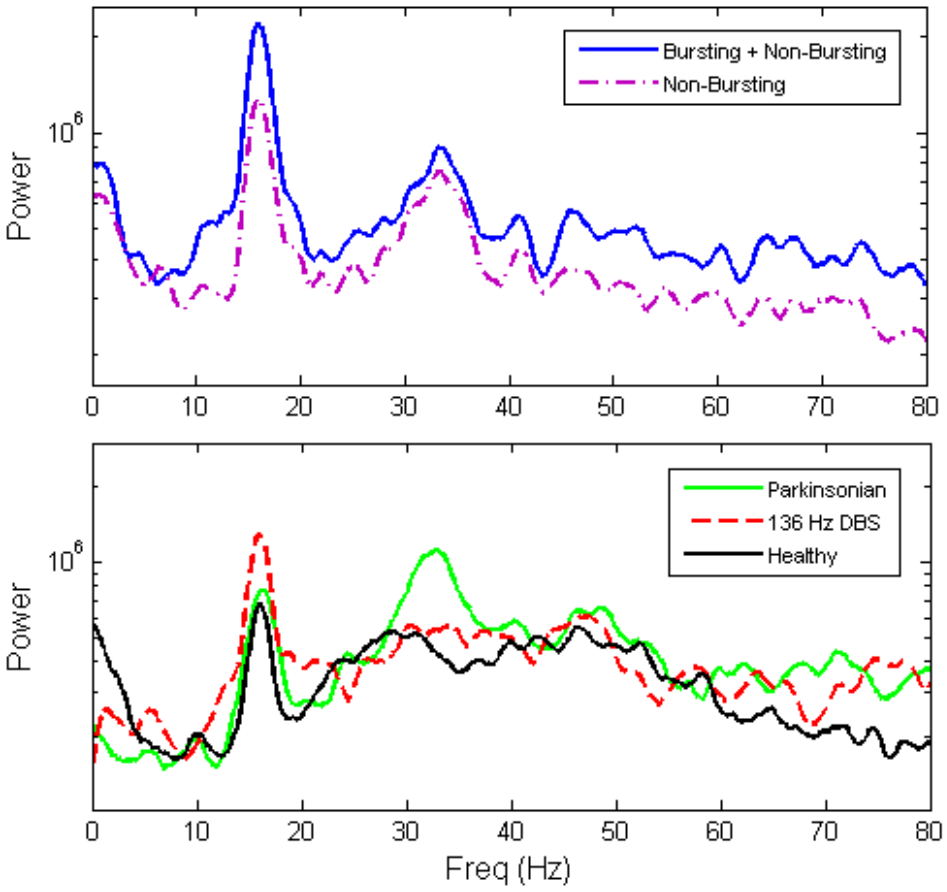

Figure 6. Parkinsonian 34 Hz oscillation present in power spectrum. An oscillation at 34 Hz arises in the Parkinsonian (PD) state in the non-bursting phase of spiking that is suppressed with DBS. Top: Power spectrum showing the emergence of a 34 Hz oscillation. X-axis is frequency (Hz) and y-axis is power. The peak at 16 Hz is from the cortical input at that frequency. All characteristics are preserved when spikes in the bursting phase are removed (dashed line). Bottom: A 34 Hz oscillation is seen in the power spectrum of the PD state (light) that is not present in that of the healthy state (dashed). Application of 136 Hz DBS (black) suppresses the 34 Hz oscillation. The 16 Hz peak due to the cortical input is not affected across conditions.

Limitations

As with any computational model, there are limitations when using the HM model to understand and optimize DBS. First, while the neurons in the HM model are coupled in a somewhat realistic manner, the actual wiring arrangements in the basal ganglia network are much more complex. Second, heterogeneity within the cells is produced by random input to identical model neurons, while neurons in the basal ganglia have a lot of heterogeneity in their firing rate and response to stimulus pulses (Farries & Wilson, 2012). Third, there is a complex topology to any neural network, which is not represented in this model. Fourth, the effects of stimulation are a simplification. For computational efficiency, dendritic arbors are not simulated and therefore stimulation is applied as a direct injection of current to the cells. The efferent effects of stimulation are the focus of this model; however, stimulation affects the neural tissue in a variety of ways. For example, it has been shown that STN DBS results in antidromic activation of cortical neurons (S. Li et al., 2007), however this is not included in the HM model.

Conclusion

Computational models of DBS can be useful in many ways. They can help understand complex experimental results, develop hypotheses on mechanisms of action, design experiments, and test novel stimulation approaches in a repeatable manner. First, the HM model will be used in chapter 3 to develop methods to understand the emergence of pathological oscillations. Next, in chapter 4 the model will be used to develop methods

for estimating phase response curves (PRC) from population data as well as to test a subject-specific approach to optimizing stimulation frequency. Finally, in chapter 5 a novel closed-loop phasic approach to stimulation optimized based on subject-specific responses to stimulation will be tested.

We do not suggest that results found in the computational model will be the same as those found in a clinical setting. Instead the HM model provides a platform to test methods for optimizing the suppression of a population parkinsonian oscillation with DBS.

Chapter 3

Origins of a Parkinsonian Oscillation in a Computational Model

The work presented in this chapter is from: Holt AB, Netoff TI (2014). Origins and suppression of oscillations in a computational model of Parkinson's disease. *J Comput Neurosci*, 37(3): 505-521.

Introduction

Enhanced beta oscillations (12-35 Hz) within the basal ganglia network and its thalamo-cortical targets have been implicated in anti-kinetic motor signs of PD (Bhidayasiri & Truong, 2008; P. Brown, 2006; Chen et al., 2007; Marsden et al., 2001). This enhanced oscillatory activity can be detected in single basal ganglia neurons as well as in local field potentials (LFPs) (P. Brown, 2007; Priori et al., 2002; Priori et al., 2004; Williams et al., 2002). While beta oscillations have been proposed as a putative biomarker for PD and a control signal for DBS (Adamchic et al., 2014; Bronte-Stewart et al., 2009; Kuhn et al., 2006; Little et al., 2013; Meissner et al., 2005), it remains unclear how these oscillations emerge.

Pathological beta oscillations could arise in various ways: 1) as periodic drive from an external source, such as the cortex, which is patterned onto the basal ganglia network; 2) as a synchronous population of neurons in the basal ganglia firing periodically at the beta frequency; or 3) as an emergent property of the basal ganglia network. Recordings of neurons in STN, GPe, and GPi show bursting behavior in the beta frequency range under PD conditions, but the neurons do not show highly precise spike synchrony (Bergman et al., 1998; P. Brown, 2007; Israel & Burchiel, 2004). Therefore, it is unlikely that oscillations are caused by synchronous firing of a single population of neurons (Hashimoto et al., 2003; Mallet et al., 2008). There is evidence both supporting and refuting the hypotheses that 1) the oscillation arises from the cortex and 2) that the oscillation is generated within the basal ganglia (Bevan & Wilson, 1999; P. Brown & Williams, 2005;

Courtemanche, Fujii, & Graybiel, 2003; Dejean, Hyland, & Arbuthnott, 2009; Goldberg, Bourad, & Bergman, 2004; Gradinaru, Mogri, Thompson, Henderson, & Deisseroth, 2009; Hammond, Bergman, & Brown, 2007; Holgado, Terry, & Bogacz, 2010; Kuhn et al., 2005; McCarthy et al., 2011; Moran et al., 2011; Nevado-Holgado, Mallet, Magill, & Bogacz, 2014; Pasillas-Lépine, 2013; Pavlides, Hogan, & Bogacz, 2015; Plenz & Kital, 1999; Sharott et al., 2005; Terman et al., 2002).

It has been hypothesized that beta oscillations emerge due to interactions between the GPe and STN (Holgado et al., 2010; Plenz & Kital, 1999; C. J. Wilson, 2014). The STN sends excitatory glutamatergic projections to the GPe, and the GPe sends inhibitory GABAergic projections back onto the STN (Albin et al., 1989). This excitatory-inhibitory feedback loop makes the system conducive to generating oscillations (Bevan, Magill, Terman, Bolam, & Wilson, 2002; Marreiros, Cagnan, Moran, Friston, & Brown, 2012).

In this chapter, I will use the Hahn and McIntyre model (HM model), as described in Chapter 2, to test a method for understanding the emergence of a 34 Hz parkinsonian oscillation. The oscillation is an emergent property of the network; however, the complexity of the HM model makes it difficult to determine the origin. The approach presented here involves fitting a simplified mean field model to the complex HM model to understand how changes in the parkinsonian state result in a propensity of the network to oscillate.

Mean field Modeling

To determine the origin of the pathological oscillation in the HM model, discrete time mean field models were fit to impulse responses. As briefly described in chapter 1, mean field models describe the average firing rate of a population (H. R. Wilson & Cowan, 1972). Sets of equations determine the population firing rate given the history of the population's firing rate and its synaptic input. Populations can be connected using various time delays and strengths. Mean field models are conducive to mathematical analysis because they reduce the dimensionality of the system. The systems-level analysis can be used to determine the necessary conditions for the system to oscillate and how changes in parameters affect behaviors.

Mean field models have previously been used to understand the origins of parkinsonian oscillations within the basal ganglia thalamo-cortical loop (Holgado et al., 2010; Nevado-Holgado et al., 2014; Pavlides et al., 2015; van Albada et al., 2009; van Albada & Robinson, 2009). However, for analysis purposes time delays between nuclei were assumed equal and the system was linearized around a specific point. Accurate delays are likely an important factor in determining the behavior of a closed-loop system and the origin of oscillations. While it is possible to calculate the stability of the system with delays (Pasillas-Lépine, 2013), we propose using a discrete mean field model. This allows for a simple analytical analysis of the system with variable delays and allows for the visualization of all poles.

Methods

The HM model, described in chapter 2 (Hahn & McIntyre, 2010), was used to test whether a simplified discrete time mean field model can be used to determine the origin of the 34 Hz parkinsonian oscillation. We hypothesize that the 34 Hz parkinsonian oscillation in the HM model emerges due to a change in interactions between the STN and GPe.

Models of the target nuclei (STN and GPe) were generated by measuring the stimulus triggered histogram of the target population's response to a stimulus applied to the pre-synaptic population. This was done in open-loop, where all connections to the target population except the connection from the stimulated pre-synaptic population were cut, to avoid any interactions between the two populations or a separate population (Figure 7). Removing connections can easily be done in a computational model but is difficult experimentally, although can be done pharmacologically in animal models (Tachibana, Iwamuro, Kita, Takada, & Nambu, 2011). The open-loop models for the STN and GPe were combined to make a closed-loop systems-level model of the STN-GPe loop. The analysis of this closed-loop system was then used to investigate if and how oscillations are generated.

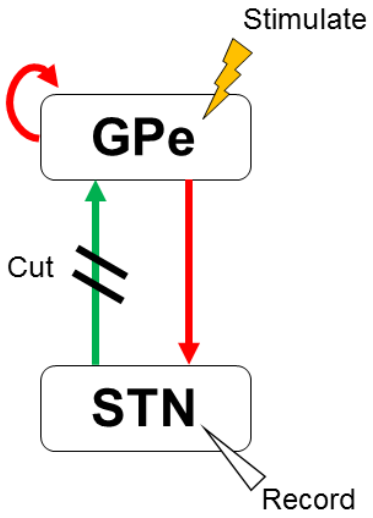

Figure 7. Open-loop stimulation protocol for measuring neural responses to stimulation. To model the connection between the globus pallidus external (GPe) and the subthalamic nucleus (STN) impulse responses were measured in the STN in response to stimulation to the GPe. The connection from the STN to the GPe was set to zero in the computational model in order to avoid interactions. The impulse response measured in the STN was used to fit a discrete transfer function model. The reverse was done to model the connection from the STN to the GPe.

Transfer Function Fits

Time delays between nuclei are an important aspect of the closed-loop system. While the emergence of oscillations in the closed-loop system can be done using the Laplace transform of the mean field fits for each connection, analysis of continuous systems with time delays is difficult. In contrast, analyzing discrete time systems with delays is relatively easy (Oppenheim, Willsky, & Nawab, 1996). Therefore, discrete time models were fit to spiking data from the Hahn and McIntyre model measured in open-loop. This allows for a discrete version of the Laplace transform, the Z-transform, to be used when generating the model of the closed-loop STN-GPe system.

Discrete time models were fit to peristimulus time histograms, $PSTH[n]$, measured from the STN and GPe in open-loop. Before fitting a function to the PSTH, it was normalized to describe the proportional change from the mean firing rate: $NPSTH[n] = \frac{PSTH[n]}{<R>} - 1$. Each NPSTH was generated by averaging 120 stimulus pulses applied at 2 Hz. Transfer functions were fit to the $NPSTHs$ to describe the time course of the response of the post-synaptic population to the stimulus applied to the presynaptic population. Delays between the two populations were also incorporated. Combinations of damped sine and cosine waves were used for the fits:

$$NPSTH[n] = Ae^{-\gamma n}\sin(\omega * (n-d)) * u[n-d]$$

$$\overset{z}{\Leftrightarrow} \frac{A * \gamma * z^{-1} * \sin(\omega)\, z^{-d}}{1 - 2 * \gamma * z^{-1} * \cos(\omega) + \gamma^2 * z^{-2}}$$

or

$$NPSTH[n] = Ae^{-\gamma n}\cos(\omega * (n-d)) * u[n-d] \overset{z}{\Leftrightarrow} \frac{A * (1 - \gamma * z^{-1} * \cos(\omega) z^{-d}}{1 - 2 * \gamma * z^{-1}\cos(\omega) + \gamma * z^{-2}}$$

Where ω is the frequency of the oscillation, γ is the dampening time constant, A is the amplitude of the response, and d is the delay between the stimulus and the response. A robust fit was used to fit the models and minimize absolute values of the error over 16 msec using Matlab's (Natick, MA) fminsearch function. In the future this could be done using the tfest function in Matlab's system identification toolbox.

Transfer function fits to the normalized PSTH in the healthy and PD state are shown in Figure 8. Coefficients used for each model are provided in Table 1. STN was fit with a cosine and sine wave under parkinsonian and healthy conditions. GPe was fit with two cosine waves under each condition.

Table 1. Values used in transfer function fits. STN was fit with a cosine and sine wave under parkinsonian and healthy conditions. GPe was fit with two cosine waves under each condition.

	Frequency (ω)	Amplitude (A)	γ	Delay (d)
STN				
Cosine	0.1824	-0.0297	0.9651	-3
Sine	0.2236	-0.0512	0.9510	-9
HSTN				
Cosine	0.1555	-0.0282	0.9607	-3
Sine	0.1953	-0.0567	0.9499	-9
GPe				
Cosine 1	0.2288	0.0445	0.9664	-7
Cosine 2	0.3357	0.1585	0.8310	-3
HGPe				
Cosine 1	0.1775	0.0422	0.9604	-6
Cosine 2	0.2979	0.1516	0.8204	-3

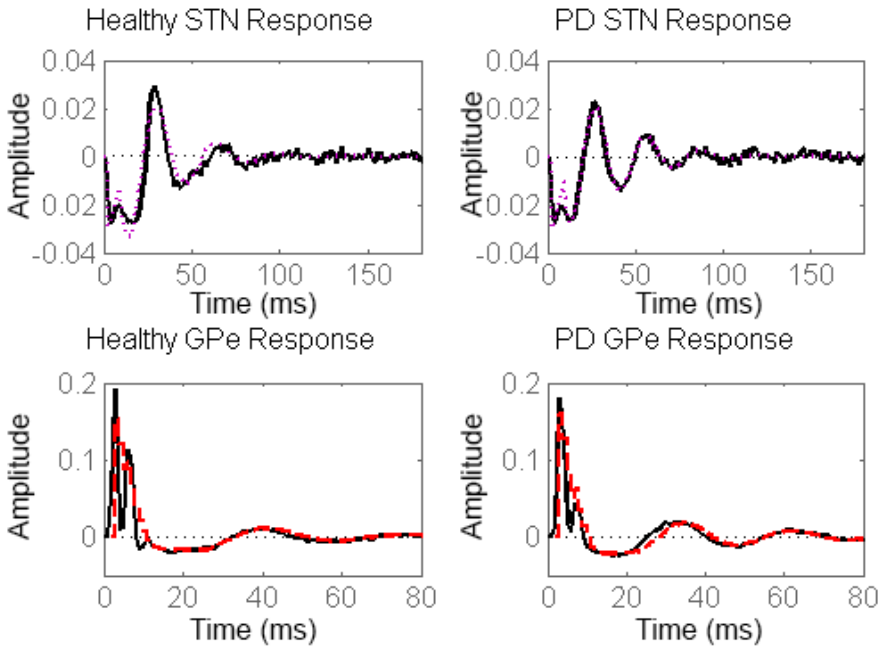

Figure 8. Impulse responses and fits. Impulse response fits to stimulus triggered histograms accurately reproduce oscillations. Black: Stimulus triggered histograms. Dashed: Impulse response fits. **Top:** STN response to a stimulus pulse to GPe in open loop in the healthy (left) and PD (right) state. **Bottom:** GPe response to a stimulus pulse in STN in the healthy (left) and PD (right) state.

Generating the closed-loop system

To analyze the emergence of oscillations in the closed-loop GPe-STN system, the transfer functions of each individual open-loop connection were coupled together to create a systems-level model, illustrated in Figure 9. The closed-loop model describes the basal ganglia output given cortical inputs. The GPe-STN loop, $Q_{GPe,STN}$, can be modeled as follows:

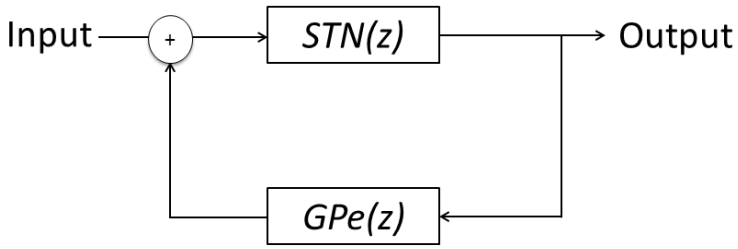

Figure 9. Box diagram of the closed-loop systems-level model. The Subthalamic nucleus (STN) receives input from the cortex and sends excitatory projections to the Globus Pallidus External (GPe). The GPe sends inhibitory projections back to STN. The transfer function of the closed-loop system describes the output of the system given the input.

$$Q_{GPe,STN}(z) = \frac{STN(z)}{1 + GPe(z) \times STN(z)}$$

Where $STN(z)$ is the transfer function describing the connection from STN to GPe, and $GPe(z)$ is the transfer function describing the connection from GPe to STN. This model is easily extensible to incorporate more nuclei. Delays between the nuclei are incorporated.

$Q_{GPe,STN}(z)$ was then analyzed to determine the stability and characteristics of oscillatory activity. Two complimentary approaches to represent the behavior of the model were used: the pole-zero plot and the power spectrum. The roots of the denominator (the characteristic equation), $1 + GPe(z) \times STN(z) = 0$, describe the stability, dampening rate, and frequency of the oscillation emerging from the system. These roots are plotted on a pole-zero plot to graphically represent the behavior of the system. The Bode plots were generated by solving $Q_{GPe,STN}(z)$ at particular frequencies and plotting the amplitudes of the resulting complex numbers to estimate the power spectrum of the system.

Results

Using a discrete mean field model of the STN-GPe system, we are able to determine that the 34 Hz parkinsonian oscillation emerges due to interactions between neurons in the STN and GPe resulting in a half-center oscillator. Furthermore, this simplified mean-field

model of the STN-GPe loop is able to predict how changes to parameters in the HM model would affect the 34 Hz oscillation.

34 Hz oscillation emerges from the STN-GPe feedback loop

In the basal ganglia network the STN and GPe constitute an excitatory-inhibitory feedback loop (Albin et al., 1989). To test if the 34 Hz oscillation in the HM model emerges in this loop, a systems-level mean field model of the STN-GPe loop was analyzed.

The pole-zero plot of the simplified mean field STN-GPe system, $Q_{GPe,STN}(z)$, can be used to characterize oscillatory activity. The poles, roots of the denominator of $Q_{GPe,STN}(z)$, and the zeros, the roots of the numerator, of the z-transform are plotted on the complex plane (Figure 10). The poles of the PD state (green), $Q^{PD}_{GPe,STN}(z)$, and healthy state (black), $Q^{H}_{GPe,STN}(z)$, are both plotted on the same graph for comparison. The two systems both contain complex poles, indicating an oscillatory component. Both the healthy and parkinsonian closed-loop systems are stable as all poles are within the unit circle. This indicates that the system's response to a bounded input decays with time. The poles of $Q^{PD}_{GPe,STN}(z)$ are closer to the edge of the unit circle than $Q^{H}_{GPe,STN}(z)$, indicating the parkinsonian system has a slower decay constant and therefore has a more dominant oscillation (Figure 10A inset). As poles move around the circle, away from the real axis, the frequencies of the oscillations increase. Poles of $Q^{PD}_{GPe,STN}(z)$ are further from the real axis than $Q^{H}_{GPe,STN}(z)$, indicating that the PD model oscillates at a slightly higher frequency.

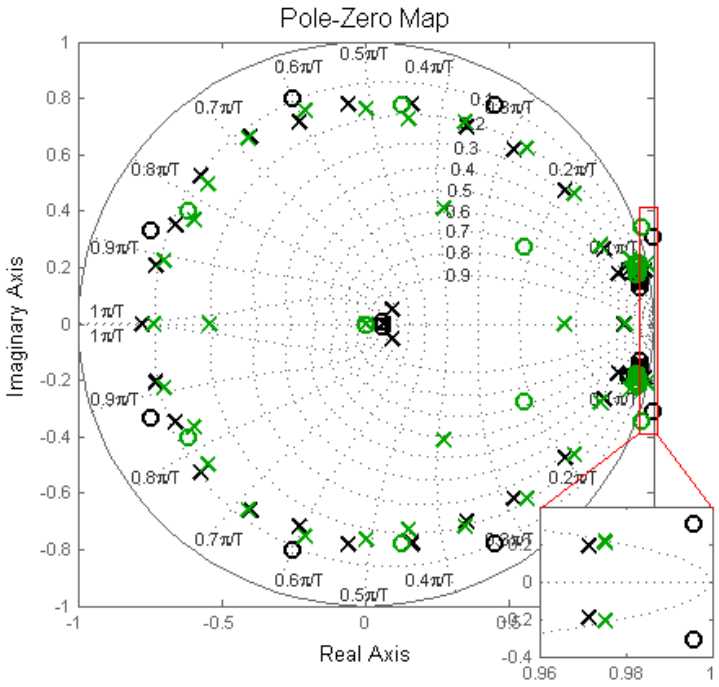

Figure 10. The PZ plot shows the poles and zeroes of the transfer function of a dynamical system. Poles are represented with X's and zeroes are represented with O's. The closed system in the PD state oscillates at a slightly shifted frequency and is less damped than the healthy state system. A pole-zero map showing the poles and zeros of the closed-loop GPe-STN system in the healthy (black) and PD (light) state. The x-axis is the real axis and the y-axis is the imaginary axis. All poles are within the unit circle, indicating they are stable. The poles closest to the edge of the unit circle characterize the oscillation seen in each state. The PD state will exhibit a less dampened oscillation, indicated by the pole being closer to the edge, at a slightly shifted frequency, indicated by the shift along the curved isodampening lines.

The power spectrum of $Q_{GPe,STN}(z)$ is used to visualize how the system will amplify or dampen inputs (Figure 11). The healthy system resonates at 30 Hz, while the parkinsonian system resonates at 34 Hz with a much higher magnitude. This oscillation frequency matches what we see in the HM model. Both the STN and GPe have some resonant properties in the healthy state and PD state, which can be seen in the impulse response curve in Figure 8 as well as the bode plot in Figure 11. However, the two nuclei resonate better with each other in the PD state than in the healthy state (inset Figure 11), resulting in an oscillation of much higher magnitude in the closed-loop system.

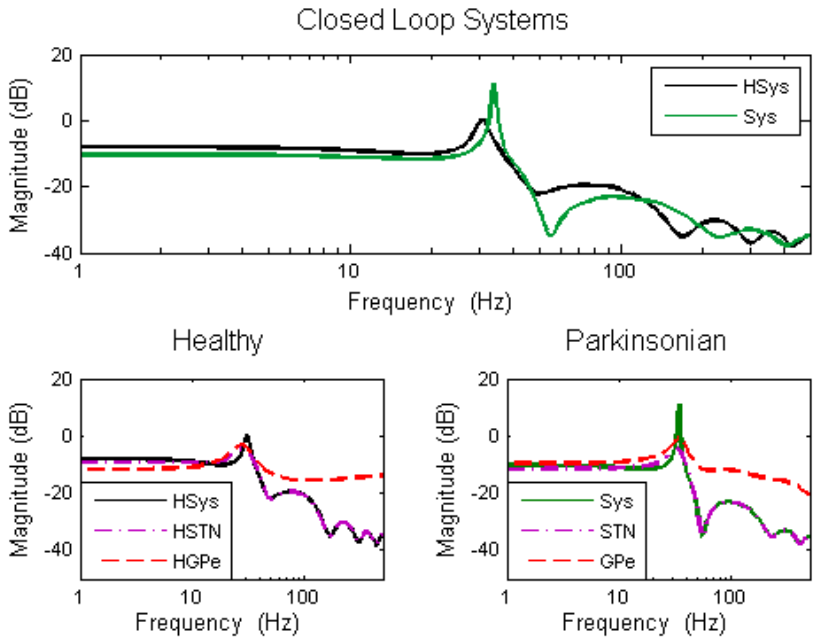

Figure 11. The Parkinsonian closed loop STN-GPe system resonates better than the healthy system due STN and GPe resonating better with each other. Top: The PD system (light/green) resonates at 33 Hz while the healthy system resonates around 28 Hz at about half the magnitude. Bottom left: In the healthy state, STN (dotted/purple) and GPe (dashed/red) do not resonate as well with each other. Bottom right: STN (dotted/purple) and GPe (dashed/red) resonate better with each other in the PD state, resulting in better resonance in the closed system.

Comparing the output of the simplified mean field model and the HM model

In order to validate the simplified mean field model, $Q_{GPe,STN}(z)$, the output was compared to that of the HM model. The simplified model is able to produce outputs similar to the HM model as well as make predictions about how the full network model will behave under altered conditions.

To model the time response of the GPe-STN loop, simulated cortical input similar to that used by the HM model was applied to $Q^{PD}_{GPe,STN}(z)$ and $Q^{H}_{GPe,STN}(z)$. Cortical input was simulated using a pulse train generated by a double stochastic process. The firing rate was modulated by an oscillation with a mean of 16 Hz, and the mean frequency was varied using an Ornstein-Uhlenbeck process with a standard deviation of 1Hz (Figure 12 top). The time series of the output of the STN shows a peak at 34 Hz in the PD state, which is not present in the healthy state (Figure 12 bottom). The power spectrum from the simple closed-loop transfer function of the GPe-STN system was able to reproduce all the important spectral features of the full HM model (Figure 12).

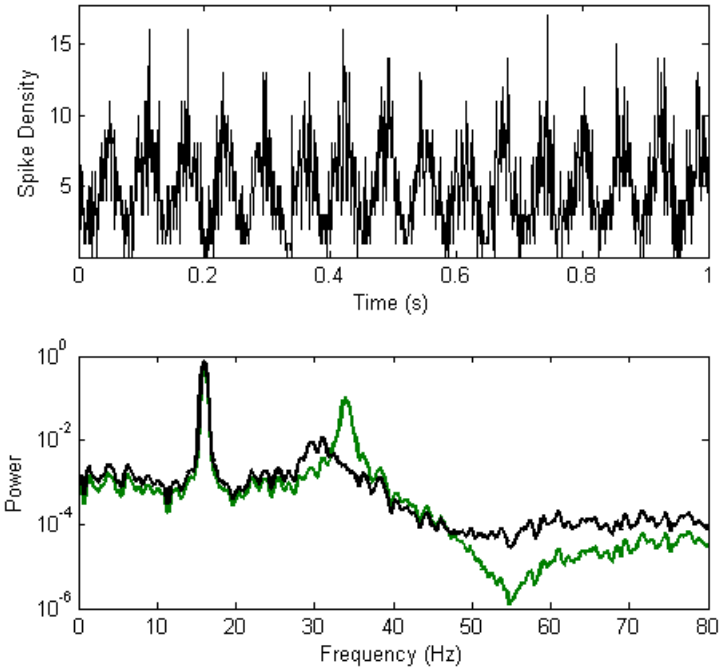

Figure 12. Simulated cortical input used to drive the systems-level GPe-STN mean-field model produces spectral features similar to that seen in the Hahn and McIntyre model. Top: Input to the GPe-STN closed-loop transfer function. An Ornstein-Uhlenbeck process with a mean of 16 Hz was used to simulate cortical input applied in the Hahn and McIntyre model. Bottom: Power spectrum of the healthy GPe-STN system (black) and PD closed-loop GPe-STN system (green/light).

Next, we tested if the simplified model could be used to predict how changes in parameters, such as delays, result in changes in the behavior of the 34 Hz oscillation in the full HM model. First, the delay from GPe to STN was increased from 4 to 7 msec. The simplified mean-field model of the GPe-STN loop, $Q^{PD}_{GPe,STN}(z)$ predicts a decrease in the resonant frequency from 34 Hz to 30 Hz with little effect on the magnitude of the oscillation. The same shift is seen in the Hahn and McIntyre model when the synaptic delay was increased proportionally (Figure 13 left column). Next, the coupling strength between GPe and STN was altered. In the mean-field model, $Q^{PD}_{GPe,STN}(z)$, the gain of GPe was increased. This resulted in an increase in the magnitude of the resonant frequency, but had little effect on the frequency. The same result was seen in the Hahn and McIntyre model when the synaptic strength of STN onto GPe was increased (Figure 13 right column).

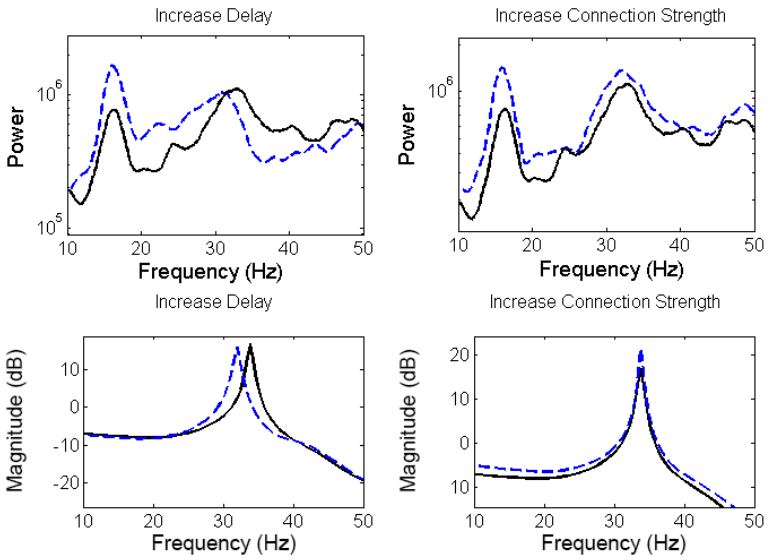

Figure 13. Changes in the closed-loop STN-GPe transfer function model predict changes seen in the Hahn & McIntyre model. Top left: By increasing the delay between GPe and STN from 4 ms to 6 ms, the peak oscillation shifts from 34 Hz to 30 Hz. Bottom left: By similarly changing the delays in the transfer function systems-level model, the resonance shifts in a similar way. Top right: Changing the connection strength between GPe and STN by increasing the maximum conductance increases the power in the oscillation. Bottom right: By increasing the connection strength in the transfer function model, the resonance has a higher magnitude.

Discussion

Here I have presented a method for investigating the emergence of oscillatory activity. This approach involves fitting a systems-level mean field model, consisting of discrete time models and their Z-transforms, to impulse responses. The mean field model was effectively used to explain the origins of an emergent pathological oscillation in the HM model. The analysis of the mean field model indicated that the resonant frequencies of the GPe and STN were better matched in the PD condition, enabling the population to oscillate stronger than in the healthy condition. Cortical drive is still needed for the emergence of the oscillation in the full HM model, but does not need to be oscillatory.

Systems-level mean field models have previously been used to understand the emergence of oscillatory activity in the basal ganglia network; however, the model developed here differs in that it can easily incorporate various time delays between nuclei (Holgado et al., 2010; Pasillas-Lépine, 2013; van Albada et al., 2009; van Albada & Robinson, 2009). Generally, delays between the nuclei have been constrained to be equal, but changes in delays can have large effects on oscillatory activity, making them an important aspect of the system. The advantage of the discrete time mean-field model is that it allows for a simple analytical analysis of the closed-loop behavior of a system with various time delays between the nuclei.

The simple mean field model of the STN-GPe system was able to capture all important spectral features of the full HM model. The hallmark in verifying a model is

testing whether it can make accurate predictions. The mean field model was able to accurately predict how changes in excitability and time delays affect the frequency and amplitude of the pathological oscillation in the HM model.

Simplified mean field models fit to LFP data recorded in response to pre-synaptic stimulation, could be used to help answer the debate about how pathological oscillations emerge in PD. The models can disambiguate between oscillations that emerge from the cortex and are patterned onto the basal ganglia nuclei from oscillations that arise within the basal ganglia network. The mean field model presented here only accounts for the STN-GPe loop; however, other nuclei can be added to make a more complete model if necessary.

Simplified mean-field models may also be used to help explain subject-specific differences in oscillatory activity. The method developed in this paper could help determine why some patients exhibit beta oscillations and others do not, or why the peak beta frequency is different across subjects (Kühn et al., 2009; Tsang et al., 2012). Subject-specific characteristics of pathological oscillations has implications in tuning DBS frequencies to suppress motor signs (Tsang et al., 2012). While it would not be possible to implement an open-loop approach to generate impulse responses in patients, this method could be used in animal models of PD, where pharmacological block of connections is possible (Tachibana et al., 2011). Through understanding the time course of responses in the basal ganglia network, it may be possible to fit transfer functions to the portion of activity recorded from impulse responses in closed-loop associated with the connection of interest. This would enable a similar approach to be used in human subjects

Simplified mean field models may provide an accurate representation of the basal ganglia network beneficial for understanding where and how oscillatory activity emerges, understanding why oscillatory activity is different in some patients, and the design optimal therapies.

Chapter 4

Optimizing Stimulus Frequency to Suppress a Parkinsonian Oscillation in a Computational Model of the Basal Ganglia

The work presented in this chapter is from: Holt AB, Netoff TI (2014). Origins and suppression of oscillations in a computational model of Parkinson's disease. *J Comput Neurosci*, 37(3): 505-521.

Introduction

Efficacy of deep brain stimulation (DBS) depends in part of postoperative tuning of stimulus parameters. Currently, this is done by a clinician using a time-intensive trial-and-error process (Volkmann et al., 2002). The overall goal of this thesis is to develop a systematic approach to tuning stimulation parameters based on patient physiology. Potential stimulus parameters to adjust include amplitude, frequency, waveform, and pattern. The stimulus parameters are tuned to optimally modulate pathological oscillatory activity seen in Parkinson's disease (PD). The focus of this chapter is on testing whether the optimization approach can be used to predict the effects of stimulus frequency on a pathological 34 Hz oscillation seen in a computational model developed by Hahn and McIntyre (described in Chapter 2).

Stimulation frequency affects the therapeutic outcome of DBS for patients with PD. High frequency DBS (>100 Hz) improves motor signs, while there is little to no efficacy at low frequencies (Alberts, Wright, & Feinstein, 1969). Furthermore, frequency effects are patient specific; certain patients show a reduction in motor signs with 50 Hz stimulation, while others do not (Chen et al., 2007; Limousin et al., 1995; Moro et al., 2002; Rizzone et al., 2001; Timmermann et al., 2004; Tsang et al., 2012). This highlights the need an approach to optimize DBS frequencies using patient-specific physiology.

We propose to use patient-specific neuronal responses to stimulation to predict optimal stimulus frequencies to suppress pathological synchrony. This method is based on

the hypothesis that DBS works through chaotic desynchronization of a population oscillation (C. J. Wilson et al., 2011). It is well known in the physics literature that periodic forcing of an oscillating system can induce chaos (Glass & Mackey, 1988). The "chaotic desynchronization" hypothesis suggests that DBS works by inducing a chaotic response in the basal ganglia. This results in differences in how neurons respond to stimulation, which grow exponentially over multiple cycles of stimulation until the system is no longer synchronized, thereby disrupting the pathological "beta oscillation". While there are many hypotheses for how DBS works in PD (Dorval et al., 2008; Warren M. Grill & Dorval II, 2014; Kühn et al., 2009; P. A. Tass, 2003) (explained in detail in chapter 1), "chaotic desynchronization" accounts for the fact that the pattern of stimulation, not just the rate, is important for effective treatment.

The feedback loop from GPe-STN, found to be the origin of the pathological oscillation in the HM model, can be thought of as a periodic oscillator. Specific frequencies of stimulation can either entrain or desynchronize the oscillator (Glass & Mackey, 1988). A simple measure called a phase response curve (PRC) can be used to predict stimulus frequencies which induce a chaotic response in an oscillating system (Nathan W. Schultheiss, Prinz, & Butera, 2012). The PRC characterizes how a subthreshold stimulus alters the period of an oscillation.

PRCs have been used to characterize the response of the interspike interval of periodically firing single cells to stimulation (Lengyel, Kwag, Paulsen, & Dayan, 2005; Netoff et al., 2005; Ota, Omori, & Aonishi, 2009; N. W. Schultheiss et al., 2010; Stiefel,

Gutkin, & Sejnowski, 2008; Torben-Nielsen, Uusisaari, & Stiefel, 2010); however, the oscillation in the HM model emerges from populations of neurons in different nuclei. In this chapter, I first present a method to estimate PRCs from population data. From the population PRC, I next show it is possible to predict how various stimulus frequencies will modulate the 34 Hz oscillation seen in the HM model.

Methods

A phase response curve (PRC) describes how a perturbation, such as a stimulus pulse, changes the phase of an oscillator. In this section, I will describe how the stimulus phase, oscillation amplitude, and change in phase are estimated from the neuronal spike times (considered a point process), and how a PRC is fit to the resulting data. This is a novel method which can be used to estimate PRCs from population recordings.

A PRC was estimated from the GPe population in the HM model (Figure 14). Because beta oscillations were strongest in the non-bursting phase of the spiking (Chapter 2), the spikes from the bursting phase of neurons were removed for all analyses. A subthreshold stimulus was applied to the STN at 2 Hz to avoid interactions between stimuli. The amplitude of stimulation was set to $1/10^{th}$ that value used to represent clinical DBS in the original model. This was done so that stimulation modulated the oscillation without resetting the phase. To estimate the PRC, it is necessary to know the phase at the time of the stimulus as well as the change in phase immediately following the stimulus. Fourier

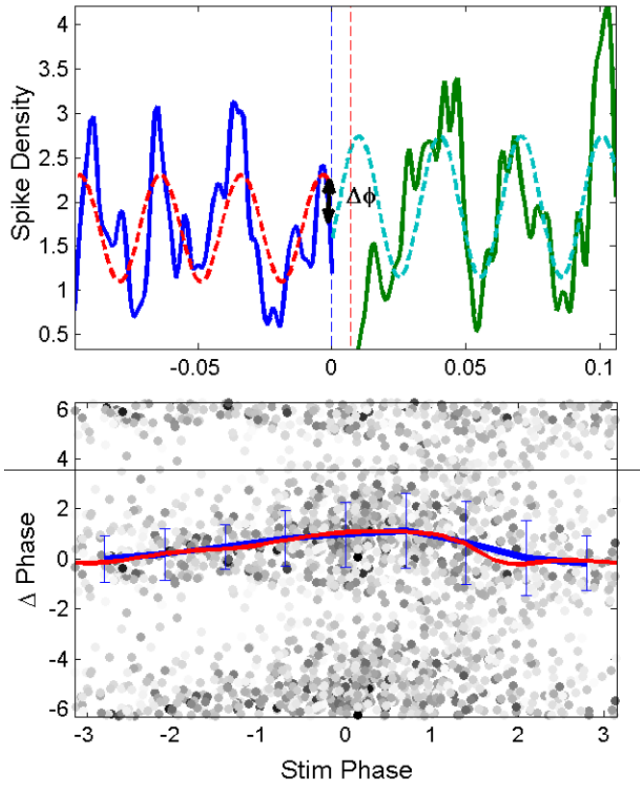

Figure 14. A phase response curve can be estimated from population local-field potential data. Top: Spike density preceding (solid/blue) and following (solid/green) a single stimulus, fit separately with a 34 Hz sine wave (dashed lines). Spikes evoked by the stimulus in a narrow window of time (between vertical dotted lines) are removed from analysis. Bottom: Phase change plotted against phase at stimulus onset with intensity of the dot indicating the amplitude of beta at the time of the stimulus.

coefficients were used to describe the phase and amplitude of the pathological oscillation immediately before and after the time of the stimulus.

Estimating the Phase and Phase Change from Spike Time Data

There are many approaches that can be taken to estimate the instantaneous amplitude and phase of the population oscillation at the time of stimulation from spike time data. One is to generate a PSTH of the spikes across the population and calculate the Fourier coefficient at the oscillation frequency, illustrated at the top of Figure 14. The Fourier coefficient, the Fourier transform at a selected frequency, $\omega = \beta$, can be calculated from the spike density histogram $h(t)$ as follows: $c^{\beta} = \sum_{k=0}^{N} e^{-j\beta s_k}$. The Fourier coefficient c_β is a complex number which can be represented as $c_\beta = Ae^{-j\phi}$, where $A = \sqrt{re(c_\beta)^2 + im(c_\beta)^2}$ is the amplitude of the oscillation and $\phi = \arctan\left(\frac{im(c_\beta)}{re(c_\beta)}\right)$ is the phase. However, the Fourier coefficient can be calculated directly from the spike times without time binning, providing a more accurate estimation of the phase and amplitude.

A Fourier coefficient is fit to a window immediately prior to the stimulus i, $c_i^{prestim}$ and a window immediately after the stimulus $c_i^{poststim}$, excluding any time containing stimulus artifacts. The amplitude and phase of the coefficients represent the amplitude and phase of the oscillation at the time of the stimulus. In the HM model, all spikes in a window 94 msec (approximately 3 oscillations) before and after the stimulus were Fourier transformed at the oscillation frequency, 34 Hz.

Estimating the Phase Response Curve

The phase change can be estimated given the phase of the oscillation estimated from the data preceding and following the stimulus, $\Delta\phi_i^{\beta} = \angle c_i^{prestim} - \angle c_i^{poststim}$.

To fit the PRC, a function is fit to the mean and standard deviation of the phase advance. This is done by dividing the stimuli into phase bins and fitting a wrapped normal distribution to estimate the mean, μ_k, and standard deviation, σ_k , of the phase advance for each bin. The wrapped Gaussian is written as $\frac{1}{\sigma\sqrt{2\pi}} \sum_{k=-\infty}^{\infty} e^{-\frac{(\phi-\phi_\mu+2\pi k)^2}{2\phi_\sigma^2}}$. To estimate the mean phase difference, a weighted average of the phases is used, weighting the changes proportionally to the amplitude of the oscillation at the time of the stimulus $\overline{\Delta\phi^{\beta}} = \frac{1}{\sum\left|c_i^{pre-\beta}\right|}\sum_i \left|c_i^{prestim}\right| \Delta\phi_i^{\beta}$. This is done because the fit is more accurate with a stronger oscillation. The mean phase is the angle of the averaged vector $\phi_\mu = \angle\left(\overline{\Delta\phi^{\beta}}\right)$. The standard deviation of the distribution of phase changes is inversely proportional to the length of the average phase change vector, $R^2 = \frac{1}{\overline{\Delta\phi^{\beta}\Delta\phi^{\beta *}}}$, where the $*$ indicates the complex conjugate of $\overline{\Delta\phi^{\beta}}$. The variance of the distribution, corrected given the number of spikes seen at a particular phase bin N_{bin}, can be calculated, $\phi_\sigma^2 = \ln\left(\frac{N_{bin}-1}{N_{bin}\left(R^2-\frac{1}{N_{bin}}\right)}\right)$. The estimated PRC is simply the mean phase, μ_k, change in phase bin k given the stimulation phase, $PRC(\phi_k) = \mu_k$.

Using the PRC to Predict Effects of Stimulus Frequency on 34 Hz Oscillation

From the PRC, it is possible to determine whether oscillators will phase lock to a periodic stimulus by calculating the Lyapunov Exponent (LE). The LE of the system can be calculated given the PRC and the steady state distribution of phases given the stimulus frequency. If the LE is negative the oscillation is predicted to phase lock to the stimulation, enhancing synchrony; if it is positive the stimulus is predicted to desynchronize the oscillation.

To calculate the LE a transition matrix must be generated, which determines the expected distribution of spike times after a stimulus from the distribution at the time of the stimulus. The transition matrix can be used to predict the steady state distribution of neuronal phases at the (*i*th+1) stimulus given the wrapped Gaussian distribution of phases at the *i*th stimulus.

$$p\left(\phi\middle|\phi_\mu,\phi_\sigma^2\right)=\frac{1}{\sigma\sqrt{2\pi}}\sum_{k=-\infty}^{\infty}e^{-\frac{\left(\phi-\phi_\mu+2\pi k\right)^2}{2\phi_\sigma^2}},$$

where $p\left(\phi\middle|\phi_\mu,\phi_\sigma^2\right)$ is the probability distribution of the phases given a mean phase ϕ_μ and variance ϕ_σ^2 of the Gaussian distribution.

To fit the PRC to the distribution of phases, the mean of the phase advances is used:

$$\mu_{post}=\mu_{pre}-PRC(\phi).$$

This curve fit to the mean phase advances represents the PRC but is a simplification that ignores variability in the cell's ISI (C. J. Wilson et al., 2011). In order to account for variability in the cell's ISI, the variance must be calculated. In Figure 14, the mean of the phase advances and the standard deviation is shown. The mean and variance of the phase after stimulation can be calculated from the PRC immediately before the stimulation.

$$\sigma_{post}^2 = \sigma_{pre}^2 + \frac{\sigma(\phi)ISI}{StimISI}.$$

Where μ_{post} represents the mean phase after stimulation and μ_{pre}, the mean phase before stimulation. The variance added at each stimulus is scaled by the average expected number of stimuli per cycle, $ISI/StimISI$, where *ISI* is the interspike-interval of the spike times, and *StimISI* is the interval between stimuli. Over many stimuli, the distributions will converge to a steady-state probability distribution independent of the starting distribution. The steady-state distribution is the eigenvector, $\lambda(\phi)$, corresponding to the largest eigenvalue of the transition matrix, $p\left(\phi\middle|\phi_\mu, \phi_\sigma^2\right)$ (G. B. Ermentrout, Beverlin, Troyer, & Netoff, 2011).

The Lyapunov exponent (LE) is a measure of the rate of divergence between two neurons firing at almost the same time in response to the stimulus. It is calculated as the average slope of the PRC, weighting each phase by the probability of neurons firing at that phase (C. J. Wilson et al., 2011). The LE can be calculated as:

$$LE = \int_0^1 \lambda(\phi) \log[1 + PRC'(\phi)]\, d\phi,$$

where PRC'(φ) is the slope of the PRC.

The LE was calculated for a range of stimulus frequencies to predict frequency dependent effects of stimulation on the 34 Hz oscillation seen in the HM model. When the LE is greater than zero, we predict that the population oscillation will be disrupted; when the LE is less than zero, the population oscillation is predicted to be enhanced (Figure 15). The most positive LE, predicted to be optimal at disrupting the pathological oscillation, was estimated to be around 85 Hz. Alternatively, stimulation at frequencies close to the natural frequency of the oscillation are predicted to entrain and enhance the oscillation.

Results

Simulations (100 seconds) of the HM model were run using various different frequencies for DBS applied to the STN. At each stimulation frequency the power of the pathological "beta" oscillation (32-38 Hz) was estimated as a ratio to the power in the unmodulated alpha (12-16 Hz) frequency band. Stimulation suppression of the pathological oscillation is defined as conditions when the ratio of beta/alpha power is less than that seen in the DBS off state. While 136 Hz stimulation suppressed the beta oscillation, the maximum suppression actually occurred at 75 Hz. The most effective stimulation frequency was close to that predicted using the LE measured from the PRC (85 Hz). Overall, predictions using the PRC matched quite well with simulations (Figure 15).

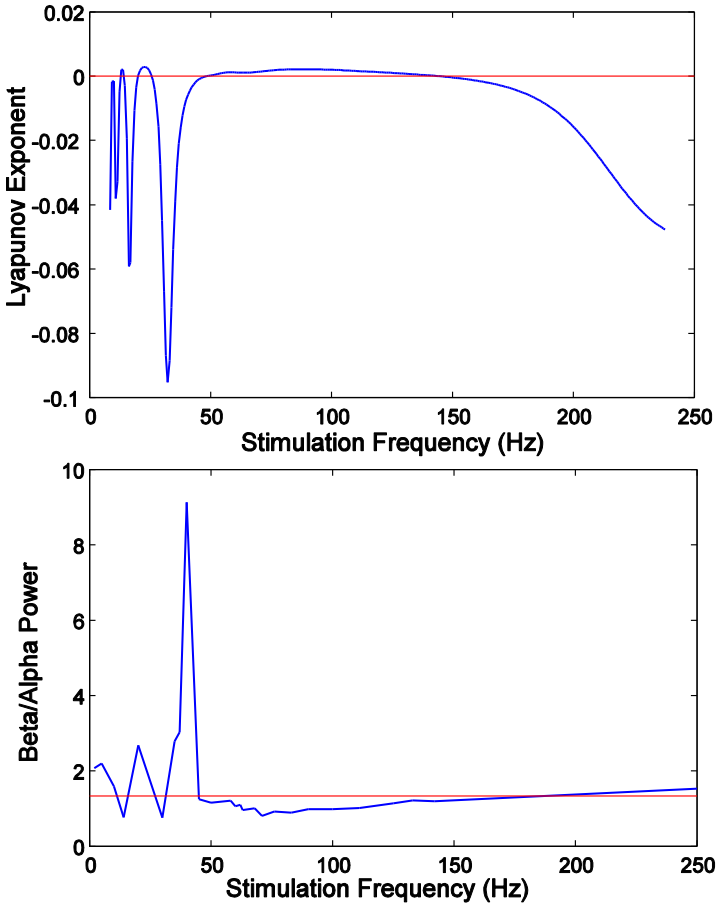

Figure 153. Predicting DBS frequencies to disrupt population oscillations using the Lyapunov exponent. Top: Lyapunov exponent as a function of DBS frequency determined from the phase-response curve. Values above the red line (above zero) are predicted to disrupt oscillations. Bottom: Ratio of beta:alpha power as a function of DBS frequency. Beta power: 32-36 Hz. Alpha power: 12-16 Hz. Red line is beta:alpha power with DBS off.

Discussion

In this chapter, we provide evidence that the phase response curve (PRC) estimated from a pathological oscillation's response to subthreshold DBS-like pulses is a physiological measure that can be used to predict optimal stimulus frequencies. This first required developing a novel method for determining the PRC from neural population data. Previously, PRCs have been applied to the spike timing of individual neurons (Lengyel et al., 2005; Netoff et al., 2005; Ota et al., 2009; N. W. Schultheiss et al., 2010; Stiefel et al., 2008; Torben-Nielsen et al., 2010). To our knowledge, this was the first PRC method developed for application to neuronal populations. Recently, PRCs have been measured from LFP recordings in human parkinsonian patients using the Hilbert Transform (Azodi-Avval & Gharabaghi, 2015). Furthermore, using predictions from the population PRC, we were able to predict how various stimulation frequencies modulate the 34 Hz oscillation seen in the HM model.

Predictions made using the PRC were able to provide valuable information regarding the optimal stimulation frequency to suppress the pathological 34 Hz oscillation in the HM model. Running simulations at various stimulation frequencies, we found that while 136 Hz DBS, the value used in the original paper to represent clinical DBS, suppressed the 34 Hz oscillation, it was not the optimal frequency. Importantly, the optimal frequency predicted from the PRC was close to the frequency which maximally suppressed the pathological oscillation in simulations.

Predictions made using the PRC were close to, but not exactly, commensurate with the findings in the full HM model. This may be because our PRC did not account for interactions between stimulus pulses, and is therefore a first order approximation. There are ways to improve predictions by accounting for higher order effects in the measurement of the PRC (Cui, Canavier, & Butera, 2009). However, we have yet to incorporate them into the estimate of the Lyapunov exponent.

The use of the PRC has the potential to aid clinicians in systematically tuning stimulus frequency based on patient physiology. This approach has several advantages over current trial-and-error methods for tuning stimulus frequencies, even as a first approximation. The first is that it provides a formal process for estimating optimal parameter settings, which may help standardize therapies and reduce tuning time. The method could also be automated and used to update the patient's stimulation parameters over time, if the patient's response to the stimulus changes. Second, a clinician generally changes parameters and monitors a behavioral output, such as tremor. When the tremor disappears, the tuning process stops. However, the final settings may only be at the edge of a window of effective parameters. After the behavioral biomarker is suppressed, it is difficult to further improve the therapy. PRC-based parameter optimization approach may find parameters closer to the center of this effective window, and therefore may produce more reliable and robust patient outcomes. Furthermore, this approach may help identify stimulus parameters outside of the standard parameter regime that may be more effective and/or robust.

With the development of DBS devices which can simultaneously record the neural signal and stimulate (Ryapolova-Webb et al., 2014), optimization using subject-specific PRCs could be a possibility in the near future. To implement this approach, 2 Hz subthreshold stimulation could be applied for a couple minutes to estimate the PRC from neural field recordings. Stimulation frequency could then be set in the neighborhood of the optimal solution predicted from the PRC. To improve predictions, the PRC could be reassessed after applying the optimal stimulus frequency initially predicted for a period of time. By iteratively predicting and testing new stimulus frequencies, an optimal stimulus may be designed within a few minutes

PRC-optimization of stimulus parameters differs from alternative methods, such as those described in Chapter 1 (Feng, Greenwald, Rabitz, Shea-Brown, & Kosut, 2007; Mera et al., 2011; Santaniello et al., 2011), in that it uses responses to subthreshold stimulation to provide an initial prediction about frequency settings. Underlying this method is the explicit assumption that DBS works by inducing chaos in the basal ganglia network, thereby disrupting a pathological oscillation. If this approach is successful in optimizing DBS therapy, it will provide insight into the mechanisms of DBS.

It remains to be determined if specifically targeting the suppression of pathological beta oscillations produces the desired reduction in motor signs of PD. The correlation between beta oscillations and motor signs of PD remains controversial (P. Brown, 2006; Dorval & Grill, 2014; Eusebio & Brown, 2007; Hammond et al., 2007; Kuhn et al., 2006), particularly in the non-human primate model (Devergnas, Pittard, Bliwise, & Wichmann,

2014). In order to predict therapeutic DBS frequencies, the correct biomarker of disease pathology must be used. If beta oscillations are not found to accurately represent behavioral output of the disease, PRC-based parameter optimization can be applied to any pathological oscillatory activity, such tremor, a behavioral oscillation. Additionally, this method can be used to identify stimulus parameters for a number of other diseases such as epilepsy, schizophrenia, or sleep disorders that involve pathological oscillations and are being considered for DBS therapy.

This work provides a method for developing a closed-loop approach to tuning DBS frequency. A closed-loop approach to parameter tuning may help conserve energy, account for changes in motor sign severity, and improve therapeutic outcome. With the development of electrodes that can simultaneously stimulate and record (Ryapolova-Webb et al., 2014), it may be possible to monitor the beta oscillation in each patient and determine the optimal stimulus frequency based on estimated PRCs.

Chapter 5

Phasic Burst Stimulation: A Novel Approach to Optimizing Closed-Loop Deep Brain Stimulation

The work presented in this chapter is from: Holt AB, Wilson D, Shinn M, Moehlis J, Netoff TI. (Under Review). Phasic burst stimulation: a novel closed-loop approach to tuning deep brain stimulation parameters for Parkinson's disease. *PLOS Computational Biology.*

Introduction

This chapter provides evidence for a phase-optimized closed-loop approach to deep brain stimulation (DBS) tested in the Hahn and McIntyre model (HM model). Implantable DBS devices have been developed for research that can simultaneously deliver stimulation while recording the neural response (Ryapolova-Webb et al., 2014). Soon these devices will enable a closed-loop approach to setting stimulation parameters, where the neural signal is used as a feedback signal. A closed-loop tuning algorithm has the potential to reduce time spent in the clinic setting stimulation parameters and may result in more robust and effective tuning. Furthermore, a closed-loop device is capable of continuously tuning parameters to maintain maximal efficacy as motor symptoms fluctuate. In this chapter we propose and test a systematic closed-loop approach termed Phasic Burst Stimulation (PhaBS) to suppress the pathological 34 Hz parkinsonian oscillation in the HM model, described in Chapter 2.

As discussed in detail in Chapter 1, therapeutic DBS has been shown to disrupt pathological oscillations ("beta" oscillations) associated with motor symptoms of PD (Bronte-Stewart et al., 2009; Kuhn et al., 2006; Meissner et al., 2005). This has led to the hypothesis that pathological oscillatory activity, particularly in the beta frequency range (12-35 Hz) could be used as a control signal to determine optimal stimulation parameters (Little et al., 2013; P. A. Tass, 2001, 2003). In support of this hypothesis, approaches designed to disrupt pathological synchrony in the basal ganglia have been effective at improving motor symptoms in patients with PD (Adamchic et al., 2014; Little et al., 2013).

Specifically, closed-loop adaptive stimulation, where high frequency stimulation is turned on when the amplitude of the beta oscillation is high, has been shown to produce greater improvement in akinetic/rigid motor symptoms while using less battery power (Little et al., 2013). This provides evidence for using the beta oscillation as a biomarker for closed-loop stimulation.

While providing high frequency stimulation at times of enhanced beta oscillations is promising, delivering electrical pulses at a specific phase of the ongoing oscillation has the potential to more efficiently and effectively disrupt this activity and provide evidence for a mechanism of action. We know high frequency DBS, >100 Hz, is more effective than low frequency (McConnell, So, Hilliard, Lopomo, & Grill, 2012) or random stimulation (Dorval et al., 2010) at disrupting pathological beta oscillations and improving motor symptoms. This may be because periodic stimulation at certain frequencies results in more stimulus pulses occurring at phases that desynchronize neurons generating the beta oscillation (Cagnan et al., 2013; C. J. Wilson et al., 2011).

The power of a phasic approach can be seen in noise canceling headphones, where external sound waves are cancelled through destructive interference by applying sound waves 180° out of phase. Using this approach to deliver transcranial current stimulation at specific phase alignments resulted in a 50% reduction in resting tremor amplitude on average (Brittain, Probert-Smith, Aziz, & Brown, 2013). Current DBS hardware does not allow for continuous stimulus waveforms, such as sinusoidal inputs. Instead we must use pulsatile electrical stimuli to disrupt oscillations.

In essential tremor patients, it has been shown that delivering pulsatile electrical stimuli to the thalamus triggered off the phase of the tremor, a behavioral oscillation, can modulate the tremor amplitude (P. Brown, 2007; Cagnan et al., 2013). This modulation involved two processes: 1) stimuli delivered at certain phases advanced or delayed the phase of the behavioral oscillation, and 2) through cumulative effects. There has not yet to our knowledge been an experiment that delivers stimulation pulses phase locked to the beta oscillation in the basal ganglia.

Provided a real-time estimation of the phase of a pathological oscillation, it is necessary to develop an algorithm that can determine the optimal phase to deliver the stimulus. In order to identify this optimal phase, we propose to use the phase response curve (PRC). A PRC is a simple measure that describes how the phase of the oscillation is affected by the phase at which the perturbation, such as an external stimulus, is delivered. The PRC can be used to predict conditions in which coupled oscillators, such as periodically firing neurons, will synchronize or desynchronize (Dodla & Wilson, 2013; Nathan W. Schultheiss et al., 2012; D. Wilson & Moehlis, 2014b). In Chapter 4, I demonstrated that a PRC estimated from spike times in the HM model can be used to predict the effects of stimulus frequency on the amplitude of the emergent 34 Hz parkinsonian oscillation. In this chapter I show it is possible to accurately predict the effects of phasic stimulation on the amplitude of the population oscillation in the HM model using the PRC.

While a single pulse delivered at the optimal phase may suppress oscillations with high efficacy, we hypothesize that delivering multiple pulses over a range of phases may be even more effective. Here we propose a phasic burst stimulation protocol (PhaBS) optimized using the PRC. The PRC can be used to determine both the stimulus phase and burst duration to suppress oscillatory activity.

This chapter demonstrates three points: 1) there is a phase dependent effect of stimulation on the parkinsonian oscillation seen in the HM model, 2) the population PRC can be used to predict these phase dependent effects, and 3) a burst of stimulus pulses over a range of phases is more effective at disrupting the oscillation than a single stimulus pulse of the same amplitude. While the focus of this chapter is on designing stimulation to suppress oscillations in this particular computational model, this approach may be generalized to other population oscillations.

Methods

In this paper we test the effects of closed-loop phasic stimulation on the amplitude of a population oscillation in a computational model of the subthalamopallidal network developed by Hahn & McIntyre (Hahn & McIntyre, 2010). To modulate the phase of the beta oscillation rather than resetting the phase, the stimulus amplitude used in this paper was 1/10th of that used in the original paper.

Closed-loop Phasic Stimulation

To test closed-loop phasic stimulation, a real-time estimation of the population phase is necessary to determine when to apply the stimulus.

The phase was estimated using a time-weighted Fourier transform of the spikes times occurring in the previous T = 400 mseconds at frequency, $\omega = 34$Hz:

$$X(f,t) = \sum_{k=1}^{N_S} e^{\frac{(S_k - t)}{\tau}} e^{-2\pi j f S_k}$$

Where S_k is the time of the k^{th}spike of the GPe population, N_S is the number of spikes in GPe from time *t*-400 until the present time, *t*, and $\tau = 3$defines the time constant of the time-weighting of the fit.

The instantaneous population phase at time *t*, $\phi(t)$can be determined as follows:

$$\phi(t) = \angle(\sum_{f=f_{min}}^{f_{max}} X(f,t) e^{2\pi j t f}$$

Where f is the frequency range of the beta oscillation, $f_{min} = 30$ Hz and $f_{max} = 36$ Hz.

Stimulation was applied at a specified delay after the midpoint of the oscillation was detected, i.e. where $\phi(t) = 0$. Simulations at ten different delays were run for 100 seconds each. Depending on the simulation being tested, either a single stimulus pulse or a burst of three equally spaced stimulus pulses were applied. The power of the pathological

beta oscillation (31-36 Hz) compared to the baseline gamma (60-64 Hz) was measured across each cycle.

Phase Response Curve Theory

We use phase response curve (PRC) theory to predict how phasic stimulation locked to an oscillation will desynchronize neurons.

The phase advance, Δ, that occurs from a stimulus applied at phase ϕ is characterized by a function $Z(\phi)$, which can be measured directly from a neuron or population of neurons. When stimulation of an oscillator is periodic, the PRC can be used to predict the phase of the stimulus on the next cycle, $\phi(i+1)$, from the phase on the current cycle $\phi(i)$ via a map, $\phi(i+1) = \phi(i) + Z(\phi(i))$.

The distance in phase between two neurons on the next cycle can be determined from the PRC and their distance, ϵ, on the current cycle $\epsilon_{i+1} = \epsilon_i * (1 + Z(\phi_i))$. If the absolute value of the slope of the map at the phase the stimulus is delivered is greater than one then the distance between the neurons will grow, as shown in Figure 16. Application of the stimulus over several cycles at these phases will cause the neurons' phases to diverge and desynchronize. The optimal stimulus phase to desynchronize the neurons with a single pulse per cycle of the oscillation is the phase at which the map has the steepest positive slope.

A burst of stimulation pulses applied over a range of phases where the slope of the map is greater than one will increase the phase difference between the neurons on the next

cycle over a single pulse, Figure 16 (assumes no interaction between pulses). We hypothesize that burst stimulation will be more effective at desynchronizing a population of neurons than pulsatile stimulation.

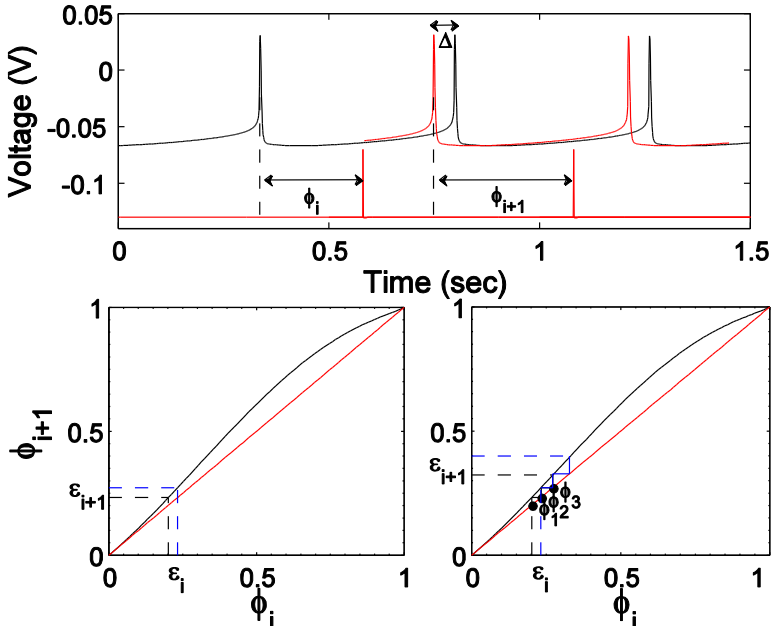

Figure 16. Phase response curves can be used to predict synchronization properties of a periodic stimulus. Top: Current pulses (red/light pulses) can be applied to a periodically firing neuron (black) to estimate PRCs. The phase in the cycle of the neuron at which the stimulus pulse is applied ($\boldsymbol{\phi_i}$), results in a change in the timing of the next action potential (red/light voltage trace), measured as the spike time advance $\boldsymbol{\Delta\phi_i}$. The stimulus will now fall at a different phase $\boldsymbol{\phi_{i+1}}$ on the next cycle. Bottom left: Given the phase of the current stimulus pulse, $\boldsymbol{\phi_i}$, the PRC map (black; PRC added to the red line of identity) can be used to predict the phase on the next cycle ($\boldsymbol{\phi_{i+1}}$). When the slope of the map is greater than one at the phase the stimulus is delivered two neurons (black and blue) starting at some small distance in phase apart ($\boldsymbol{\epsilon}$) become further apart on the next cycle, $\boldsymbol{\epsilon_{i+1} > \epsilon_i}$. Bottom right: Applying a burst of three stimulus pulses at phases where the slope of the PRC is positive results in a greater distance between the two neurons on the next cycle than when a single pulse was used (bottom left).

Estimating the PRC

As discussed in Chapter 4, the PRC was measured from population data in the HM model. Briefly, the Fourier coefficient, c_β, was estimated directly from the spike time data output from the HM model. The Fourier coefficient is a complex number represented as $c_\beta = Ae^{-j\phi}$, where $\phi = \arctan(\frac{im(c_\beta)}{re(c_\beta)}$ is the phase and $A = \sqrt{re(c_\beta)^2 + im(c_\beta)^2}$ is the amplitude of the oscillation. The phase of a Fourier coefficient fit to a window before, $c_i^{prestim}$, and after, $c_i^{poststim}$, the stimulus *i* represents the phase of the oscillation at the time of the stimulus. From the difference in phase angles of the Fourier coefficients at time of stimulus estimated from the spike times prior to the stimulus from the phase angle from the phase angle estimated from the data immediately after, the phase change can be determined $\Delta\phi_i^\beta = \angle c_i^{prestim} - \angle c_i^{poststim}$. The PRC is estimated using a function fit to the mean and standard deviation of the phase advance.

Predicting Phase Dependent Modulation of 34 Hz Oscillation

Using the PRC we are able to predict the effect of phasic stimulation on the amplitude of a population oscillation. The precise phase divergence can be calculated, taking into account the stimulus pulse interval:

$$\epsilon_{i+1} = \epsilon_i(1 + Z_1'(\phi_i))(1 + Z_2'(\phi_i + Z_1(\phi_i) + \gamma))(1 + Z_3'(\phi_i + Z_2(\phi_i) + Z_2(\phi_i + Z_1(\phi_i) + \gamma) + 2\gamma))$$

Where ϵ_{i+1} is the phase difference between two neurons after the three stimuli; ϵ_i is the starting distance between two neurons; γ is the inter-stimulus-interval; and Z_1, Z_2, and Z_3 are the PRCs in response to the 1st, 2nd, and 3rd stimulus respectively. If there is no interaction between the stimuli, the first-order PRC may be used for all three responses. This is illustrated in Figure 18. While this equation solves for effect on synchrony after three stimulus pulses, the equation can be generalized to any number of pulses. For PhaBS predictions, we used a PRC estimated using the application of three subthreshold stimulus pulses.

Results

To test whether stimulation locked to the phase of an oscillation can modulate synchrony in a population oscillation, we test closed-loop phasic stimulation in the HM model. In this model an oscillation centered around 34 Hz emerges in the "parkinsonian state" and response to high frequency stimulation. In order to implement a closed-loop phasic stimulation protocol in the computational model, a time weighted Fourier Transform of the spike trains was used to estimate the instantaneous phase of the population oscillation. This phase estimation was used to trigger the stimulus. A burst of three equally spaced stimuli was more effective at disrupting the population oscillation than a single stimulus pulse. Output from the GPe in the HM model without stimulation, and with phasic stimulation can be seen in Figure 17.

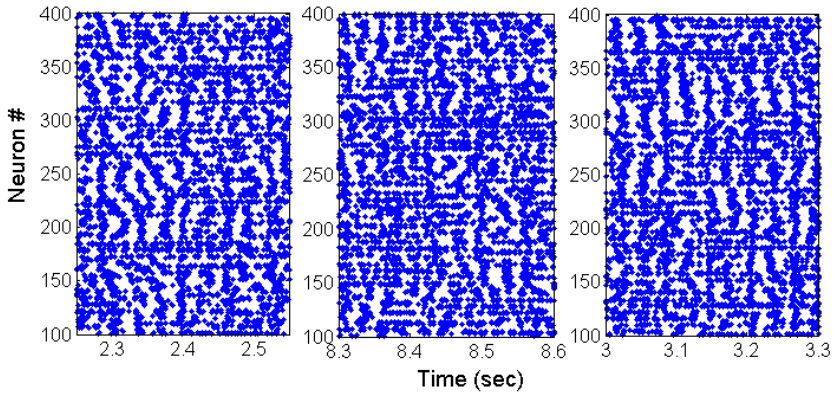

Figure 17. Rastergrams from the external globus pallidus of the Hahn & McIntyre model. Left) No stimulation, Middle) Closed-loop phasic stimulation at a phase of 0.3; Right) Closed-loop phasic stimulation at a phase of 0.7.

Phase dependent modulation of the ratio of beta to gamma amplitude is seen using a single stimulus pulse triggered off of the phase of the oscillation (Figure 18); gamma power did not change with respect to stimulation phase (data not shown). Stimulation applied early in the phase of the oscillation results in a decrease in the 34 Hz oscillation below baseline (DBS Off), while stimulation applied late in the phase of the oscillation enhances the pathological oscillation. Using 1/10th the stimulus amplitude as was used to model clinical DBS in the original paper (Hahn & McIntyre, 2010), a 30% reduction in the beta oscillation is seen at the optimal stimulus phase.

While phase-dependent effects were seen in simulations using a single pulse per cycle, we hypothesize that a burst of stimulus pulses over a range of phases will be more effective at modulating the oscillation (Figure 18). To test this, a burst of three stimulus pulses (5 msec apart) was triggered off of the instantaneous phase in the computational model. As predicted in Figure 16, the effects of the burst stimulation are stronger than the effects of the single pulse stimulation, as seen in the bottom of Figure 18. At certain phases, almost a 50% reduction in the power of the pathological 34 Hz oscillation compared to baseline (DBS off) is seen using a burst of stimulus pulses 1/10th the amplitude of the value used as the clinical value in the original HM model (Hahn & McIntyre, 2010).

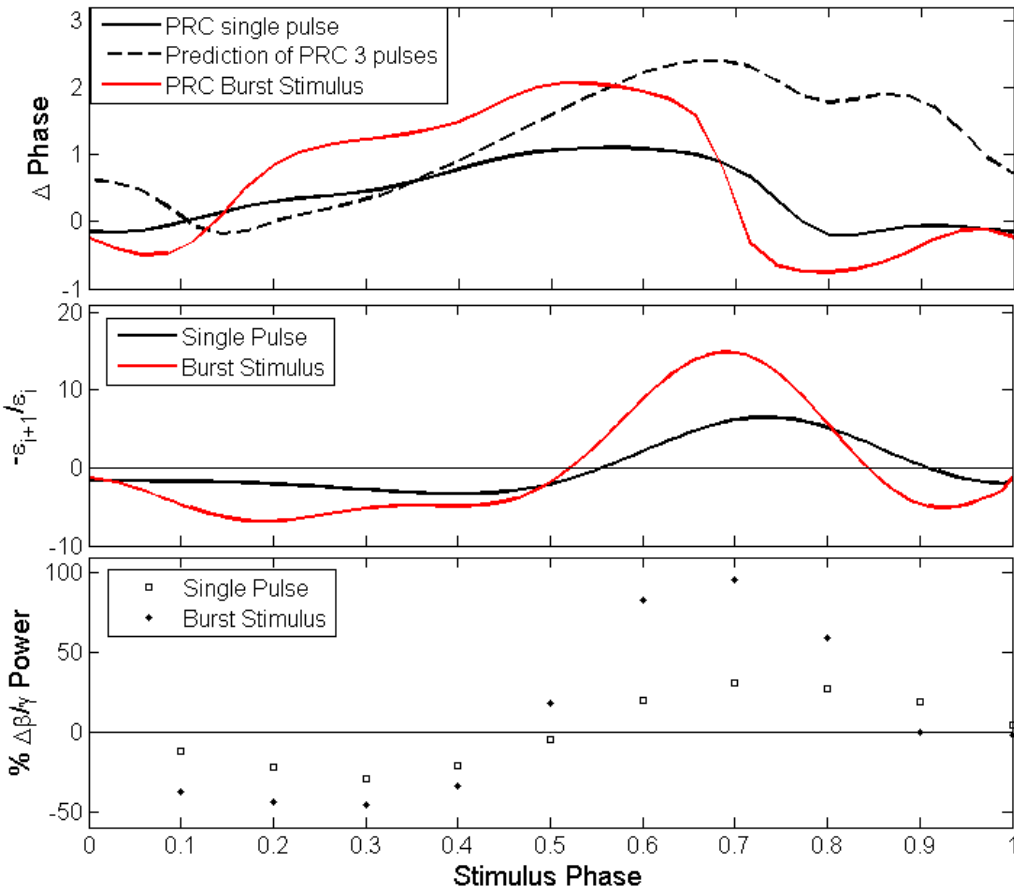

Figure 18. The phase response curve (PRC) can be used to predict the effects of phasic stimulation on the 34 Hz parkinsonian oscillation seen in the HM model. Top: PRCs estimated using, 1 (solid black) and 3 (red/light) stimulus pulses per cycle. Assuming each no interactions between pulses, the PRC for three pulses can be predicted (dotted black) from the single pulse PRC. Indicates there are higher order effects. Middle: Predictions from the single pulse PRC (black) and the 3 stimuli PRC (red). Stimulating at phases where the curve is below zero is predicted to desynchronize the oscillation. Bottom: Ratio of Beta (31-36 Hz) to Gamma (60-64 Hz) amplitude as a function of stimulus phase, shown as a percent change from stimulation off (black line at y=0). Stimulating early in the phase suppresses the 34 Hz oscillation, while stimulating late in the phase enhances it. This matches with predictions made using the PRC (middle). Furthermore, 3 pulses per cycle result in a stronger modulation of the 34 Hz oscillation.

To predict the effects of phasic stimulation, the slope of the PRC is used. The PRC can be estimated by applying a single stimulus pulse at 2 Hz and measuring the change in phase of the oscillation. Assuming no interactions between stimuli, the PRC estimated using a single pulse can be scaled 3x to account for a burst three stimulus pulses per cycle. However, when the PRC was measured by applying three stimulus pulses per cycle at 2 Hz, the results were not just a 3x scaled version of the single pulse PRC (Figure 18 top). This indicates that there are some higher order effects, and that each stimulus pulse within the burst does not result in equal phase effects. For this reason, the PRC estimated using a burst of stimuli was used to predict the effects of PhaBS.

The effects of phasic stimulation and PhaBS on the 34 Hz parkinsonian oscillation seen in the HM model can be predicted using the single pulse PRC and burst pulse PRC respectively (Figure 18). As described above, the slope of the PRC can be used to make predictions. The slope of the PRC is positive when stimuli are applied at phases early in the oscillation, which was found to suppress the pathological oscillation in simulations. Stimulating late in the phase, which enhance the pathological oscillation in simulations, corresponds to phases when the slope of the PRC is negative. Predictions from the PRC, plotted as the negative slope of the PRC ($-Z'(\phi_i)$), are shown in the middle panel of Figure 18. Negative values indicate phases predicted to desynchronize the oscillation. Furthermore, the burst pulse PRC predicts a larger modulation of the oscillation, seen in simulations. These predictions match well with the simulation results showing the % reduction of the pathological oscillation (bottom of Figure 18).

Discussion

Results in this paper provide evidence for a PRC optimized closed-loop approach to DBS to suppress pathological oscillations seen in PD. This approach was tested in a computational model of the subthalamopallidal network exhibiting an emergent population oscillation in the PD state. A novel closed-loop approach to suppress oscillations, termed Phasic Burst Stimulation (PhaBS), for which the PRC is used to optimize both the stimulus phase and burst frequency, was shown to be more effective than applying a single stimulus pulse per oscillation cycle. PhaBS triggered off of the phase of pathological oscillations has the potential to improve efficacy and robustness of DBS. While the focus of this paper has been on a parkinsonian oscillation seen in the PD state of a computational model, the approach can be generalized to disrupt or enhance other oscillatory biomarkers.

Using phasic stimulation to suppress pathological oscillations has previously been proposed and tested (Azodi-Avval & Gharabaghi, 2015; Cagnan et al., 2013; Cagnan et al., 2014; M. Rosenblum & A. Pikovsky, 2004; M. G. Rosenblum & A. S. Pikovsky, 2004). The contribution of this paper is in providing a method for determining the optimal stimulus phase and burst frequency for a burst of stimulus pulses applied over a range of phases. Azodi-Avval and Gharabaghi (Azodi-Avval & Gharabaghi, 2015) suggested using the PRC to optimize stimulation phase, but propose to stimulate at the phase of the oscillation resulting in the largest phase advance and do not test this theory. Here, we suggest that the slope of the PRC is most important in predicting phase dependent

modulation of oscillatory activity, and provide numerical and theoretical evidence for this assertion.

PhaBS was tested in the HM model, and while this is one of the most physiologically realistic computational models of DBS to the subthalamopallidal network, there are limitations. These limitations are discussed in depth in Chapter 2. However, using this model we have successfully demonstrated how a closed-loop phasic approach to DBS may work, and how a PRC estimated empirically from each subject could be used to select the optimal stimulation phase to disrupt pathological oscillations specific to that subject.

We do not suggest that the optimal phases found in this study will be the same as those found in a clinical setting. Instead, we present evidence for a method of using the PRC, estimated empirically from each patient, to select the optimal stimulation phase to disrupt pathological oscillations specific to that subject. The use of the HM model successfully demonstrates how a closed-loop approach to DBS, where stimulation is triggered off the phase of a population oscillation, may work and be systematically optimized.

Advantages of closed-loop DBS

Phasic Burst Stimulation, presented in this paper, is a closed-loop approach to DBS for PD. Currently continuous high frequency stimulation is used to treat motor symptoms of PD. Stimulation parameters for this open-loop approach are pre-programmed by a clinician and are not adjusted based on feedback. While high frequency stimulation is

effective (Sun & Morrell, 2014), it may not be optimal. One limitation of an open-loop approach is that the same level of stimulation is applied regardless of the severity of a patient's motor symptoms reference (Little et al., 2013). A closed-loop approach offers many potential benefits including improved efficacy (Little et al., 2013; Rosin et al., 2011), reduced side effects (Little et al., 2013), increased battery life, and patient-specificity (Sun & Morrell, 2014).

For PhaBS to be effective, an oscillatory biomarker related to symptom severity must be targeted. This oscillation could be a behavioral oscillation, such as tremor, or from a neural signal for non-oscillatory motor symptoms, such as rigidity. An implantable DBS system for PD (Activa PC+S) with sensing, stimulation, and detection features has been developed for investigational use (Ryapolova-Webb et al., 2014), making it possible to use the biomarkers recorded from the neural signal in a clinical setting. Here we test a PhaBS on an oscillation present in the neural signal of the HM model. The oscillation used here resembles parkinsonian beta oscillations in that it emerges in the PD state and is suppressed with high frequency DBS, but occurs at a higher frequency than those commonly seen in patients. While beta oscillations have been associated with motor symptoms of PD (Brittain, Sharott, & Brown, 2014; P. Brown, 2006, 2007; Cagnan et al., 2014; J. Dostrovsky & Bergman, 2004; C. J. Wilson, 2014), more work needs to be done to understand their role as a biomarker for closed-loop DBS.

Tremor provides a behavioral oscillation that can be recorded noninvasively from patients. It has been shown that tremor amplitude is modulated by the phase at which

stimulus pulses are applied in essential tremor patients (Cagnan et al., 2013; Cagnan et al., 2014). In these studies, researchers identified time periods over which multiple stimulus pulses were applied at the same phase of the tremor *post hoc*. Even with only 5-6 consecutive stimuli cumulative effects were observed, which may be enhanced with stimulus pulses applied for more consecutive cycles. The theory presented in this paper suggests that a PRC estimated from the tremor could be used to identify the optimal stimulation phase to suppress tremor, and that a burst of stimulus pulses may be more effective than a single stimulus per cycle.

While PhaBS works by destabilizing the current phase around which neurons synchronize, it may stabilize another phase. Therefore, continued stimulation at the same phase for many cycles may only result in transient destabilization (D. Wilson, Holt, Netoff, & Moehlis, 2015), and instead help sustain the oscillation after many cycles of stimulation. The solution is to turn off stimulation when the amplitude of the oscillation becomes small and turn it back on when the oscillation begins to emerge again.

There have been many approaches, both closed- and open-loop, for optimizing DBS for movement disorders (i.e. reference (Brocker et al., 2013; Carron, Chaillet, Filipchuk, Pasillas-Lépine, & Hammond, 2013; Warren M. Grill & Dorval II, 2014; Little et al., 2013; M. G. Rosenblum & A. S. Pikovsky, 2004; Rosin et al., 2011; Santaniello et al., 2011; P. A. Tass et al., 2012). Adaptive and on-demand closed-loop approaches (i.e. (Little et al., 2013; Rosin et al., 2011; Santaniello et al., 2011) have been used to reduce the amount of stimulation applied and improve efficacy. These approaches are reactive, where open-loop

high frequency stimulation is applied when a physiological event is detected, such as an increase in beta power. Here we are proposing a closed-loop approach where the timing of the stimulus pulses is determined by the physiology.

New open-loop approaches, such as Coordinated Reset (Adamchic et al., 2014; P. A. Tass et al., 2012) and Temporally Optimized Patterned Stimulation (TOPS) (Warren M. Grill & Dorval II, 2014) have also shown promise at improving DBS for PD. Coordinated Reset, a multi-site stimulation approach, aims to disrupt pathological synchrony by entraining sub-populations out of phase with each other thereby disrupting synchrony across the entire population. This approach may evoke plasticity effects resulting in long-lasting reductions in motor symptoms persistent after the stimulation is terminated. Current pulse generators implanted in patients are not capable of implementing this approach. Temporally Optimized Patterned Stimulation (TOPS) (Warren M. Grill & Dorval II, 2014), another open-loop approach, uses an algorithm to optimize the pattern of stimulation using a computational model. This approach depends on the accuracy of the computational model and is not patient-specific.

Phasic Burst Stimulation differs from these approaches by using a principled approach for optimization using a simple model, the PRC, estimated from a patient's physiological recordings generating a patient specific stimulation.

Chapter 6

Using the Phase Response Curve to Predict Entrainment of Single Neurons *in vitro*

The work presented in this chapter is from: Holt AB, Wilson D, Moehlis J, Netoff TI. Periodic forcing of single neurons *in vitro* (Preparing for submission).

Introduction

The goal of this chapter is to provide experimental evidence for using phase response curves (PRCs) to predict how stimulation parameters modulate synchrony in neurons. PRCs have been used to study synchrony in networks of heart cells (Guevara et al., 1986), fireflies (Mirollo & Strogatz, 1990), and networks of model neurons (E. Brown et al., 2004; Hoppensteadt & Izhikevich, 1996; Izhikevich, 2007; Kopell & Ermentrout, 2002; N. W. Schultheiss et al., 2010; Smeal et al., 2010; Wu et al., 2010). Specific to this chapter, PRCs have been used to predict the effects of various stimulation parameters in computational models of neurons (Danzl, Hespanha, & Moehlis, 2009; Dodla & Wilson, 2013; C. J. Wilson et al., 2011). However, there is a need for experimental evidence to determine principles of how stimulus parameters may affect synchrony in single neurons and provide a preliminary framework for parameter optimization.

To provide experimental evidence to support this PRC-optimization of stimulus parameters, I test whether the PRC can be used to predict how periodic and phasic stimulation modulate entrainment in patch clamped neurons. As phase can only be measured at the time of spikes in single cells, neurons which fire periodically must be used. This approach was tested in neurons in the subthalamic nucleus (STN) and substantia nigra pars reticulata (SNr). First, I show that PRCs estimated from neurons in the subthalamic nucleus (STN) can be used to predict how stimulus frequency modulates synchrony, similar to work in Chapter 4. Next, I show that the PRC can be used to predict how phasic stimulation affects the ability of single neurons in the SNr to entrain to an externally applied

oscillation, similar to the work in Chapter 5. These results provide evidence for using PRCs to predict stimulus parameters in neural systems.

PRC theory

Pulse coupled oscillator theory reduces the complex behavior of a periodically firing neuron to a simple input-output phase model, the PRC, that determines how a neuron's next spike time is changed given a stimulus at a particular phase (G. B. Ermentrout & Kopell, 1998; Winfree, 2001). The theory applies to periodic oscillators, and although the periodicity of neuronal firing is not always regular, it can still provide insight into situations when populations are oscillating, as in Parkinson's disease, or when neurons are being driven at high rates, as during a seizure.

The phase advance, $\Delta\phi$, that occurs from a stimulus applied at phase ϕ is characterized by a function $Z(\phi)$, which can be measured directly from a neuron. When stimulation of an oscillator is periodic, the PRC can be used to predict the phase of the stimulus on the next cycle, ϕ_{i+1}, from the phase on the current cycle, ϕ_i, via a map, $\phi_{i+1} = \phi_i + Z(\phi_i)$.

As discussed in Chapter 1, the slope of this map can be used to predict the effects of stimulus parameters on synchrony (stimulus phase predicted to desynchronize neurons when the slope > 1 and synchronize neurons when the slope < 1). In Chapters 5 and 6 I showed that this approach could be used to predict the effects of stimulus frequency and phase on a population oscillation in a computational network model.

PRCs used in Chapters 4 and 5 were estimated from a population of neurons; however, PRCs have been well characterized for single periodically firing cells (Miranda-Domínguez & Netoff, 2013; N. W. Schultheiss et al., 2010). When estimating PRCs from single cells, phase can only be measured at the time of spikes. Therefore, we must infer phase from time between two spikes. Applying a stimulus at a desynchronizing phase will result in the period of the neuron stretching, thereby chaotically desynchronizing the cell from the stimulus over several stimulation cycles. Applying a stimulus at a synchronizing phase will result in entrainment to the stimulus.

Methods

Patch clamp recordings were made from periodically firing neurons in brain slices containing basal ganglia nuclei. PRCs were estimated in one of two ways: 1) using square wave stimulus pulses applied periodically, and 2) using an externally applied sinusoidal current input. The PRCs from individual neurons were used to make predictions about either 1) how stimulus frequency will modulate synchrony, or 2) how phasic stimulation modulates entrainment to the sinusoidal input. All experimental procedures were performed following guidelines from Research Animal Resources of the University of Minnesota and approved by the Institutional Animal Care and Use Committee.

Slice Preparation

Brain slices containing the STN and SNr were prepared using standard methods (Bevan et al., 2002; Farries & Wilson, 2012). Briefly, brain slices were prepared from

Sprague Dawley rats aged 18-25 days. Animals were deeply anesthetized using isoflurane before being perfused transcardially with 10 ml of ice-cold artificial cerebral spinal fluid (aCSF) composed of (in mM): 126 NaCl, 26 $NaHCO_3$, 10 D-glucose, 2.5 KCl, 1.25 NaH_2PO_4, 2 $CaCl_2$, and 2 $MgSO_4$. Following decapitation, the brain was extracted and chilled in aCSF. Sagittal slices 300 μm thick were cut using a Vibratome 3000 (The Vibratome Company) in a high-sucrose cutting solution continuously oxygenated with 95% O_2 and 5% CO_2. Slices were incubated in oxygenated aCSF at room temperature for at least one hour.

Electrophysiology Recording

Slices were placed in a recording chamber perfused with oxygenated aCSF at 36°C and visualized using differential interference contrast optics (Olympus, Center Valley, PA). Recording electrodes 3-8 MΩ were pulled from borosilicate glass (P-97 micropipette puller; Sutter Instrument). Electrodes were backfilled with intracellular fluid containing (in mM): 120 K-gluconate, 10 HEPES, 1 EGTA, 20 KCl, 2 $MgCl_2$, 2 Na_2ATP, and 0.25 Na_3GTP, and then filled with intracellular fluid containing 0.5 μg/ml of gramicidin-D. Gramicidin-D is used for a perforated patch-clamp technique. The antibiotic compound pokes small holes in the cellular membrane for better stability over time than whole-cell patch-clamp.

Data were recorded using a current-clamp amplifier (MultiClamp 700B; Axon Instruments, Molecular Devices, Sunnyvale, CA), sampled at 5 kHz, and collected using the Real-Time eXperimental Interface (RTXI) software publicly available (www.rtxi.org).

Frequency Protocol

Neurons in the STN were patch clamped using perforated-patch to improve stability. The STN is an input nucleus of the basal ganglia network, and was chosen because 1) neurons in the STN intrinsically fire periodically, ideal for the estimation of a PRC, and 2) it is a common stimulation site for DBS in parkinsonian patients.

Stimulation triggered from a Grass amplifier was applied through a bipolar electrode positioned in the internal capsule, which provides synaptic input to the STN. Short-duration (0.02-0.4ms) square-wave current pulses (400μA-1mA) were applied through the bipolar stimulation electrode to elicit an EPSP and significant phase change without inducing an action potential.

Estimating the PRC using a single pulse

To estimate the PRC, $Z(\theta)$, from single STN neurons, stimuli were applied at different phases of the neuron's interspike interval and deviations from the unperturbed period were measured. PRCs were estimated as previously described in (Nabi, Stigen, Moehlis, & Netoff, 2013; Stigen, Danzl, Moehlis, & Netoff, 2009). Briefly, stimulation was applied at 2 Hz to ensure pulses occurred throughout the neuron’s period. Spike time

advances were plotted as a function of the stimulus phase. The PRC is represented as a low-order polynomial function fit to the data.

Making Predictions from the PRC

In order to predict how stimulus frequency affects synchrony, the Lyapunov exponent (LE) was calculated from the PRC of each neuron. This approach was described in detail in Chapter 4. Briefly, the LE is calculated as:

$$LE = \int_0^1 \lambda(\phi) \log[1 + PRC'(\phi)]\, d\phi,$$

where $PRC'(\phi)$ is the slope of the PRC and $\lambda(\phi)$ is the steady-state distribution of spike times. The LE is calculated for a range of stimulus frequencies. When the value is greater than zero, the stimulus frequency is predicted to chaotically desynchronize the neurons over time; when the LE is less than zero, the stimulus frequency is predicted to synchronize the neurons.

Comparing Predictions to Experimental Results

Various stimulus frequencies (0-3x the natural firing rate of the neuron) were applied to the periodically firing neuron (Figure 19). To quantify the synchrony of the spike times of the neuron to the stimulus, peri-stimulus time histograms (PSTHs) were measured. The null-hypothesis used was that the spike times should have no correlation to the stimulation times, and therefore should be uniformly distributed across the interstimulus interval phase. Distance of the measured spike time histogram from flat was used to

characterize whether the neurons synchronized to the stimulus (large distance) or not (small distance). Results were visually compared to predictions made from the PRCs.

Phasic Burst Stimulation Protocol

Neurons in the SNr were patch clamped using perforated-patch. The SNr is a major output nucleus of the basal ganglia, and was chosen because 1) neurons in the SNr intrinsically fire periodically, and 2) the output signal sent from the basal ganglia to the thalamus and on to motor cortex, is arguably the signal that influences motor output.

Estimating the PRC using a continuous input

The PRC can be estimated for a continuous stimulus input to the neuron by deconvolving the stimulus from the phase-shifts (N. W. Schultheiss et al., 2010). Here we use a sine wave stimulus to estimate the PRC, $Z(\theta)$, for each neuron given its spike times. The sinusoidal input was chosen as this was used to entrain the neuron throughout the course of the experiment. First, the stimulus over the cycle can be estimated:

$$Stimulus_i = \cos(2\pi f t + \phi_i)$$

where f is the frequency of the input, t is time, and ϕ_i is the phase of the stimulus. A matrix of stimuli compiled across all cycles is (**Stimulus**), where each row *i* is the stimulus applied prior to spike *i*.

The phase advance at each cycle is measured: $\Delta_i = 1 - \frac{ISI_i}{mean(ISI)}$. $\mathbf{\Delta}$ is a vector of phase advances where each row *i* is the phase advance at spike *i*.

If a PRC is known, the spike advances, **Δ** as a result of the stimulus can be calculated using linear algebra:

$$\boldsymbol{\Delta} = \boldsymbol{Stimlus} * \boldsymbol{Z}$$

Because the PRC is unknown, a least squares solution can be estimated using a pseudoinverse of the stimulus matrix, (**Stimulus**), and the spike advances, **Δ**:

$$\boldsymbol{Z} = \boldsymbol{Stimulus}^{\dagger}\boldsymbol{\Delta}$$

Predicting effects of phasic stimulation of synchrony

Using the PRC we are able to predict the effect of phasic burst stimulation on the ability of the neuron to entrain to an oscillatory input. As shown in Chapter 5, a burst of stimulus pulses applied over a range of phases is more effective at desynchronizing neurons than a single stimulus pulse per cycle of the same amplitude. Furthermore, a burst of stimulus pulses is more robust to errors in the phase estimation.

The phase advance resulting from the burst of stimulus pulses was calculated based on the percentage of the period over which stimulus pulses were applied. This approximation was made by integrating the slope of the PRC over the phase range of the burst, starting at the onset of the burst, ϕ_{start}, to the end of the burst,ϕ_{end}:

$$\hat{Z}'(\phi_{start}) = \int_{\phi_{start}}^{\phi_{end}} Z'(\tau)d\tau$$

When $\hat{Z}'(\phi_{start})$ is negative, the stimulus is expected to enhance entrainment of the neuron to the sine wave input, and when $\hat{Z}'(\phi_{start})$ is positive, the stimulus is expected to decrease the entrainment through chaotic desynchronization. It is important to note that this approximation does not take into account the phase advance induced by each stimulus.

Phasic burst stimulation

To simulate a population oscillation to which a neuron could synchronize, we applied a sinusoidal current (400-1000 pA) through the patch clamp electrode (Figure 21). Prior to applying the stimulus, the natural firing rate of the neuron was measured, and the sine wave was applied at the frequency of the firing rate. To investigate how stimulating at a specific phase affects how well a neuron is able to entrain to the sine wave, a burst of stimulus pulses (100-200 Hz) starting at different phases of the sine wave were applied through the patch clamp electrode in addition to the sine wave. The burst duration lasts for 30% of the sine wave. This results in a different number of stimulus pulses depending on the natural firing rate of the neuron and frequency of the burst stimulus, 4-6 pulses per cycle were used on average. Stimulus pulses were applied starting at nine different phases from 0.1-0.9 of the period of the sine wave. For each phase, at least 30 cycles of phasic stimulation were applied followed by 30 cycles without phasic stimulation. The sequence of stimulation phases was randomized.

Estimating synchrony from experimental data

To estimate entrainment of the neuron to the sine wave, we used a modified normalized entropy measure. Synchrony values, $1 - Entropy$, calculated from spike density histograms were used to compare how well a neuron was entrained to the sine wave for each stimulus phase. $P(i)$ is the probability of a neuron firing in a given phase bin i, where B is the total number of equally spaced bins dividing up the sine wave. To account for the different number of spikes in each trial, an entropy bias correction was used (Roulston, 1999):

$$Entropy_{bias} = \frac{B-1}{2N}$$

The unbiased entropy was normalized by the maximum entropy to get the normalized unbiased entropy value:

$$Entropy = \frac{\sum_{i=1}^{B} P(i) ln P(i) - Entropy_{bias}}{B ln \frac{1}{B}}$$

Standard deviations were calculated for each entropy value (Roulston, 1999):

$$SEM = \sqrt{\frac{1}{N}\sum_{i=1}^{B} (\ln(1 - P(i)) + Entropy)^2 P(i)(1 - P(i))}$$

Statistical comparisons between entropy values were made using the Student's t-test, and p values < 0.05 were considered significant.

Results

Effects of stimulus frequency

The effects of stimulus frequency on entrainment of neurons in the STN to the stimulus was investigated in 6 neurons. In all cells, we see high entrainment when the stimulation frequency matches the natural firing rate of the neuron, as is expected (Figure 19). There is high variability in significant entrainment and desynchronization to the stimulus across cells.

PRCs measured from each cell were used to predict the effects of stimulus frequency on entrainment. The PRCs were extremely noisy; with the phase advance on the order of $1/5^{th}$ the jitter in spike times (Figure 19). Despite the noisy PRCs, predictions from different cells look very different (Figure 20), indicating that the PRC contributed to the prediction and not that we are simply predicting how any oscillator would respond to periodic input. Qualitatively predictions made from the PRC match experimental results pretty well (Figure 20). Peaks in experimental results and predictions often match. While predictions may differ slightly from experimental results, the experimental results for a given cell are qualitatively more similar to predictions from the PRC for that cell than from PRCs from other cells. This supports the hypothesis that PRCs contribute significant information in predicting the entrainment effects of periodic stimulation.

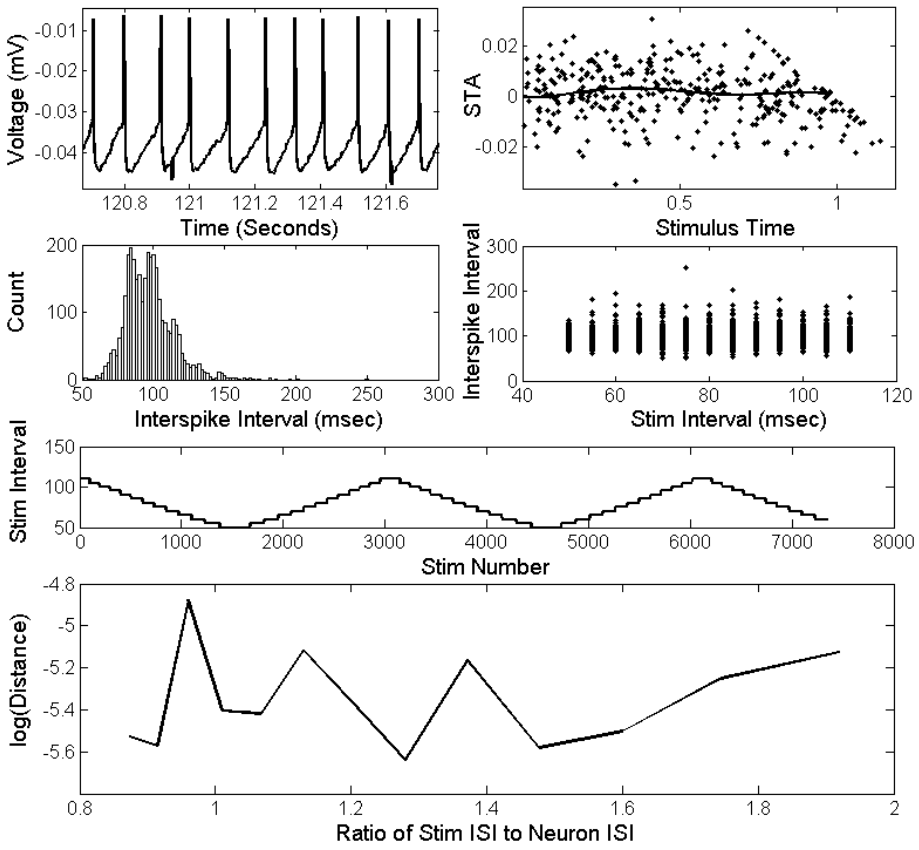

Figure 19. Periodic forcing of a single neuron in the subthalamic nucleus (STN). Top: Voltage trace recording from a patch clamped neuron in the STN. Stimulus pulses, seen in the voltage trace were applied at 2 Hz to measure a phase response curve (right). Row 2: Left, Histogram of interspike intervals shows the cell was firing periodically. Right, Interspike interval as a function of stimulus interval. Row 3: The stimulus frequency applied to the neuron was swept up and down. Bottom: Stimulus frequency modulates entrainment of the neuron to the stimulus. Distance of the peristimulus time histogram from flat was measured as a function of the ratio of the stimulus interval: the neuron interspike interval. Peaks represent entrainment to the stimulus.

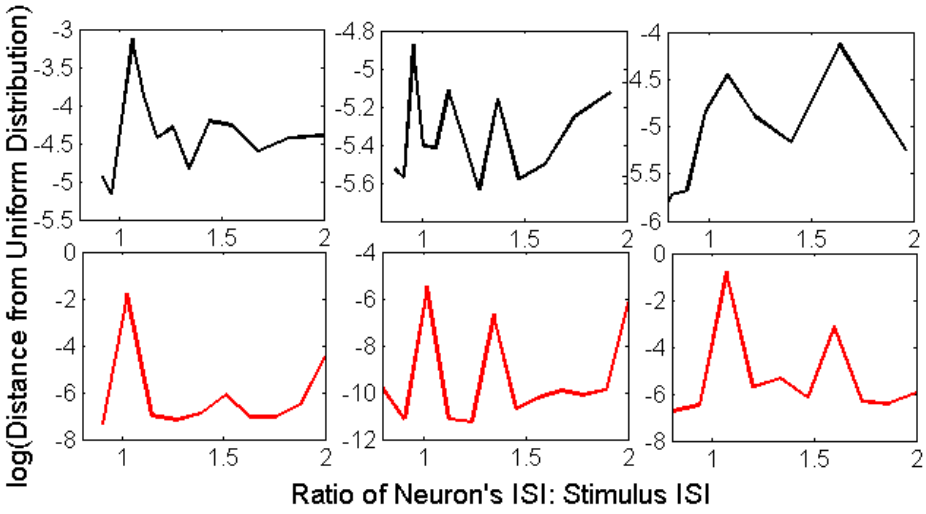

Figure 20. PRCs measured from single cells can be used to predict how stimulation frequency modulates entrainment. Examples from three subthalamic nucleus neurons. Distance of the peristimulus time histogram from flat is plotted as a function of the ratio of the neuron's interstimulus interval to the interstimulus interval. Experimental results (top row/black) match decently with predictions made from the PRCs (bottom row/red). Peaks represent entrainment.

Phasic burst stimulation

The effect of phasic burst stimulation on a neuron's ability to phase lock to an oscillatory input was investigated in 18 substantia nigra pars reticulata (SNr) neurons in the rat brain slice. Significant entrainment to the oscillation was seen in 15 neurons; however, in 3 cells, the amplitude of the oscillation was too low or the neuron was not firing periodically enough to elicit significant entrainment (t-test, $p<0.05$). On top of the oscillatory input, a burst of stimulus pulses at 100-200Hz was applied for 30% of the period, starting at a specified phase of the oscillatory input.

The stimulus phase affected the ability of the neurons to phase lock to the oscillatory input. An example from one neuron is shown in Figure 21. In the absence of burst stimulation, the neuron is somewhat entrained to the oscillation. However, burst stimulation applied at certain phases, such as 0.7, disrupts the ability of the neuron to entrain to the oscillation, while stimulation applied at other phases, such as 0.1, enhances entrainment. Significant modulation of entrainment as a function of burst phase onset was seen in all cells (N=15, ANOVA, $p<0.05$). However, in 2 neurons only an increase in synchronization was observed, indicating that these neurons most likely changed their natural frequency over the duration of the experiment. This results in an inaccurate baseline synchronization measurement. These cells were eliminated from further analysis.

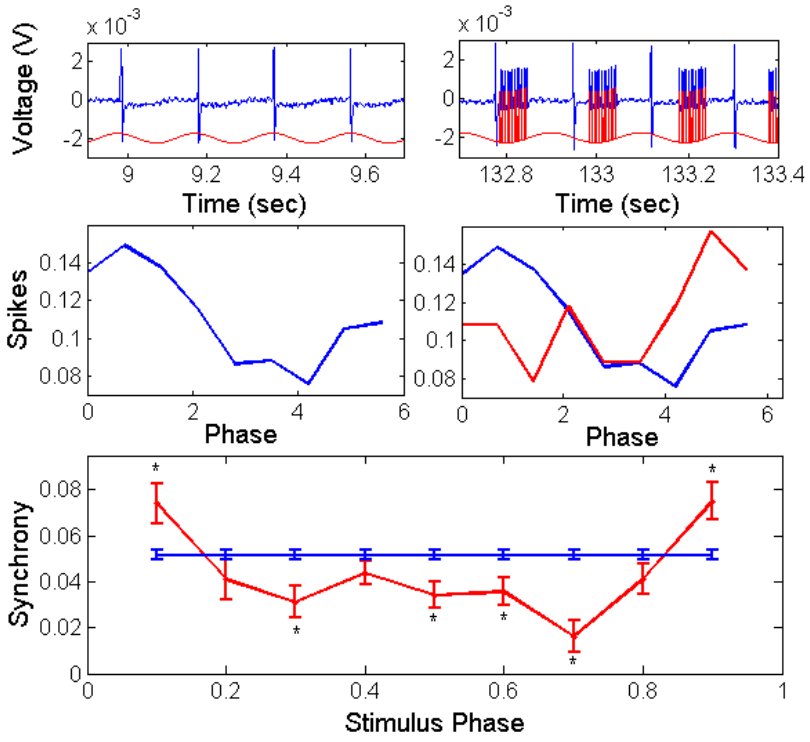

Figure 21. Example from a Substantia nigra pars reticulata cell. Top left: Voltage trace of neuron and oscillatory current input. The neuron is phase locked to the oscillation. Below: spike density histograms showing the number of spikes occurring at each phase of the sine wave. It can be seen that the neuron prefers to fire early in the phase of the oscillatory input. Top right: Oscillatory input and phasic burst stimulation applied at 0.7 of the phase. Burst stimulation at this phase prevents the neuron from locking to the oscillation. Below: spike density histogram provided with the phasic stimulation (red/light) is flatter compared to the oscillatory input alone (blue/dark), indicating that the phasic burst stimulation decreases synchrony. A peaked histogram indicates strong entrainment; a flat histogram indicates low entrainment. Bottom: Summary of synchrony calculated from the spike density histograms. Blue is the the mean and standard deviation estimated from synchrony due to oscillatory input alone (this is same value across all phases), the red line shows the synchrony values as a function of the burst phase onset (StimPhase). Asterisks indicate stimulation significantly modulated entrainment from baseline (* $p < 0.01$)

Next, we test if the PRC can be used to predict the effects of stimulus phase on the ability to enhance or disrupt entrainment to the oscillatory input. The effect of stimulation at each phase was predicted by integrating the slope of the PRC over the phase range for which the stimulus burst was applied. If the average slope of the PRC is negative, burst stimulation is predicted to increase entrainment to the oscillation; if the average slope is positive, stimulation is predicted to disrupt entrainment. The predicted modulation on entrainment was compared to the measured effect of phasic stimulation; examples from 3 neurons are shown in Figure 22. In these examples, it can be seen that the predicted modulation of synchrony, $-\hat{Z}'(\phi_{start})$, matches the measured synchrony quite well. Notice that we plot the negative of the average slope to match the synchrony measure. Peaks in the expected synchrony occur at phases of stimulation where the average slope is the most negative, and low values of synchrony occur when average slope is most positive.

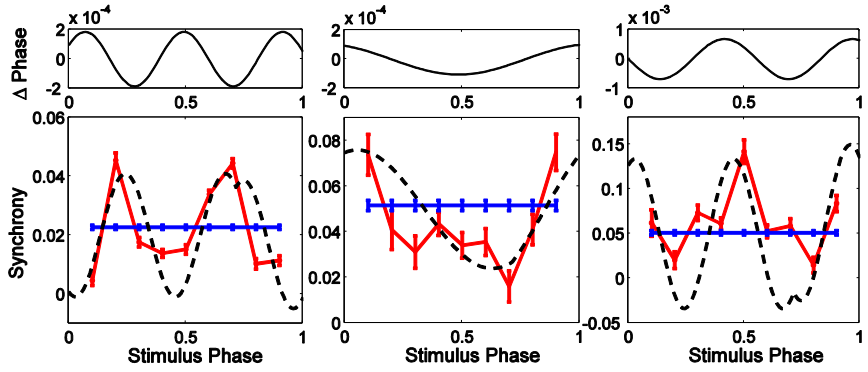

Figure 22. Using phase response curves to predict entrainment of single cells in the substantia nigra pars reticulate to an oscillatory input. Top: Phase response curves (PRCs) for each cell. Bottom: Solid/red: Experimental values of synchrony as a function of the phase of burst stimulation. Blue/horizontal line: Synchrony value with burst stimulation off. Black dotted: Values of synchrony predicted from the PRC of the neuron $-\hat{Z}'(\phi_{start})$.

To summarize our single neuron findings, in 13 of the 15 cells phase dependent stimulation significantly modulated entrainment of the neuron to the applied sine wave. Figure 23 shows the measured synchrony versus the predicted synchrony in all 13 cells. The correlation coefficient (Pearson R value) across all cells is $R=0.53$ (significant at $p < 0.01$), indicating that 28% ($R^2=0.28$) of all variance in synchrony can be explained by the stimulus phase on average.

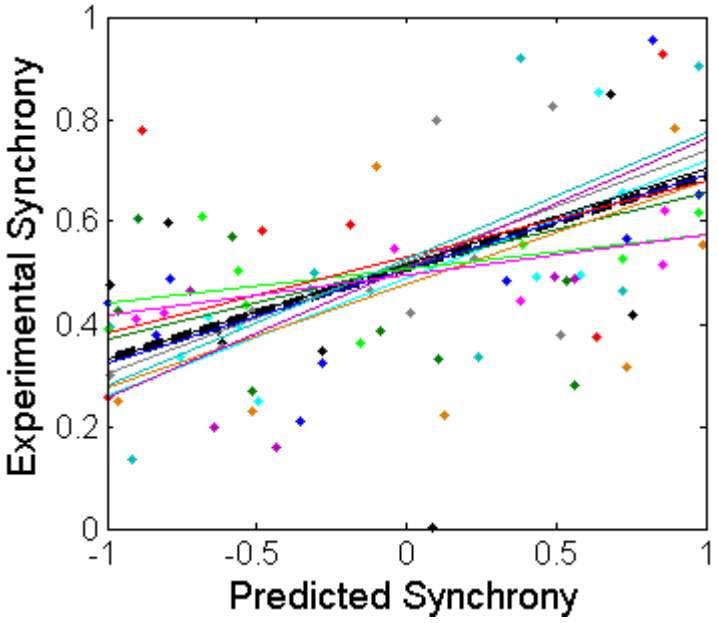

Figure 23. Correlation between experimental and predicted synchrony across all cells. Plot of experimental synchrony compared to predicted synchrony at each stimulus phase for each cell, with a regression line fit to each cell. Each of the 13 cells is represented with a different color. Black dotted line: regression fit using all cells, $R^2 = 0.53$.

Discussion

In this chapter we show that the PRC can be used to predict the effects of periodic forcing on synchrony in single neurons. First, we show that PRCs measured from periodically firing neurons in the STN can be used to predict the effects of stimulus frequency. Next, we show PRCs measured from neurons in the SNr can be used to predict the effects of phasic stimulation on entrainment to an external oscillation. These results provide experimental evidence supporting the use of the PRC to optimize stimulation to either suppress or enhance synchronous neural activity.

PRCs have been used to predict pulsatile stimulus parameters (Dodla & Wilson, 2013) and non-pulsatile stimulus shapes (D. Wilson & Moehlis, 2014a) to disrupt synchronous activity in model neurons. In previous chapters, I have discussed how a PRC estimated from a population oscillation can be used to optimize DBS parameters in a computational model. However, to our knowledge, this is the first example of using the PRC to 1) predict stimulus frequencies which modulate synchrony of a neuron to the stimulus and 2) test stimulus phases that synchronize or desynchronize a neuron from oscillatory input *in vitro*.

While the PRC only accounts for first order effects of stimulation, and the neuron's dynamics may be drifting over time, the PRC estimated prior to the onset of stimulation can be used to predict the effects of periodic stimulation fairly accurately. However, results might be improved by estimating the PRC during the experimental protocol.

This work was motivated by using measured PRCs to predict stimulation parameters which will disrupt pathological synchrony in patients with DBS. For example, in PD we hypothesize that under healthy conditions neurons only synchronize transiently to produce oscillations, while under pathological conditions they synchronize more robustly to produce pathological beta oscillations. As the enhanced beta oscillation emerges in the population, it begins to entrain neurons, strengthening and stabilizing the oscillation. We propose that chaotically desynchronizing neurons through periodic forcing will prevent them from entraining to the oscillatory population input and eventually disrupt the pathological activity.

The results presented here provide experimental evidence for using the PRC to estimate the effects of periodic forcing on synchrony in single neurons. It should be noted that results vary from cell to cell, which fits with previous studies showing a lot of heterogeneity of PRCs within basal ganglia neurons (Farries & Wilson, 2012). This variability suggests that PRCs estimated from single cells may not be not be accurate for predicting stimulation effects on synchrony in a heterogeneous network of neurons. Instead, it may be necessary to estimate the PRC from population data, which will be discussed in Chapter 7.

Chapter 7

Testing Phase Response Curve Optimized Stimulus Waveforms *in vitro*

The work presented in this chapter is from: Wilson D, Holt AB, Netoff TI, Moehlis J. (2015). Optimal entrainment of heterogeneous noisy neurons. *Frontiers in Neuroscience*.

Introduction

Neurostimulation therapies have been effective at modulating various pathological activity, such as deep brain stimulation (DBS) for Parkinson's disease, epilepsy, and other psychiatric disorders (Hardesty & Sackeim, 2007); vagus nerve stimulation for epilepsy (Groves & Brown, 2005); cochlear stimulation to restore hearing (Shepherd & McCreery, 2006); and spinal cord stimulation for chronic pain (Turner, Loeser, Deyo, & Sanders, 2004). The waveform used for these therapies is a charge balanced square wave pulse (Foutz & McIntyre, 2010). While the square wave pulse has been effective, alternative waveforms may offer many advantages, such as decreasing power consumption (Danzl et al., 2009; Foutz & McIntyre, 2010; Jezernik & Morari, 2005; Nabi et al., 2013; D. Wilson & Moehlis, 2014a; Wongsarnpigoon & Grill, 2010), decreasing tissue damage (Lilly, Hughes, Alvord, & Galkin, 1955), decreasing side effects, and increasing charge injection (Sahin & Tie, 2007).

It has been suggested that the phase response curve (PRC) can be used to design optimal stimulus waveforms to synchronize or desynchronize neural activity specific to each patient (Danzl et al., 2009; Nabi et al., 2013; D. Wilson & Moehlis, 2014b). In this chapter I test the efficacy of a PRC-optimized stimulus waveform designed to entrain neurons. The stimulus waveforms, designed by Dr. Jeff Moehlis and Dan Wilson at the University of California Santa Barbara (UCSB), are tested *in vitro* on pyramidal neurons from the CA1 region of the hippocampus. This work focuses on waveforms which promote synchrony, useful for situations such as restoring hearing loss, where a loss in synchrony

is associated with the pathology (Henry & Heinz, 2012; Wang & Manis, 2006). However, the same theory can be used to design waveforms optimized to desynchronize neurons, useful for disrupting pathological synchrony, such as enhanced beta oscillations seen in Parkinson's disease (Kühn et al., 2009).

Methods

To test the efficacy of the PRC-optimized stimulus waveform in a biological system, stimulus waveforms were designed to entrain hippocampal CA1 pyramidal neurons in a brain slice preparation. PRCs were first measured from several pyramidal neurons to estimate the variability in the PRC. Then, optimized stimulus waveforms were designed and applied to neurons using patch clamp recording techniques. All experimental procedures were performed following guidelines from Research Animal Resources of the University of Minnesota and approved by the Institutional Animal Care and Use Committee.

Electrophysiology Recordings

Hippocampal brain slices were prepared from Long Evans rats aged 14-21 days old. Rats were deeply anesthetized using isoflurane before decapitation and extraction of the brain. Following extraction, the brain was chilled in artificial cerebral spinal fluid (aCSF) composed of (in mM): 125 NaCl, 25 $NaHCO_3$, 11 D-glucose, 3 KCl, 1.25 NaH_2PO_4, 2 $CaCl_2$, and 1 $MgCl_2$. Transverse slices of the hippocampus were sectioned 400 μm thick using a Vibratome (The Vibratome Company). Slices were oxygenated with 95%

O_2 and 5% CO_2 and incubated at 37º C for at least one hour. Slices were visualized using differential interference contrast optics (Olympus, Center Valley, PA) while in a chamber with circulating aCSF. Patch-clamp electrodes (3-6 MΩ) were pulled from borosilicate glass (P-97 micropipette puller; Sutter Instrument) and filled with intracellular recording fluid composed of (in mM): 120 K-gluconate, 10 HEPES, 1 EGTA, 20 KCl, 2 $MgCl_2$, 2 Na_2ATP, and 0.25 Na_3GTP. Recordings from whole-cell patch clamped CA1 pyramidal neurons in the hippocampus were made using a current-clamp amplifier (MultiClamp 700B; Axon Instruments, Molecular Devices, Sunnyvale, CA). Data were collected using the Real-Time eXperimental Interface (RTXI) software publicly available (www.rtxi.org) and sampled at 5 kHz.

Estimating PRCs from single neurons

To estimate the PRC, $Z(\theta)$, from CA1 pyramidal neuron, stimuli were applied at different phases of the neuron's interspike interval and deviations from the unperturbed period were measured. PRCs were estimated as previously described in (Nabi et al., 2013; Stigen et al., 2009). Briefly, short-duration (0.02-0.4ms) current pulses (300-400pA) were injected into the periodically firing neuron through the patch clamp electrode to elicit a significant phase change without inducing an action potential. Each data point was obtained by stimulating at a random phase θ, and measuring the change in spike time with the resulting value equal to $\Delta\theta/Q$ where $\Delta\theta$ is the change in phase and Q is the charge injected by the pulse. Constant drive or an oscillatory input to these neurons causes them to fire

periodically. To compensate for drift in the neuron's natural firing rate over the experiment, a proportional-integral (PI) controller was used to adjust the current applied to the neuron slowly to maintain the neuron at a target firing rate (Miranda-Dominguez, Gonia, & Netoff, 2010). Spike advances as a function of the stimulus phase were fit with a low order polynomial constrained to zero at the beginning and end of the phase by minimizing least squares error (Matlab's fminsearch). Examples of PRCs are shown in Figure 24. We note that the waveform optimization requires the mean phase advance estimated by the PRC to be within the envelope, but the phase advance on any particular cycle can be outside the envelope, due to noise.

Stimulus waveform

PRCs from ten CA1 pyramidal cells, collected for previous experiments under similar conditions described here (Miranda-Domínguez & Netoff, 2013; Nabi et al., 2013), were used to design optimal stimulus waveforms.

The approach for designing the optimal waveform was developed by Dan Wilson and Dr. Jeff Moehlis at the UCSB and has been explained in detail (D. Wilson et al., 2015; D. Wilson & Moehlis, 2014a). Briefly, the approach involves considering a heterogeneous group of neural oscillators. A periodically firing neuron, the oscillator, can be defined using a phase response model:

$$\frac{d\theta}{dt} = \omega + Z(\theta)u(t)$$

Where ω is the natural frequency of the neuron, $Z(\theta)$ is the neuron's infinitesimal PRC, and $u(t)$ is the control stimulus.

The optimal control stimulus is found using a Hamilton-Jacobi Bellman approach (Kirk, 2004; D. Wilson & Moehlis, 2014a). The stimulus waveform optimized to minimize energy and maximize entrainment will minimize the cost function:

$$J[u(t)] = \alpha \int_0^T [u(t)]^2 dt - \beta \int_0^T Z'\big(\theta(t)\big)u(t)dt,$$

where α and β are constants to weight the importance of the input energy term and Lyapunov exponent term respectively. The synchronization properties of the stimulus are based on the Lyapunov exponent calculated from the PRC. To maximize entrainment to the stimulus, the Lyapunov exponent is minimized from time 0 to time *T*. Essentially this approach involves applying a positive stimulus at phases where the PRC, $Z'(\theta)$, is predicted to be negative, resulting in a negative Lyapunov exponent. This leads to oscillating neurons exponentially converging. This equation only requires knowledge of the system's PRC.

The significant advancement in the optimization of stimulus waveforms presented in this chapter over previously designed waveforms (Moehlis, Nabi, & Danzl, 2010; Nabi et al., 2013; D. Wilson & Moehlis, 2014b) is that they are developed for an envelope of PRCs instead of for a single neuron. This approach was taken because a distribution of PRCs was seen within a population, and therefore the stimulus waveform is optimized

based on the distribution. Instead of having to optimize stimulus waveforms for each individual PRC, this allows us to optimize waveforms for a heterogeneous population of neurons, provided the PRC from the individual neuron fits within the envelope of distributions used for the optimization.

The PRCs used for optimization had slightly different shapes, so four envelopes, together incorporating all shapes, and their corresponding stimulus waveforms were calculated; shown in Figure 24. We assume that we have direct control over the natural frequency of the neuron, ω, with the PI controller. Each optimal waveform was defined by an envelope containing all PRCs within that group of cells. For each envelope, one optimal and two suboptimal stimulus waveforms with equal energy were generated. The suboptimal waveforms were created by either 1) inverting and time-shifting the optimal waveform, or 2) by stretching out the positive portion of the optimal waveform and renormalizing to preserve the total energy.

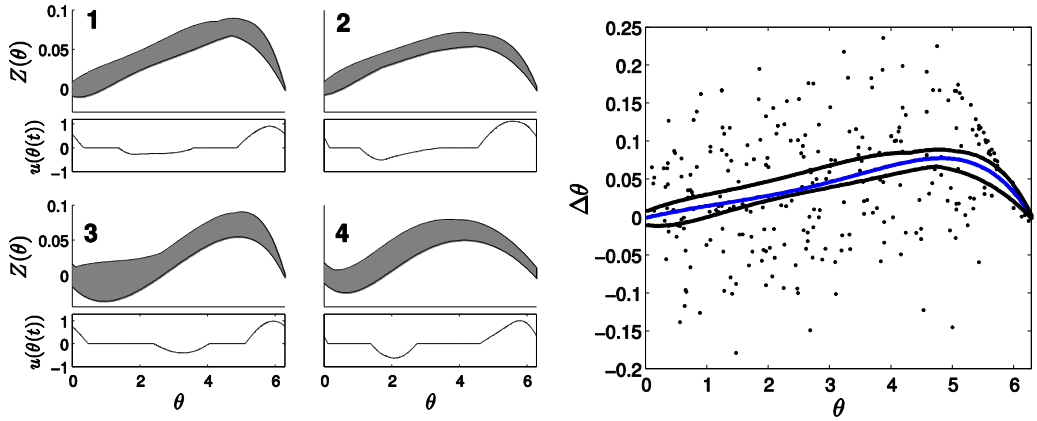

Figure 24. Four envelopes with separate optimal waveforms were used to determine which stimuli to use on a given cell. The left panels show envelopes in gray with corresponding optimal stimulus waveforms directly below. On the right panel, a PRC (blue/middle) calculated from individual measurements of $\boldsymbol{\Delta\theta/Q}$ (dots) from a CA1 pyramidal neuron fits within the black curves of envelope 1.

Applying stimulus waveforms in vitro

For *in vitro* experiments, whole-cell patch clamp recordings were made from CA1 pyramidal neurons. For each cell, Matlab was used to determine which envelopes the measured PRC fit within. Once an envelope was determined, the 3 stimulus waveforms associated with that envelope (1 optimal and 2 suboptimal) were applied as current through the patch clamp electrode. For some cells, PRCs fit within multiple envelopes; in this case stimulus waveforms associated with each relevant envelope were tested if possible. Each of the three waveforms were applied continuously for at least 30 seconds to a few minutes. The stimulus waveform was applied at the target frequency of the neuron, set at 10 Hz using the PI controller, for the duration of the experiment. The peak-to-peak amplitude of the waveform was less than 1 nA. The sequence in which the waveforms were applied was selected at random. In most cases the PI controller was used to hold the neuron at the target firing while the stimulus waveforms were being applied. However, in a few cases the PI controller was turned off to ensure it was not affecting the synchrony measures. The amplitude of stimulation was chosen so that the stimulus waveform could be seen in the baseline membrane potential without eliciting a spike. I was blinded to which stimulus was optimal until after completion and analysis of all experiments.

Entropy estimation

Entropy values calculated from spike density histograms were used to compare how well a stimulus entrained the neuron Figure 25. Data were analyzed using Matlab. For

entropy calculations, phases were subdivided into *B* equally spaced bins and *P(i)* was used to denote the probability that a spike occurs in bin *i*. An entropy bias term was used to correct for the different number of spikes in each trial (Roulston, 1999):

$$Entropy_{bias} = \frac{B-1}{2N}$$

Where *N* is the total number of spikes. To calculate the unbiased normalized entropy measure from each spike density histogram, the entropy, accounting for the bias, was normalized by the maximum possible entropy:

$$Entropy = \frac{\sum_{i=1}^{B} P(i) ln P(i) - Entropy_{bias}}{B ln \frac{1}{B}}$$

The standard error of the entropy was estimated as follows (Roulston, 1999):

$$SEM = \sqrt{\frac{1}{N}\sum_{i=1}^{B} (\ln(1-P(i)) + Entropy)^2 P(i)(1-P(i))}$$

Statistical comparisons between entropy values were made using the Student's t-test, and *p* values < 0.05 were considered significant.

Results

Stimulus waveforms were applied to ten CA1 pyramidal neurons. An example cell can be seen in Figure 25. The PRC from this example neuron best fit within envelope 3. For each stimulus the coefficient of variation of the interspike intervals, and the entropy of

the spike times with respect to the phase of the stimulus waveform was measured. In this cell, the optimal stimulus waveform resulted in the lowest coefficient of variation in the interspike intervals, indicating that the cell fired more periodically with the optimal waveform than with the suboptimal waveforms. Furthermore, the optimal stimulus waveform had the lowest entropy of spike times with respect to the stimulus phase, indicating that the neurons phase locked to the optimal stimulus better than the suboptimal stimulus waveforms.

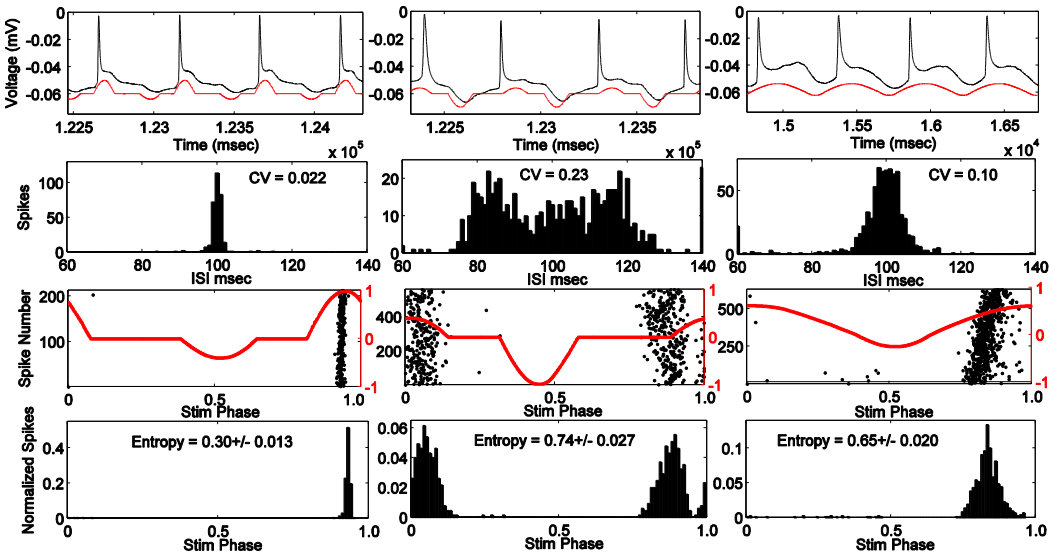

Figure 25. Example cell using envelope 3. Response to optimal stimulus is plotted in left column and two suboptimal stimuli applied in right columns. Top Row: voltage trace (black) and applied stimulus waveform (red/light). Second row: Histograms of inter-spike-intervals. Coefficient of variation (CV) values are indicated. Third row: phase of the stimulus at each action potential (black dots) with stimulus waveform (red/light). Bottom row: spike density histogram with respect to stimulus phase. Entropy values +/- SEM are indicated.

Across all cells significantly affected by the stimulus waveforms, the optimal stimulus was the most effective at entraining neurons (Figure 26). Stimuli from envelope 1 were applied to seven cells. For six out of the seven cells, the entropy values for the optimal waveform were significantly lower ($p<0.05$) than the non-optimal waveforms, as tested with a Student's T-test. For cell number 1, the entropy remained high across all stimuli without any noticeable effect from any of the waveforms, perhaps because the stimulus amplitude was too low. Stimuli from envelope 2 were applied to one cell, from envelope 3 were applied to four cells, and from envelope 4 were applied to one cell. For each of these cells, the entropy values were significantly lower for the optimal waveform than the suboptimal waveforms. We conclude that the PRC-optimized stimulus waveform was the most effective at entraining the neurons to the stimulus. In three cells experiments were done without the PI controller to control the firing rate to confirm that the PI controller was not affecting the findings; the results in these cells were consistent with the experiments done with the PI controller.

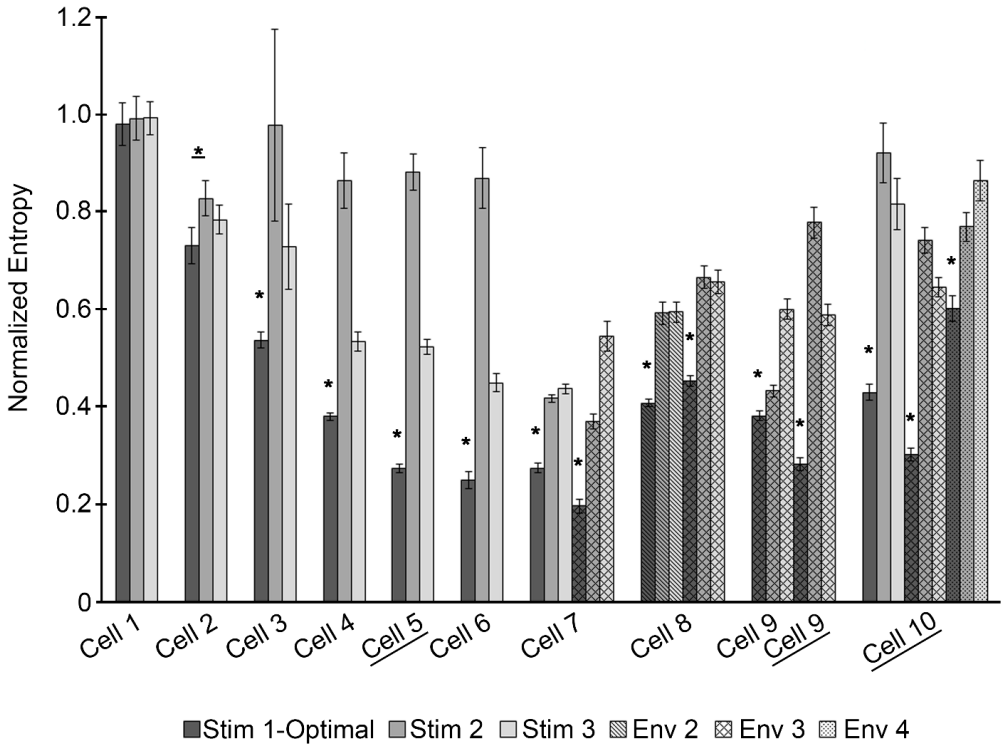

Figure 26. The PRC-optimized stimulus waveform is significantly better at entraining neurons to the stimulus across cells. Entropy values for each stimulus applied are shown for 10 cells. Some cells had stimuli from more than one envelope applied. Envelopes are indicated by different patterns, with envelope 1 being the solid fill. For each envelope, three stimuli were applied: the waveform optimized for entraining the neuron (dark gray) and two sub-optimal waveforms (gray and white). Certain cells did not have the PI controller on to control the firing rate of the neuron (underlined). Significant differences between the optimal stimulus waveform and the alternative waveforms at $p < 0.05$ are indicated by *.

Discussion

In this chapter I have shown that a PRC-optimized stimulus waveform can be used to entrain neurons *in vitro* more effectively than alternative waveforms. The optimal waveform, designed by collaborators at UCSB, was determined using PRCs characteristic of the CA1 pyramidal population in brain slice. The Lyapunov exponent (LE), calculated using the slope of the PRC, determines the synchronization properties of a stimulus. A stimulus associated with a positive LE will desynchronize an oscillation, while a stimulus associated with a negative LE will synchronize an oscillation. A cost function that takes the slope of the PRC into account can be used to design a stimulus waveform which minimizes the Lyapunov exponent, thereby synchronizing neurons.

It is difficult to experimentally prove that a given stimulus is truly optimal. However, the experimental evidence suggests that the PRC-optimized waveforms are probably at least close to optimal. Simulations *in silico*, done by collaborators at UCSB, demonstrated that the optimized stimulus resulted in better entrainment than other stimuli (D. Wilson et al., 2015). Furthermore, the experimental results presented here show that this optimization method can be used to entrain CA1 pyramidal neurons from the hippocampal brain slice better than alternative waveforms with the same power. These waveforms are robust, in that deviations from the exact PRCs used for optimization does not cause much degradation in performance.

There are a number of ways the optimization approach could be improved. First, the natural firing rate of the periodically firing neurons likely drifts over the course of the experiment, changing the shape of the PRC (Thounaojam, Cui, Norman, Butera, & Canavier, 2014). While we used a PI controller to keep the firing rate of the neuron constant, explicitly accounting for the uncertainty in the shape of the PRC over time could help improve entrainment over the duration of the experiment. Second, the optimization approach only considered entrainment and energy minimization. There are other important constraints, such as requiring a charge balanced stimuli (Nabi et al., 2013) and limiting harmful Faradaic reactions (D. Wilson & Moehlis, 2014b), that could be included into the cost function.

The evidence in this chapter suggests that PRCs could be used to design stimulus waveforms optimal at synchronizing neurons. This could be used to design stimulus waveforms to target pathologies associated with a loss of synchrony, such as in hearing loss (Shepherd & McCreery, 2006). Furthermore, while the approach presented here aimed to entrain neurons, the same theory can be applied to optimally desynchronize neurons by using a cost function that maximizes instead of minimizes the LE (D. Wilson & Moehlis, 2014b). A PRC-optimized stimulus waveform designed to chaotically desynchronize neurons could be used to more efficiently disrupt pathological oscillations seen in PD. With an optimal stimulation waveform tailored to the dynamics of the system's response to the stimulus, entrainment or desynchronization of oscillators may be done with greater

reliability and less energy than other stimulus waveforms, such as periodic pulsing or sine wave stimulation.

Chapter 8

Estimating Phase Response Curves from Local Field Potential Recordings in Non-Human Primates

Introduction

It has recently been shown that PRCs can be measured from field recordings in parkinsonian patients intraoperatively (Azodi-Avval & Gharabaghi, 2015). Here I show it is possible to measure PRCs from local field potential recordings (LFP) from chronically implanted leads in the non-human primate (NHP). Existence of a PRC suggests that optimal stimulus parameters can be predicted using the PRC and that there are phase dependent effects. PRCs estimated from spike data have been used to predict optimal stimulus parameters in previous chapters. While it is possible to collect single unit recordings intraoperatively from parkinsonian patients undergoing DBS surgery, electrodes that sense neural field activity, such as Medtronic's PC+S device are more likely to provide long-term recording approaches (Ryapolova-Webb et al., 2014). Furthermore, single cells in the basal ganglia exhibit bursts of activity at the beta frequency (Figure 2), instead of firing periodically at the beta frequency (necessary for approaches presented in Chapter 4).

To measure PRCs in NHPs in this chapter, I investigate how a subthreshold stimulus pulse affects the phase of an oscillation in the beta frequency range seen in the LFP recordings of both the naïve and parkinsonian NHP.

Methods

All experiments and data analyzed in this chapter were performed and collected by Dr. Luke Johnson in Dr. Jerrold Vitek's laboratory and Dr. Allison Connolly in the

laboratory of Dr. Matthew Johnson. Recordings were made in naïve and parkinsonian NHPs. All animal work was approved by the Institutional Animal Care and Use Committee and conducted in accordance with the National Institutes of Health policy on the humane care and use of laboratory animals.

LFP Recordings

Naïve NHP

Two eight contact DBS leads were implanted in the naïve, female Rhesus monkey (*Macaca mulatta*, 5.7 kg, 7.5 years). The STN and GP were targeted with each electrode respectively. Bipolar stimulation was applied through contacts 2 and 3 (100 μs) of the lead targeting the STN. Here we look at the first order PRC, which assumes no interaction between stimuli. To avoid interactions between stimulus pulses, 2 Hz stimulation was used. After testing a range of amplitudes (100-500 μA), 300 μA stimulation was selected because it induced a significant phase change without phase resetting.

A PRC looks at how an oscillation is modulated depending on the phase of the stimulus. In PD, the emergence of pathological oscillations in the beta frequency range (12-35 Hz) is thought to lead to motor symptoms. However, beta oscillations play a role in normal motor function and have been seen in the naïve/healthy NHP (Connolly et al., 2015; Davis, Tomlinson, & Morgan, 2012; Feingold, Gibson, DePasquale, & Graybiel, 2015). The goal of this chapter is to test methods to estimate PRCs from LFP recordings in NHPs. Therefore, the only requirement is that an oscillation be present in the LFP recording. The

approach was first tested using recordings from a healthy NHP showing a strong beta oscillation. The power spectrum of a 60 second recording shows the presence of an oscillation centered around 12.35 Hz (Figure 27).

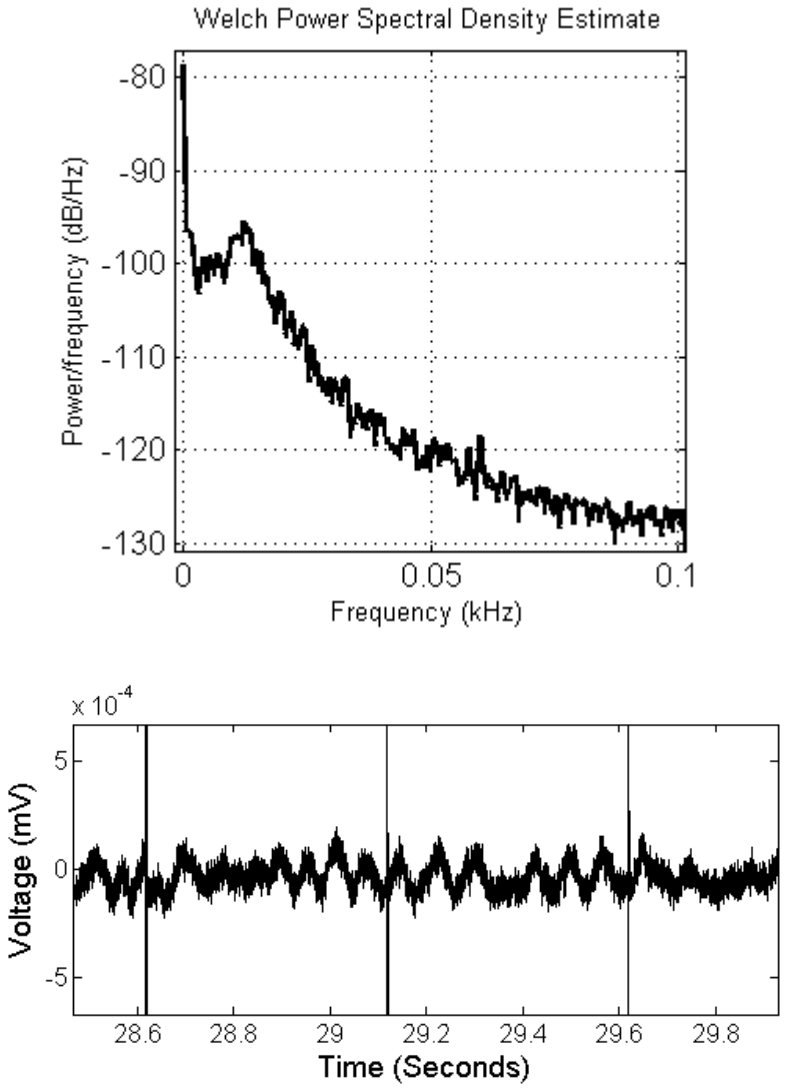

Figure 27. 12.35 Hz oscillation present in the local field potential recordings of a naïve non-human primate. Top: The power spectrum of LFP recordings from the STN of a naïve NHP reveal a peak at 12.35 Hz. Bottom: Beta oscillations can be seen in the LFP recordings.

MPTP Recording

Next, PRCs were estimated using LFP recordings from a second adult female rhesus monkey (*macaca mulatta*, 17 years, 9.0 kg). This subject was treated with the neurotoxin 1-methyl-4-phenyl-1,2,3,6-tetrahydropyridine (MPTP) to induce parkinsonian-like motor symptoms (Langston, Ballard, Tetrud, & Irwin, 1983; Rivlin-Etzion, Elias, Heimer, & Bergman, 2010). Systemic injections on two consecutive days (total of 0.7 mg/kg) were given. MPTP results in the death of dopaminergic neurons in the substantia nigra pars compacta (SNc), the hallmark of PD in humans. Importantly, a strong beta oscillation is seen in the LFP recording of this NHP (Figure 28).

A research deep brain stimulation array with 40 electrodes segmented around the lead (NeuroNexus) was implanted targeting the globus pallidus and the STN of the MPTP-treated NHP. An Alpha Lab SNR (Alpha Omega, Nazareth, Israel) was used to provide biphasic 200 μsec current controlled pulses at 2 Hz through 3 contacts. LFPs were recorded using the AlphaLab SNR system, sampled at 22.321 kHz.

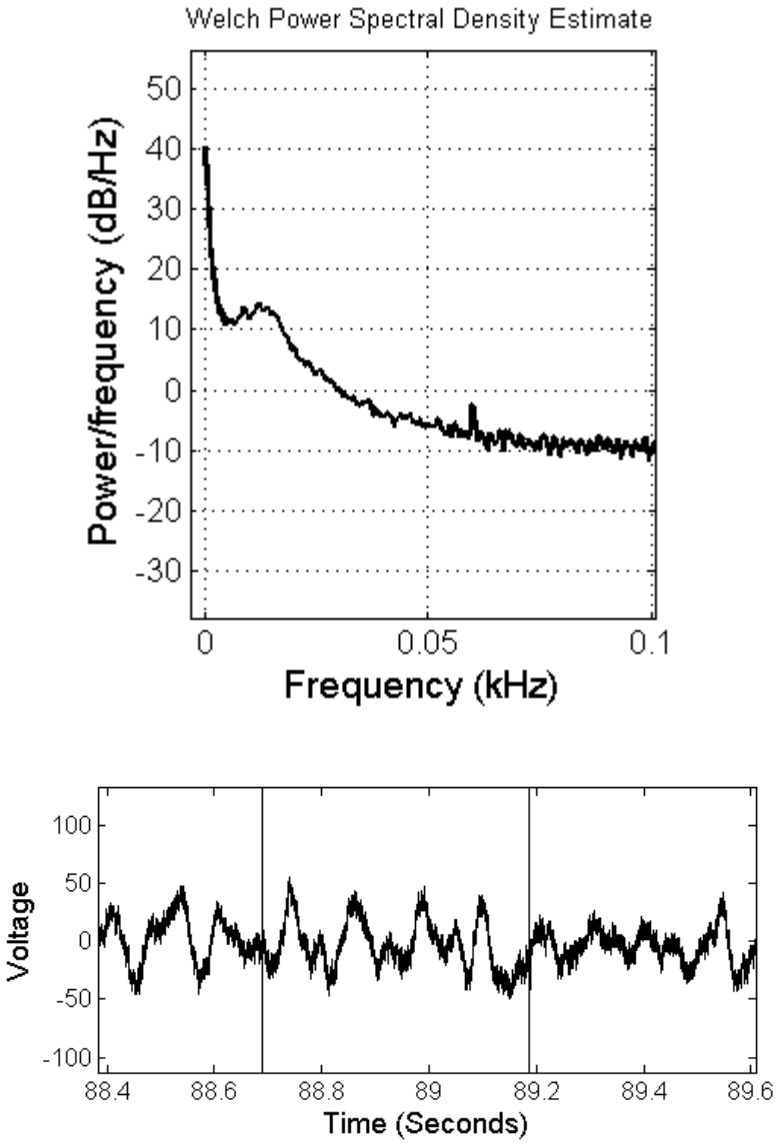

Figure 28. 12.65 Hz oscillation present in the local field potential recordings of an MPTP-treated non-human primate. Top: The power spectrum of LFP recordings from the GPe of an MPTP-treated NHP reveals a peak at 12.35 Hz. Bottom: Beta oscillations can be seen in the LFP recordings.

Estimating the PRC

To estimate the PRC from LFP recordings, it is necessary to get an accurate estimation of the phase at the time of the stimulus. Stimulus artifacts must be removed from the data as they may disrupt the phase estimate. In the recordings used in this chapter, the effects of the stimulus only lasted a few milliseconds. This made it possible to replace sample points around the stimulus with samples linearly interpolated from neighboring sample points.

Differing from methods presented in Chapter 4, in this chapter a causal method was used to estimate the PRCs. First, the data were band pass filtered from 8-82 Hz. Here we used a time weighted estimation of the phase and fit the change in phase with a time weighted polynomial fit. Time-weighting methods improved accuracy of phase and amplitude estimation at the time of stimulation by emphasizing data closest to the time of the stimulus. A similar method has been used without the time weighted estimation to measure PRCs in humans (Azodi-Avval & Gharabaghi, 2015; Cagnan et al., 2013).

The Hilbert transform is a linear operator, like the fast Fourier transform, that allows you to estimate the instantaneous amplitude and phase from a signal from which we calculate the PRC. A window, $lfpwin(t)$, large enough for six periods of the beta oscillation, three before and three after the time of the stimulus, was taken around each stimulus. A Hann window, $hannwin$, was applied to the data window to emphasize the

time around the stimulus, and the Hilbert transform was applied, $H(lfpwin(t) * hannwin)$.

The Hilbert transform takes a time series and estimates the analytic representation of the signal representing it as a series of complex numbers with a real part, $v(t)$, and an imaginary part, $u(t)$. The amplitude can be determined by: $Amp(t) = \sqrt{v^2(t) + u^2(t)}$. The phase, $\varphi(t)$, can be determined by: $\varphi(t) = \arctan(\frac{u(t)}{v(t)})$ where the phase is between 0 and 2π as the phase wraps around the circle. The phase was then unwrapped, to get phase as a function of time (Figure 29 bottom). A weighted polynomial was fit to the unwrapped phase from the data preceding the stimulus, with greatest weight at the time of the stimulus. Then, the fit phase was subtracted from the entire window to detrend the unwrapped phase (Figure 29 bottom). The change in phase, $\nabla\varphi$, was calculated by taking the difference of the between the mean detrended phase before and after the stimulus. Finally, the change in phase, $\nabla\varphi$, was plotted as a function stimulus phase, $\varphi(t)$, for each stimulus pulse. Each data point was weighted depending on the amplitude of the beta oscillation. Strong weights were given to large amplitudes due to improved confidence in our estimation of the phase. The PRC is represented as the polynomial fit to this data.

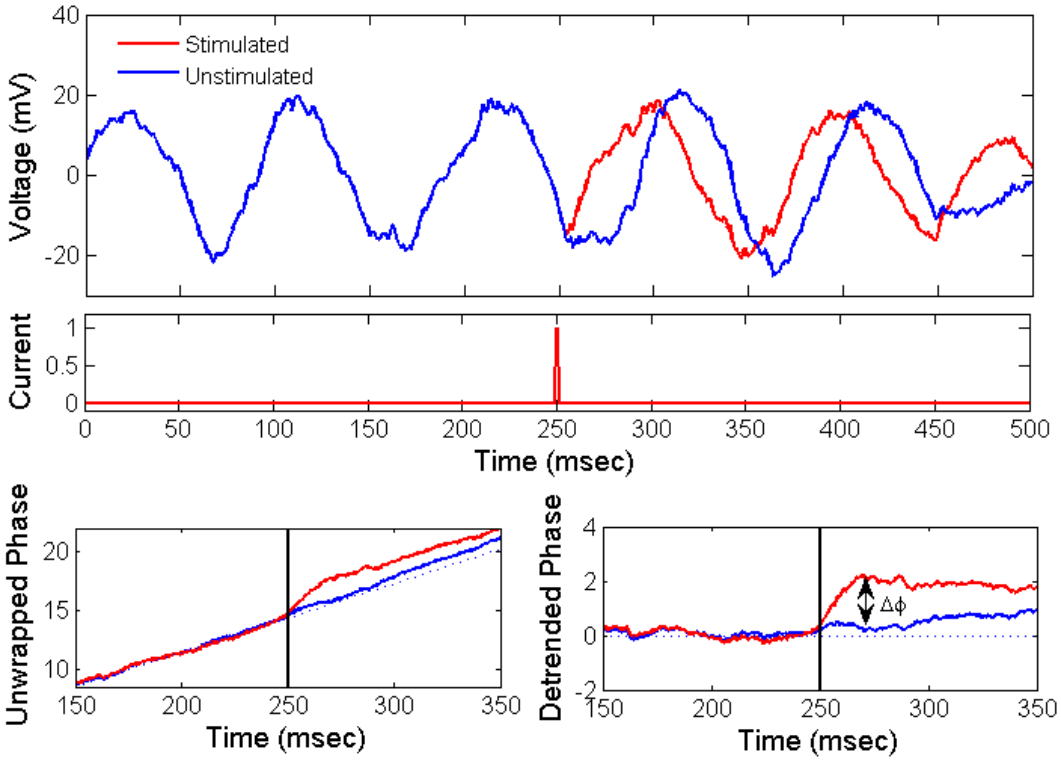

Figure 29. Estimating instantaneous phase using the Hilbert Transform. Oscillator model showing how the change in phase as a result of a stimulus pulse is measured using the Hilbert Transform. Top: Oscillatory signal (blue/dark) which is shifted as a result of the application of a stimulus pulse (red/light). Bottom: Left: Unwrapped phase around the time of the stimulus (250 msec). Right: The change in phase after the time of the stimulus is measured from the difference in the detrended phase.

The significance of the PRC was evaluated by comparing entropy values between the PRC and surrogate PRCs. The surrogate PRCs were generated by randomly shuffling the stimulus phase of data points and repeatedly fitting PRCs to the resulting data. A Bonferroni correction to account for multiple comparisons was used for the evaluation of significant z-scores (95% confidence level). A significant z-score was determined to be a value greater than 3.0233 when using the 40 contact lead, and greater than 2.7344 when using the 8 contact leads.

Predicting the effects of stimulus frequency using the PRC

The PRC can be used to predict how stimulus frequency will modulate the oscillation seen in both the naïve and MPTP-treated NHP recordings. Methods described in depth in Chapter 4 and 6 were used to make predictions. Briefly, the Lyapunov exponent (LE) was calculated at various different frequencies. When the LE > 0 we predict stimulation will disrupt the oscillation; when the LE < 0 we predict stimulation will enhance the oscillation.

Results

Local field potential recordings were made from two non-human primates; one in the naïve state and one treated with MPTP to induce parkinsonian-like symptoms. Significant PRCs were measured from a number of contacts.

A significant oscillation (12.35 Hz) can be seen in field recording of the naïve NHP. We looked at how stimulation affects the phase of this “beta oscillation”. The naïve

monkey was implanted with 8 contact leads. Bipolar stimulation was applied to the STN through contacts 2 and 3 at 300 μA. Significant PRCs (z-score > 2.7344, $\alpha = 0.05$) were seen in recordings from 8 contacts in the naïve NHP (Figure 30). Contacts 1-8 are located on the lead targeting the STN. Significant PRCs were measured from channels 1,4,5,7, and 8. We found significant PRCs in 5 out of 6 possible recording electrodes (as 2 electrodes were used for stimulation). Contacts 9-16 are located on the lead targeting the globus pallidus. Significant PRCs were measured from channels 13, 14, and 15. We found significant PRCs in only 3 out of 8 possible recording electrodes.

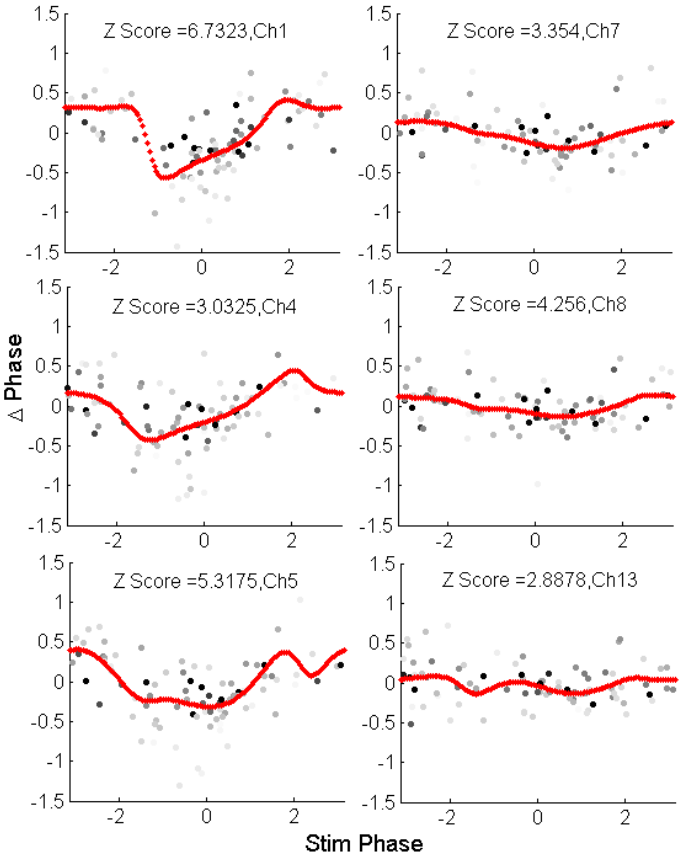

Figure 30. Phase response curves estimated from local field potential recordings in the naïve NHP. Recordings from macroelectrodes were used to look for phase dependent effects of subthreshold stimulation to the STN on the 12.35 Hz oscillation. Significant PRCs (z-score > 2.7344, $\alpha = 0.05$) were seen in 5 out of 6 viable recording contacts in on the lead targeting the STN (stimulation applied through contacts 2 and 3), and 3 out of 8 contacts from the lead targeting the GP (not all shown).

A significant oscillation (12.65 Hz) was also seen in the field recording of the MPTP treated NHP. The parkinsonian-like monkey was implanted with 40 contact leads targeting the STN and GP. On the lead targeting the GP, 15 of the 40 electrode contacts were functional; 27 of the 40 on the lead targeting the STN were functional at the time of recording. Stimulation was applied to the STN lead through 4 contacts, 100μA/contact at 2 Hz. LFPs recorded from the GP lead were used to estimate PRCs in response to STN stimulation. Significant PRCs (z-score > 3.0233, $\alpha = 0.05$) were seen in recordings from 8 of the 15 usable contacts in the MPTP-treated NHP (Figure 31).

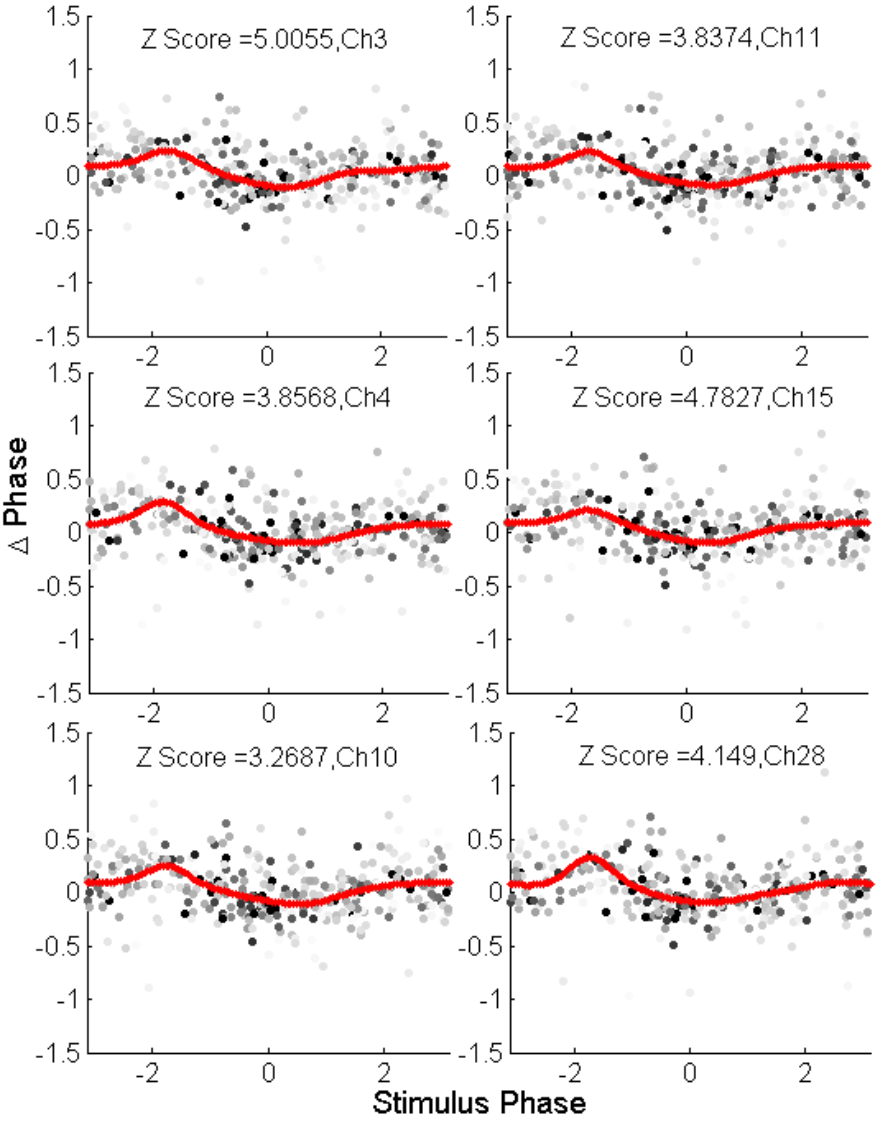

Figure 317. Phase response curves estimated from local field potential recordings in the MPTP-treated NHP. Recordings from the 40 contact lead targeting the GP were used to look for phase dependent effects of subthreshold stimulation to the STN on the 12.65 Hz oscillation. Significant PRCs (z-score > 3.0233, $\alpha = 0.05$) were seen in 8 out of 15 viable recording contacts in the GP (100 μA stimulation applied through 4 contacts in the STN).

Predictions regarding how stimulus frequency modulates the oscillation seen in the LFP recordings can be made using the PRC, as was done in Chapters 4 and 6. Here, predictions were made using a PRC estimated from the naïve NHP recordings (Figure 32). Predictions made from contact 5, located on the lead implanted in the STN of the naïve NHP, indicate a window from 20-60 Hz that should disrupt the 12.35 oscillation. The purpose is to simply show that we can make predictions. Validation of these predictions must still be investigated.

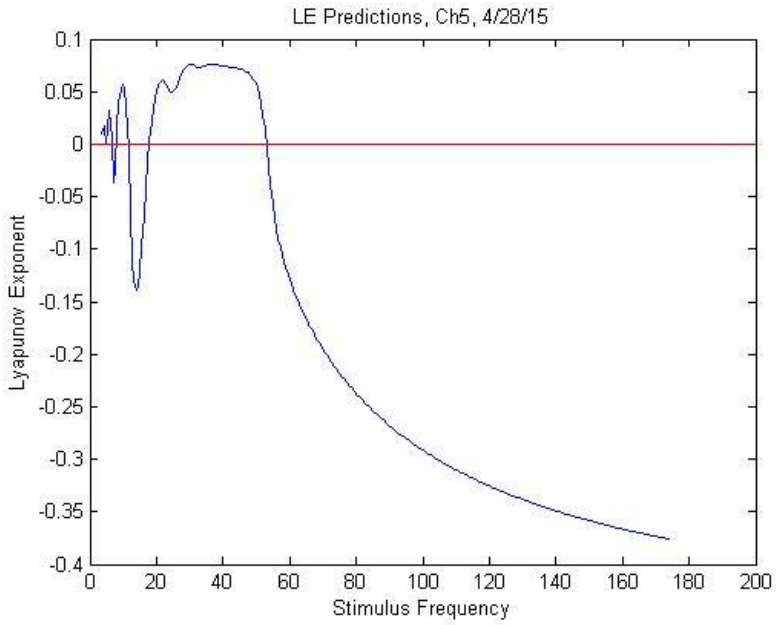

Figure 32. Predicting the effects of stimulus frequency on the 12.35 Hz oscillation in the naïve non-human primate. Predictions were made using the PRC measured from contact 5 of the naïve NHP. The Lyapunov exponent (LE) is plotted as a function of stimulus frequency. When the LE > 0, we predict the stimulus frequency to disrupt the oscillation; when the LE < 0, we predict the stimulus frequency to enhance the oscillation.

Conclusion

Here I have shown it is possible to estimate PRCs from field recordings. By using the Hilbert transform, we are able to measure the change in phase of a beta oscillation in both the naïve and MPTP-treated NHP. This provides support for future testing of PRC-optimized DBS as it will be necessary to use field recordings in humans.

The presence of a PRC indicates there are phase dependent effects of stimulation on the amplitude of the oscillation. This suggests that PRCs could be used to develop optimization approaches to DBS. However, we have yet to establish that these PRCs can be used to make accurate predictions about optimal stimulus parameters. Accurately being able to make predictions will validate the estimated PRC. Furthermore, here we estimated PRCs from two different NHPs, one in the naïve state and one in the parkinsonian-like state. We were able to use these subjects as recordings from both exhibited strong beta oscillations.

In the future, we will test if the PRC can be estimated from the same NHP in both the healthy and MPTP-treated state. This will tell us if the PRC changes as a result of MPTP treatment. Furthermore, we have shown that the PRCs can be used to make predictions about stimulus frequency. However, the predictions indicate a window from 20-60 Hz that will be effective at disrupting the 12.35 oscillation in the naïve NHP. It is thought that high frequency stimulation (< 100 Hz) is necessary to reduce beta oscillations, at least in the parkinsonian state. If predictions made here were validated, our results would

provide interesting information about optimal stimulus frequency. The next step is to validate our predictions in the NHPs used for recordings.

Chapter 9

Conclusions & Future Directions

The overall goal of this doctoral dissertation is to investigate a systematic approach to tuning deep brain stimulation (DBS) parameters based on patient physiology. Specifically, this work has contributed to the advancement of optimization approaches for DBS in Parkinson's disease by: 1) providing evidence for using phase response curves (PRCs) to optimize stimulus parameters, such as frequency; 2) providing evidence for a novel closed-loop approach to DBS – Phasic Burst Stimulation; and 3) developing methods for estimating PRCs from neural field recordings in non-human primates. PRC-optimization provides a platform to optimize various stimulus parameters and closed-loop approaches to DBS.

Summary and Significance of Results

Deep brain stimulation is used to treat motor symptoms of patients with PD. The efficacy of DBS depends in part on post-operative programming of stimulation parameters. Currently, stimulation parameters, such as frequency and amplitude, are tuned post-operatively by a clinician using a time-intensive trial-and-error process (Volkmann et al., 2002). In this thesis, I propose using a simple measure, the PRC, estimated from each patient to systematically tune stimulation parameters. This has the potential to reduce time spent tuning parameters and improve therapeutic outcome.

DBS has been hypothesized to work through "chaotic desynchronization," where certain subthreshold stimulation parameters induce chaotic behavior, thereby disrupting pathological oscillatory activity, particularly in the beta frequency range (12-35 Hz), seen

in PD (C. J. Wilson et al., 2011). Underlying this theory of chaotic desynchronization is the idea that the PRC can be used to predict when coupled oscillators, such as periodically firing neurons, will synchronize or desynchronize. In this thesis, I have provided evidence for using PRCs to optimize simulation to suppress neural synchrony in a computational model of the subthalamopallidal network displaying an emergent parkinsonian oscillation in the parkinsonian state (HM model) as well as in single neurons in basal ganglia brain slices *in vitro*. A computational model offers a platform to develop and test the approach in a repeatable way. Single cell experiments provide proof-of-concept evidence for using this approach in a neural system. Finally, I have shown that PRCs can be estimated from local field potential (LFP) recordings in non-human primates (NHPs); this suggests that this approach could be applied to an animal model of PD. A PRC-optimized approach offers a systematic method for tuning DBS parameters based on patient physiology and moving towards a closed-loop approach to DBS.

Using PRCs to Optimize Stimulus Parameters for Open-Loop DBS

Using DBS devices currently implanted in PD patients, a PRC could be used to optimize stimulus frequency. This approach was successfully used to optimize the suppression of a parkinsonian oscillation in the HM model in Chapter 4, and to disrupt entrainment of single STN neurons in Chapter 6. Intraoperative recordings during DBS surgery are often used for targeting, and could be used to measure a patient's physiological response to stimulation. This patient-specific PRC could then aid a clinician in determining

a window of frequencies predicted to disrupt the pathological oscillation. The PRC-optimized approach has the potential to reduce time spent tuning stimulation frequency post-operatively and perhaps offer a more robust solution.

It is likely that the PRC changes over time or with the state of the patient. Re-measuring the PRC periodically may provide more optimal results. DBS leads that can record the neural signal, currently used for research purposes, could be used in the future to re-measure the PRC over time (Ryapolova-Webb et al., 2014). This would allow for the periodic readjustment of stimulus parameters.

While current DBS devices only allow for pulsatile, square-wave pulses (Butson & McIntyre, 2007), future technology could allow for continuous stimulus waveforms. This has the potential to reduce the total power used, thereby saving battery life, and improve therapeutic outcome. Results in Chapter 7 demonstrated that the PRC could be used to optimize a stimulus waveform to entrain neurons. This same theory could be applied to desynchronize parkinsonian oscillations.

Using PRCs to Optimize a Closed-Loop Approach to DBS

The development of stimulation devices that can sense neuronal signals enables the use of closed-loop approaches for DBS, where activity in the recorded signal is continuously used to adjust stimulation (Rouse et al., 2011; Ryapolova-Webb et al., 2014). Closed-loop algorithms have many advantages over solely physician tuned approaches as they have the potential to: 1) improve efficacy; 2) reduce negative side effects with

decreased stimulation amplitude 3) achieve optimal stimulus settings in less time 4) enhance battery life; and 5) stabilize fluctuations in motor symptoms.

In Chapter 7, a novel closed-loop approach to DBS was proposed, termed Phasic Burst Stimulation (PhaBS). PhaBS involves applying a burst of stimulus pulses over a range of phases to optimally disrupt enhanced pathological synchrony in PD. The slope of the PRC can be used to predict both the phase window as well as the inter-stimulus interval. Closed-loop stimulation triggered off the phase of the beta oscillation has been proposed, but the advancement of PhaBS is that applying a burst of stimulus pulses over a range of phases is more effective at modulating oscillatory activity than a single pulse per cycle at the same amplitude and that parameters can be predicted using patient-specific PRCs. A similar level of modulation could be achieved by using a single pulse at a higher amplitude. However, there are limits to stimulation amplitude. High amplitude stimulation can lead to irreversible faradaic reactions, which may be damaging to neural tissue (Merrill, Bikson, & Jefferys, 2005). Furthermore, a higher amplitude may result in activation of a larger volume of tissue, potentially leading to negative side effects. Lower amplitude stimulation could be reduced by using lower amplitude stimulation.

Estimation of Phase Response Curves

To implement PRC-optimized DBS in patients, PRCs must be measured from field recordings. Recently it has been shown that it is possible to estimate PRCs from LFP recordings from the STN of PD patients (Azodi-Avval & Gharabaghi, 2015). This suggests

that the pathological beta oscillation implicated in PD is sensitive to the phase at which a stimulus is applied and that closed-loop phasic stimulation and PRC-optimized stimulus parameters may be successful. In Chapter 8, significant PRCs are measured from LFP recordings in naïve and MPTP-treated non-human primates. This provides a basis for testing PRC-optimized DBS in NHPs in the future.

In Chapters 4-8, PRCs were estimated using a single stimulus pulse applied at 2 Hz. This is done to ensure stimulus pulses occur at a range of phases. For most predictions made in these chapters, the first order PRC is used, which assumes no interaction between stimuli. While the first order PRC was used to make fairly accurate predictions in Chapters 4-8, predictions could potentially be improved by incorporating higher order effects. In Chapter 8, a PRC measured using a burst of 3 stimulus pulses per oscillation cycle, was used to predict the effects of PhaBS. A large difference was seen when comparing the PRC estimated using a burst of pulses to the PRC estimated using a single pulse (Figure 18). Assuming no higher order effects, the 3 stimulus PRC should simply be the single PRC scaled 3 times; however, results indicate the presence of higher order effects. Incorporating higher order effects moving forward has the potential to make predictions more accurate.

Clinical Limitations

Here we propose using PRCs to predict stimulus parameters to optimally disrupt beta oscillations seen in PD. However, there are a number of potential issues with suppressing this activity. 1) While beta oscillations are implicated in anti-kinetic motor

symptoms of PD, a causal role is highly debated (Brittain et al., 2014). It has been shown that the beta oscillation is reduced upon therapeutic DBS and dopamine replacement therapy, but this may be an epiphenomenon (Kühn et al., 2009). 2) Strong beta oscillations are not seen in all PD patients and are seen in healthy subjects, such as the naïve NHP used in Chapter 8 (Connolly et al., 2015). This suggests that beta oscillations may not be a great biomarker. The approach presented here can be used to target any oscillatory activity found to be implicated in PD in the future. Furthermore, restricting high frequency stimulation to times of enhanced beta oscillations has shown promise for specifically targeting this activity (Little et al., 2013). 3) Enhanced beta activity is not constant, there may be periods of high beta and periods of low beta synchrony (Feingold et al., 2015). For this reason, a closed-loop approach to DBS, where beta oscillations are tracked, may offer a more efficient approach to stimulation. If beta oscillations are truly causing motor symptoms, this would suggest stimulation is not needed during times when beta power is low. 4) It is not known how eliminating the beta oscillation will impact normal motor control. Oscillatory activity is necessary for normal function throughout the brain. Eliminating beta oscillations may impair motor control in a different way, or may allow new pathological activity to emerge. While there are many potential clinical limitations to using PRCs to optimize DBS to suppress beta oscillations, because this method can specifically target the beta oscillation, it may be useful to help settle this debate.

Oscillatory activity is seen throughout the nervous system. Enhanced oscillations have been implicated in many neurological disorders other than PD, such as essential

tremor, epilepsy, and schizophrenia (Golomb, Wang, & Rinzel, 1994; Milton, Gotman, Remillard, & Andermann, 1987; Peter A. Tass, 2007; Uhlhaas & Singer, 2006, 2013; Zijlmans et al., 2012). However, oscillatory activity can also be necessary or important for proper function, such as such as in cognition and perception (Ainsworth et al., 2012; Buzsáki & Draguhn, 2004; Jacobs, Kahana, Ekstrom, & Fried, 2007; Lakatos, Karmos, Mehta, Ulbert, & Schroeder, 2008). While this dissertation focuses on using PRCs to optimize stimulus parameters to suppress pathological oscillations seen in PD, the theory can be applied to enhance or disrupt any oscillatory signals.

While using PRCs to predict how stimulus parameters modulate oscillatory activity, it may not be the most efficient method to optimize stimulus parameters clinically. Sweeping through potential parameters, such as frequencies or phases for closed-loop phasic stimulation, may be more clinically realistic. However, when the parameter space is too large, such as for designing stimulus waveforms, using the PRC may offer the best approach. In the future, the approach presented here should be compared to alternative methods.

Future Experiments

PRC-optimized DBS must be tested in parkinsonian subjects *in vivo*, where the effect on motor output can be monitored. Chapter 8 sets up for future experiments in MPTP-treated NHPs. The predictions made from the PRCs in Chapter 8 can be compared to experimental results in the future. Evidence for a PRC-based optimization approach

could also be gathered from human subjects with PD via intraoperative recordings in patients undergoing DBS surgery or from implanted leads which can sense the neural signal implanted in patients for research. As PRCs have been measured from intraoperative recordings (Azodi-Avval & Gharabaghi, 2015), the next step is to use patient-specific PRCs to make predict the effects of testable stimulus parameters in open-loop, such as stimulus frequency or amplitude. It is important to not only evaluate the effect of PRC-optimized stimulus parameters on the power of beta oscillations, but also on the motor output, as the ultimate goal of DBS therapy is to improve motor symptoms in PD.

Conclusion

While many approaches, both closed- and open-loop, for optimizing DBS for PD have been proposed (Carron et al., 2013; Hauptmann & Tass, 2007; Little et al., 2013; M. Rosenblum & A. Pikovsky, 2004; Rosin et al., 2011; Santaniello et al., 2011; P. A. Tass, 2001), PRC-optimized closed-loop phasic stimulation provides a principled approach optimized using patient-specific physiology. This approach has the potential to more efficiently and effectively stimulate using subthreshold stimulus pulses, thereby improving patient quality of life and improving battery life. Furthermore, this approach tests an underlying theory of "chaotic desynchronization," offering insight into mechanisms-of-action and offering an explanation as to why HF DBS is effective.

References

Adamchic, I., Hauptmann, C., Barnikol, U. B., Pawelczyk, N., Popovych, O., Barnikol, T. T., . . . Tass, P. A. (2014). Coordinated reset neuromodulation for Parkinson's disease: Proof-of-concept study. *Mov Disord*. doi:10.1002/mds.25923

Agnesi, F., Connolly, A. T., Baker, K. B., Vitek, J. L., & Johnson, M. D. (2013). Deep brain stimulation imposes complex informational lesions. *PLoS One, 8*(8), e74462. doi:10.1371/journal.pone.0074462

Ainsworth, M., Lee, S., Cunningham, M. O., Traub, R. D., Kopell, N. J., & Whittington, M. A. (2012). Rates and rhythms: a synergistic view of frequency and temporal coding in neuronal networks. *Neuron, 75*(4), 572-583. doi:10.1016/j.neuron.2012.08.004

Alberts, W. W., Wright, E. W., Jr., & Feinstein, B. (1969). Cortical potentials and Parkinsonian tremor. *Nature, 221*(5181), 670-672.

Albin, R. L., Young, A. B., & Penney, J. B. (1989). The functional anatomy of basal ganglia disorders. *Trends Neurosci, 12*(10), 366-375.

Alexander, G. E., DeLong, M. R., & Strick, P. L. (1986). Parallel organization of functionally segregated circuits linking basal ganglia and cortex. *Annu Rev Neurosci, 9*, 357-381. doi:10.1146/annurev.ne.09.030186.002041

Alhourani, A., McDowell, M. M., Randazzo, M. J., Wozny, T. A., Kondylis, E. D., Lipski, W. J., . . . Richardson, R. M. (2015). Network effects of deep brain stimulation. *J Neurophysiol, 114*(4), 2105-2117. doi:10.1152/jn.00275.2015

Alvarez, L., Macias, R., Guridi, J., Lopez, G., Alvarez, E., Maragoto, C., . . . Obeso, J. A. (2001). Dorsal subthalamotomy for Parkinson's disease. *Mov Disord, 16*(1), 72-78.

Alvarez, L., Macias, R., Lopez, G., Alvarez, E., Pavon, N., Rodriguez-Oroz, M. C., . . . Obeso, J. A. (2005). Bilateral subthalamotomy in Parkinson's disease: initial and long-term response. *Brain, 128*(Pt 3), 570-583. doi:10.1093/brain/awh397

Anderson, M. E., Postupna, N., & Ruffo, M. (2003). Effects of high-frequency stimulation in the internal globus pallidus on the activity of thalamic neurons in the awake monkey. *J Neurophysiol, 89*(2), 1150-1160. doi:10.1152/jn.00475.2002

Anderson, T. R., Hu, B., Iremonger, K., & Kiss, Z. H. (2006). Selective attenuation of afferent synaptic transmission as a mechanism of thalamic deep brain stimulation-induced tremor arrest. *J Neurosci, 26*(3), 841-850. doi:10.1523/JNEUROSCI.3523-05.2006

Ariano, M. A., Larson, E. R., & Noblett, K. L. (1995). Cellular dopamine receptor subtype localization. In M. A. Ariano & D. J. Surmeier (Eds.), *Molecular and cellular mechanisms of neostriatal function* (pp. 59-79). Austin, TX: Landes.

Aström, M., Lemaire, J. J., & Wårdell, K. (2012). Influence of heterogeneous and anisotropic tissue conductivity on electric field distribution in deep brain stimulation. *Med Biol Eng Comput, 50*(1), 23-32. doi:10.1007/s11517-011-0842-z

Aziz, T. Z., Peggs, D., Agarwal, E., Sambrook, M. A., & Crossman, A. R. (1992). Subthalamic nucleotomy alleviates parkinsonism in the 1-methyl-4-phenyl-1,2,3,6-tetrahydropyridine (MPTP)-exposed primate. *Br J Neurosurg, 6*(6), 575-582.

Azodi-Avval, R., & Gharabaghi, A. (2015). Phase-dependent modulation as a novel approach for therapeutic brain stimulation. *Front Comput Neurosci, 9*, 26. doi:10.3389/fncom.2015.00026

Barbeau, A., Sourkes, T., & Murphy, C. (1962). Les catecholamines de la maladie de Parkinson. In J. de Ajuriaguerra (Ed.), *Monoaimnes et systeme Nerveux Central* (pp. 247-262). Geneva.

Bergman, H., Feingold, A., Nini, A., Raz, A., Slovin, H., Abeles, M., & Vaadia, E. (1998). Physiological aspects of information processing in the basal ganglia of normal and parkinsonian primates. *Trends Neurosci, 21*(1), 32-38.

Bergman, H., Wichmann, T., & DeLong, M. R. (1990). Reversal of experimental parkinsonism by lesions of the subthalamic nucleus. *Science, 249*(4975), 1436-1438.

Bergman, H., Wichmann, T., Karmon, B., & DeLong, M. R. (1994). The primate subthalamic nucleus. II. Neuronal activity in the MPTP model of parkinsonism. *J Neurophysiol, 72*(2), 507-520.

Beurle, R. L. (1956). Properties of a mass of cells capable of regenerating pulses. *Philos.Trans.R.Soc.Lond.B.Biol.Sci., 240*, 55.

Beurrier, C., Bioulac, B., Audin, J., & Hammond, C. (2001). High-frequency stimulation produces a transient blockade of voltage-gated currents in subthalamic neurons. *J Neurophysiol, 85*(4), 1351-1356.

Bevan, M. D., Magill, P. J., Terman, D., Bolam, J. P., & Wilson, C. J. (2002). Move to the rhythm: oscillations in the subthalamic nucleus-external globus pallidus network. *Trends in neurosciences, 25*(10), 525-531.

Bevan, M. D., & Wilson, C. J. (1999). Mechanisms underlying spontaneous oscillation and rhythmic firing in rat subthalamic neurons. *The Journal of neuroscience : the official journal of the Society for Neuroscience, 19*(17), 7617-7628.

Bhidayasiri, R., & Truong, D. D. (2008). Motor complications in Parkinson disease: clinical manifestations and management. *Journal of the neurological sciences, 266*(1-2), 204-215. doi:10.1016/j.jns.2007.08.028

Boraud, T., Bezard, E., Bioulac, B., & Gross, C. E. (2000). Ratio of inhibited-to-activated pallidal neurons decreases dramatically during passive limb movement in the MPTP-treated monkey. *J Neurophysiol, 83*(3), 1760-1763.

Braak, H., Del Tredici, K., Rüb, U., de Vos, R. A., Jansen Steur, E. N., & Braak, E. (2003). Staging of brain pathology related to sporadic Parkinson's disease. *Neurobiol Aging, 24*(2), 197-211.

Brittain, J. S., Probert-Smith, P., Aziz, T. Z., & Brown, P. (2013). Tremor suppression by rhythmic transcranial current stimulation. *Curr Biol, 23*(5), 436-440. doi:10.1016/j.cub.2013.01.068

Brittain, J. S., Sharott, A., & Brown, P. (2014). The highs and lows of beta activity in cortico-basal ganglia loops. *Eur J Neurosci, 39*(11), 1951-1959. doi:10.1111/ejn.12574

Brocker, D. T., Swan, B. D., Turner, D. A., Gross, R. E., Tatter, S. B., Koop, M. M., . . . Grill, W. M. (2013). Improved efficacy of temporally non-regular deep brain stimulation in Parkinson's disease. *Exp Neurol, 239*, 60-67. doi:10.1016/j.expneurol.2012.09.008

Bronte-Stewart, H., Barberini, C., Koop, M. M., Hill, B. C., Henderson, J. M., & Wingeier, B. (2009). The STN beta-band profile in Parkinson's disease is stationary and shows prolonged attenuation after deep brain stimulation. *Experimental neurology, 215*(1), 20-28. doi:10.1016/j.expneurol.2008.09.008; 10.1016/j.expneurol.2008.09.008

Brown, E., Moehlis, J., & Holmes, P. (2004). On the phase reduction and response dynamics of neural oscillator populations. *Neural Comput, 16*(4), 673-715. doi:10.1162/089976604322860668

Brown, P. (2006). Bad oscillations in Parkinson's disease. *J Neural Transm Suppl*(70), 27-30.

Brown, P. (2007). Abnormal oscillatory synchronisation in the motor system leads to impaired movement. *Current opinion in neurobiology, 17*(6), 656-664. doi:10.1016/j.conb.2007.12.001

Brown, P., Oliviero, A., Mazzone, P., Insola, A., Tonali, P., & Di Lazzaro, V. (2001). Dopamine dependency of oscillations between subthalamic nucleus and pallidum in Parkinson's disease. *J Neurosci, 21*(3), 1033-1038.

Brown, P., & Williams, D. (2005). Basal ganglia local field potential activity: character and functional significance in the human. *Clinical neurophysiology : official*

journal of the International Federation of Clinical Neurophysiology, 116(11), 2510-2519. doi:10.1016/j.clinph.2005.05.009

Burchiel, K. J. (1995). Thalamotomy for movement disorders. *Neurosurg Clin N Am, 6*(1), 55-71.

Butson, C. R., Cooper, S. E., Henderson, J. M., & McIntyre, C. C. (2007). Patient-specific analysis of the volume of tissue activated during deep brain stimulation. *Neuroimage, 34*(2), 661-670. doi:10.1016/j.neuroimage.2006.09.034

Butson, C. R., & McIntyre, C. C. (2006). Role of electrode design on the volume of tissue activated during deep brain stimulation. *Journal of neural engineering, 3*(1), 1-8. doi:10.1088/1741-2560/3/1/001

Butson, C. R., & McIntyre, C. C. (2007). Differences among implanted pulse generator waveforms cause variations in the neural response to deep brain stimulation. *Clin Neurophysiol, 118*(8), 1889-1894. doi:10.1016/j.clinph.2007.05.061

Butson, C. R., & McIntyre, C. C. (2008). Current steering to control the volume of tissue activated during deep brain stimulation. *Brain Stimul, 1*(1), 7-15. doi:10.1016/j.brs.2007.08.004

Buzsáki, G., & Draguhn, A. (2004). Neuronal oscillations in cortical networks. *Science, 304*(5679), 1926-1929. doi:10.1126/science.1099745

Cagnan, H., Brittain, J. S., Little, S., Foltynie, T., Limousin, P., Zrinzo, L., . . . Brown, P. (2013). Phase dependent modulation of tremor amplitude in essential tremor through thalamic stimulation. *Brain, 136*(Pt 10), 3062-3075. doi:10.1093/brain/awt239

Cagnan, H., Little, S., Foltynie, T., Limousin, P., Zrinzo, L., Hariz, M., . . . Brown, P. (2014). The nature of tremor circuits in parkinsonian and essential tremor. *Brain, 137*(Pt 12), 3223-3234. doi:10.1093/brain/awu250

Carlsson, A., Lindqvist, M., Magnusson, T., & Waldeck, B. (1958). On the presence of 3-hydroxytyramine in brain. *Science, 127*(3296), 471.

Carron, R., Chaillet, A., Filipchuk, A., Pasillas-Lépine, W., & Hammond, C. (2013). Closing the loop of deep brain stimulation. *Front Syst Neurosci, 7*, 112. doi:10.3389/fnsys.2013.00112

Chaturvedi, A., Foutz, T. J., & McIntyre, C. C. (2012). Current steering to activate targeted neural pathways during deep brain stimulation of the subthalamic region. *Brain Stimul, 5*(3), 369-377. doi:10.1016/j.brs.2011.05.002

Chaudhuri, K. R., Healy, D. G., Schapira, A. H., & Excellence, N. I. f. C. (2006). Non-motor symptoms of Parkinson's disease: diagnosis and management. *Lancet Neurol, 5*(3), 235-245. doi:10.1016/S1474-4422(06)70373-8

Chen, C. C., Litvak, V., Gilbertson, T., Kühn, A., Lu, C. S., Lee, S. T., . . . Brown, P. (2007). Excessive synchronization of basal ganglia neurons at 20 Hz slows movement in Parkinson's disease. *Exp Neurol, 205*(1), 214-221. doi:10.1016/j.expneurol.2007.01.027

Chiken, S., & Nambu, A. (2015). Mechanism of Deep Brain Stimulation: Inhibition, Excitation, or Disruption? *Neuroscientist*. doi:10.1177/1073858415581986

Coffey, R. J. (2009). Deep brain stimulation devices: a brief technical history and review. *Artif Organs, 33*(3), 208-220. doi:10.1111/j.1525-1594.2008.00620.x

Connolly, A. T., Jensen, A. L., Bello, E. M., Netoff, T. I., Baker, K. B., Johnson, M. D., & Vitek, J. L. (2015). Modulations in oscillatory frequency and coupling in globus pallidus with increasing parkinsonian severity. *J Neurosci, 35*(15), 6231-6240. doi:10.1523/JNEUROSCI.4137-14.2015

Connolly, A. T., Vetter, R. J., Hetke, J. F., Teplitzky, B. A., Kipke, D. R., Pellinen, D. S., . . . Johnson, M. D. (2016). A Novel Lead Design for Modulation and Sensing of Deep Brain Structures. *IEEE Trans Biomed Eng, 63*(1), 148-157. doi:10.1109/TBME.2015.2492921

Contarino, M. F., Bour, L. J., Verhagen, R., Lourens, M. A., de Bie, R. M., van den Munckhof, P., & Schuurman, P. R. (2014). Directional steering: A novel approach to deep brain stimulation. *Neurology, 83*(13), 1163-1169. doi:10.1212/WNL.0000000000000823

Copernicus, N., Herrmann, J., & Akademie der Wissenschaften der DDR. (1973). *Nicolaus Copernicus. 1473-1973. Das Bild vom Kosmos u. d. Copernican. Revolution in d. gesellschaftl. u. geistigen Auseinandersetzgn. Studien zum Copernicus-Jahr 1973*. Berlin,: Akademie-Verl.

Cotzias, G. C., Papavasiliou, P. S., & Gellene, R. (1969). Modification of Parkinsonism--chronic treatment with L-dopa. *N Engl J Med, 280*(7), 337-345. doi:10.1056/NEJM196902132800701

Courtemanche, R., Fujii, N., & Graybiel, A. M. (2003). Synchronous, focally modulated beta-band oscillations characterize local field potential activity in the striatum of awake behaving monkeys. *The Journal of neuroscience : the official journal of the Society for Neuroscience, 23*(37), 11741-11752.

Cui, J., Canavier, C. C., & Butera, R. J. (2009). Functional phase response curves: a method for understanding synchronization of adapting neurons. *J Neurophysiol, 102*(1), 387-398. doi:10.1152/jn.00037.2009

Danzl, P., Hespanha, J., & Moehlis, J. (2009). Event-based minimum-time control of oscillatory neuron models: phase randomization, maximal spike rate increase, and

desynchronization. *Biological cybernetics, 101*(5-6), 387-399. doi:10.1007/s00422-009-0344-3

Dauer, W., & Przedborski, S. (2003). Parkinson's disease: mechanisms and models. *Neuron, 39*(6), 889-909.

Davis, N. J., Tomlinson, S. P., & Morgan, H. M. (2012). The role of β-frequency neural oscillations in motor control. *J Neurosci, 32*(2), 403-404. doi:10.1523/JNEUROSCI.5106-11.2012

de Bie, R. M., de Haan, R. J., Schuurman, P. R., Esselink, R. A., Bosch, D. A., & Speelman, J. D. (2002). Morbidity and mortality following pallidotomy in Parkinson's disease: a systematic review. *Neurology, 58*(7), 1008-1012.

de Hemptinne, C., Ryapolova-Webb, E. S., Air, E. L., Garcia, P. A., Miller, K. J., Ojemann, J. G., . . . Starr, P. A. (2013). Exaggerated phase-amplitude coupling in the primary motor cortex in Parkinson disease. *Proc Natl Acad Sci U S A, 110*(12), 4780-4785. doi:10.1073/pnas.1214546110

de Hemptinne, C., Swann, N. C., Ostrem, J. L., Ryapolova-Webb, E. S., San Luciano, M., Galifianakis, N. B., & Starr, P. A. (2015). Therapeutic deep brain stimulation reduces cortical phase-amplitude coupling in Parkinson's disease. *Nat Neurosci, 18*(5), 779-786. doi:10.1038/nn.3997

Deco, G., Jirsa, V. K., Robinson, P. A., Breakspear, M., & Friston, K. (2008). The dynamic brain: from spiking neurons to neural masses and cortical fields. *PLoS computational biology, 4*(8), e1000092. doi:10.1371/journal.pcbi.1000092

Dejean, C., Hyland, B., & Arbuthnott, G. (2009). Cortical effects of subthalamic stimulation correlate with behavioral recovery from dopamine antagonist induced akinesia. *Cereb Cortex, 19*(5), 1055-1063. doi:10.1093/cercor/bhn149

DeLong, M. R. (1990). Primate models of movement disorders of basal ganglia origin. *Trends Neurosci, 13*(7), 281-285.

DeLong, M. R., Alexander, G. E., Miller, W. C., & Crutcher, M. D. (1992). Anatomical and functional aspects of basal ganglia-thalamocortical circuits. In J. W. Ironside, R. H. S. Mindham, R. J. Smith, E. G. S. Spokes, & W. Winlow (Eds.), *Function and dysfunction in the basal ganglia* (pp. 3-32). OxfordNew YorkSeoulTokyo Rergamon Press.

Devergnas, A., Pittard, D., Bliwise, D., & Wichmann, T. (2014). Relationship between oscillatory activity in the cortico-basal ganglia network and parkinsonism in MPTP-treated monkeys. *Neurobiol Dis, 68C*, 156-166. doi:10.1016/j.nbd.2014.04.004

Dodla, R., & Wilson, C. J. (2013). Spike width and frequency alter stability of phase-locking in electrically coupled neurons. *Biol Cybern, 107*(3), 367-383. doi:10.1007/s00422-013-0556-4

Dorval, A. D., & Grill, W. M. (2014). Deep Brain Stimulation of the Subthalamic Nucleus Reestablishes Neuronal Information Transmission in the 6-OHDA Rat Model of Parkinsonism. *J Neurophysiol*. doi:10.1152/jn.00713.2013

Dorval, A. D., Kuncel, A. M., Birdno, M. J., Turner, D. A., & Grill, W. M. (2010). Deep brain stimulation alleviates parkinsonian bradykinesia by regularizing pallidal activity. *Journal of neurophysiology, 104*(2), 911-921. doi:10.1152/jn.00103.2010

Dorval, A. D., Panjwani, N., Qi, R. Y., & Grill, W. M. (2009). Deep brain stimulation that abolishes Parkinsonian activity in basal ganglia improves thalamic relay fidelity in a computational circuit. *Conf Proc IEEE Eng Med Biol Soc, 2009*, 4230-4233. doi:10.1109/IEMBS.2009.5333611

Dorval, A. D., Russo, G. S., Hashimoto, T., Xu, W., Grill, W. M., & Vitek, J. L. (2008). Deep brain stimulation reduces neuronal entropy in the MPTP-primate model of Parkinson's disease. *Journal of neurophysiology, 100*(5), 2807-2818. doi:10.1152/jn.90763.2008; 10.1152/jn.90763.2008

Dostrovsky, J., & Bergman, H. (2004). Oscillatory activity in the basal ganglia--relationship to normal physiology and pathophysiology. *Brain : a journal of neurology, 127*(Pt 4), 721-722. doi:10.1093/brain/awh164

Dostrovsky, J. O., Levy, R., Wu, J. P., Hutchison, W. D., Tasker, R. R., & Lozano, A. M. (2000). Microstimulation-induced inhibition of neuronal firing in human globus pallidus. *J Neurophysiol, 84*(1), 570-574.

Ehringer, H., & Hornykiewicz, O. (1960). [Distribution of noradrenaline and dopamine (3-hydroxytyramine) in the human brain and their behavior in diseases of the extrapyramidal system]. *Klin Wochenschr, 38*, 1236-1239.

Engel, A. K., & Fries, P. (2010). Beta-band oscillations--signalling the status quo? *Curr Opin Neurobiol, 20*(2), 156-165. doi:10.1016/j.conb.2010.02.015

Ermentrout, G., & Kopell, N. (1991). Multiple pulse interactions and averaging in systems of coupled neural oscillators. *Journal of Mathematical Biology, 29*, 195-217.

Ermentrout, G. B., Beverlin, B., 2nd, Troyer, T., & Netoff, T. I. (2011). The variance of phase-resetting curves. *Journal of computational neuroscience, 31*(2), 185-197. doi:10.1007/s10827-010-0305-9; 10.1007/s10827-010-0305-9

Ermentrout, G. B., & Kopell, N. (1998). Fine structure of neural spiking and synchronization in the presence of conduction delays. *Proceedings of the National Academy of Sciences of the United States of America, 95*(3), 1259-1264.

Eusebio, A., & Brown, P. (2007). Oscillatory activity in the basal ganglia. *Parkinsonism Relat Disord, 13 Suppl 3*, S434-436. doi:10.1016/s1353-8020(08)70044-0

Farries, M. A., & Wilson, C. J. (2012). Phase response curves of subthalamic neurons measured with synaptic input and current injection. *J Neurophysiol, 108*(7), 1822-1837. doi:10.1152/jn.00053.2012

Feingold, J., Gibson, D. J., DePasquale, B., & Graybiel, A. M. (2015). Bursts of beta oscillation differentiate postperformance activity in the striatum and motor cortex of monkeys performing movement tasks. *Proc Natl Acad Sci U S A, 112*(44), 13687-13692. doi:10.1073/pnas.1517629112

Feng, X. J., Greenwald, B., Rabitz, H., Shea-Brown, E., & Kosut, R. (2007). Toward closed-loop optimization of deep brain stimulation for Parkinson's disease: concepts and lessons from a computational model. *Journal of neural engineering, 4*(2), L14-21. doi:10.1088/1741-2560/4/2/L03

Feng, X. J., Shea-Brown, E., Greenwald, B., Kosut, R., & Rabitz, H. (2007). Optimal deep brain stimulation of the subthalamic nucleus--a computational study. *J Comput Neurosci, 23*(3), 265-282. doi:10.1007/s10827-007-0031-0

Filali, M., Hutchison, W. D., Palter, V. N., Lozano, A. M., & Dostrovsky, J. O. (2004). Stimulation-induced inhibition of neuronal firing in human subthalamic nucleus. *Exp Brain Res, 156*(3), 274-281. doi:10.1007/s00221-003-1784-y

Folkerts, M., & Kühne, A. (2006). *Astronomy as a model for the sciences in early modern times: papers from the international symposium, Munich, 10-12 March 2003* (Vol. Heft 59). Augsburg: Rauner.

Follett, K. A., Weaver, F. M., Stern, M., Hur, K., Harris, C. L., Luo, P., . . . Group, C. S. (2010). Pallidal versus subthalamic deep-brain stimulation for Parkinson's disease. *N Engl J Med, 362*(22), 2077-2091. doi:10.1056/NEJMoa0907083

Foutz, T. J., & McIntyre, C. C. (2010). Evaluation of novel stimulus waveforms for deep brain stimulation. *J Neural Eng, 7*(6), 066008. doi:10.1088/1741-2560/7/6/066008

Franks, A. J. (1990). *Function and dysfunction in the basal ganglia*. Manchester ; New York, New York, NY, USA: Manchester University Press ; Distributed exclusively in the USA and Canada by St. Martin's Press.

Freeman, W. J. (1975). *Mass action in the nervous system: examination of the neurophysiological basis of adaptive behavior through the EEG*. New York: Academic Press.

Gerfen, C. R., Engber, T. M., Mahan, L. C., Susel, Z., Chase, T. N., Monsma, F. J., & Sibley, D. R. (1990). D1 and D2 dopamine receptor-regulated gene expression of striatonigral and striatopallidal neurons. *Science, 250*(4986), 1429-1432.

Gertler, T. S., Chan, C. S., & Surmeier, D. J. (2008). Dichotomous anatomical properties of adult striatal medium spiny neurons. *J Neurosci, 28*(43), 10814-10824. doi:10.1523/JNEUROSCI.2660-08.2008

Gilbertson, T., Lalo, E., Doyle, L., Di Lazzaro, V., Cioni, B., & Brown, P. (2005). Existing motor state is favored at the expense of new movement during 13-35 Hz oscillatory synchrony in the human corticospinal system. *J Neurosci, 25*(34), 7771-7779. doi:10.1523/JNEUROSCI.1762-05.2005

Gillies, A., & Arbuthnott, G. (2000). Computational models of the basal ganglia. *Mov Disord, 15*(5), 762-770.

Glass, L., & Mackey, M. C. (1988). *From clocks to chaos: the rhythms of life*. Princeton, N.J.: Princeton University Press.

Goldberg, J. A., Bourad, T., & Bergman, H. (2004). Microrecording in the Primate MPTP Model (pp. 46).

Goldman, J. G., & Postuma, R. (2014). Premotor and nonmotor features of Parkinson's disease. *Curr Opin Neurol, 27*(4), 434-441. doi:10.1097/WCO.0000000000000112

Golomb, D., Wang, X. J., & Rinzel, J. (1994). Synchronization properties of spindle oscillations in a thalamic reticular nucleus model. *J Neurophysiol, 72*(3), 1109-1126.

Gradinaru, V., Mogri, M., Thompson, K. R., Henderson, J. M., & Deisseroth, K. (2009). Optical deconstruction of parkinsonian neural circuitry. *Science (New York, N.Y.), 324*(5925), 354-359. doi:10.1126/science.1167093

Grannan, E., Kleinfeld, D., & Sompolinsky, H. (1993). Stimulus-dependent synchronization of neuronal assemblies. *Neural Computation, 4*, 550-569.

Grill, W. M., & Dorval II, A. (2014). USA Patent No.: D. University.

Grill, W. M., Snyder, A. N., & Miocinovic, S. (2004). Deep brain stimulation creates an informational lesion of the stimulated nucleus. *Neuroreport, 15*(7), 1137-1140.

Groves, D. A., & Brown, V. J. (2005). Vagal nerve stimulation: a review of its applications and potential mechanisms that mediate its clinical effects. *Neurosci Biobehav Rev, 29*(3), 493-500. doi:10.1016/j.neubiorev.2005.01.004

Guevara, M. R., Shrier, A., & Glass, L. (1986). Phase resetting of spontaneously beating embryonic ventricular heart cell aggregates. *Am J Physiol, 251*(6 Pt 2), H1298-1305.

Guo, Y., Rubin, J. E., McIntyre, C. C., Vitek, J. L., & Terman, D. (2008). Thalamocortical relay fidelity varies across subthalamic nucleus deep brain

stimulation protocols in a data-driven computational model. *J Neurophysiol, 99*(3), 1477-1492. doi:10.1152/jn.01080.2007

Guridi, J., & Lozano, A. M. (1997). A brief history of pallidotomy. *Neurosurgery, 41*(5), 1169-1180; discussion 1180-1163.

Gurney, K., Prescott, T. J., & Redgrave, P. (2001). A computational model of action selection in the basal ganglia. I. A new functional anatomy. *Biol Cybern, 84*(6), 401-410.

Hahn, P. J., & McIntyre, C. C. (2010). Modeling shifts in the rate and pattern of subthalamopallidal network activity during deep brain stimulation. *Journal of computational neuroscience, 28*(3), 425-441. doi:10.1007/s10827-010-0225-8

Hahn, P. J., Russo, G. S., Hashimoto, T., Miocinovic, S., Xu, W., McIntyre, C. C., & Vitek, J. L. (2008). Pallidal burst activity during therapeutic deep brain stimulation. *Exp Neurol, 211*(1), 243-251. doi:10.1016/j.expneurol.2008.01.032

Hammond, C., Bergman, H., & Brown, P. (2007). Pathological synchronization in Parkinson's disease: networks, models and treatments. *Trends in neurosciences, 30*(7), 357-364. doi:10.1016/j.tins.2007.05.004

Hansel, D., Mato, G., & Meunier, C. (1993). Phase dynamics of weakly coupled Hodgkin-Huxley neurons. *Europhysics Letters, 23*, 367-372.

Hardesty, D. E., & Sackeim, H. A. (2007). Deep brain stimulation in movement and psychiatric disorders. *Biol Psychiatry, 61*(7), 831-835. doi:10.1016/j.biopsych.2006.08.028

Hashimoto, T., Elder, C. M., Okun, M. S., Patrick, S. K., & Vitek, J. L. (2003). Stimulation of the subthalamic nucleus changes the firing pattern of pallidal neurons. *The Journal of neuroscience : the official journal of the Society for Neuroscience, 23*(5), 1916-1923.

Hassler, R., & Riechert, T. (1954). [Indications and localization of stereotactic brain operations]. *Nervenarzt, 25*(11), 441-447.

Hauptmann, C., & Tass, P. A. (2007). Therapeutic rewiring by means of desynchronizing brain stimulation. *Bio Systems, 89*(1-3), 173-181. doi:10.1016/j.biosystems.2006.04.015

Hemm, S., Mennessier, G., Vayssiere, N., Cif, L., El Fertit, H., & Coubes, P. (2005). Deep brain stimulation in movement disorders: stereotactic coregistration of two-dimensional electrical field modeling and magnetic resonance imaging. *J Neurosurg, 103*(6), 949-955. doi:10.3171/jns.2005.103.6.0949

Henry, K. S., & Heinz, M. G. (2012). Diminished temporal coding with sensorineural hearing loss emerges in background noise. *Nat Neurosci, 15*(10), 1362-1364. doi:10.1038/nn.3216

Hines, M. L., & Carnevale, N. T. (1997). The NEURON simulation environment. *Neural Comput, 9*(6), 1179-1209.

Hines, M. L., & Carnevale, N. T. (2001). NEURON: a tool for neuroscientists. *Neuroscientist, 7*(2), 123-135.

Hodgkin, A. L., & Huxley, A. F. (1952a). Currents carried by sodium and potassium ions through the membrane of the giant axon of Loligo. *The Journal of physiology, 116*(4), 449-472.

Hodgkin, A. L., & Huxley, A. F. (1952b). The components of membrane conductance in the giant axon of Loligo. *The Journal of physiology, 116*(4), 473-496.

Holgado, A. J., Terry, J. R., & Bogacz, R. (2010). Conditions for the generation of beta oscillations in the subthalamic nucleus-globus pallidus network. *The Journal of neuroscience : the official journal of the Society for Neuroscience, 30*(37), 12340-12352. doi:10.1523/JNEUROSCI.0817-10.2010

Holt, A. B., & Netoff, T. I. (2014). Origins and suppression of oscillations in a computational model of Parkinson's disease. *J Comput Neurosci, 37*(3), 505-521. doi:10.1007/s10827-014-0523-7

Hoppensteadt, F. C., & Izhikevich, E. M. (1996). Synaptic organizations and dynamical properties of weakly connected neural oscillators. I. Analysis of a canonical model. *Biological cybernetics, 75*(2), 117-127.

Humphries, M. D., & Gurney, K. (2012). Network effects of subthalamic deep brain stimulation drive a unique mixture of responses in basal ganglia output. *Eur J Neurosci, 36*(2), 2240-2251. doi:10.1111/j.1460-9568.2012.08085.x

Hunka, K., Suchowersky, O., Wood, S., Derwent, L., & Kiss, Z. H. (2005). Nursing time to program and assess deep brain stimulators in movement disorder patients. *The Journal of neuroscience nursing : journal of the American Association of Neuroscience Nurses, 37*(4), 204-210.

Huss, D. S., Dallapiazza, R. F., Shah, B. B., Harrison, M. B., Diamond, J., & Elias, W. J. (2015). Functional assessment and quality of life in essential tremor with bilateral or unilateral DBS and focused ultrasound thalamotomy

Movement Disorders Volume 30, Issue 14. *Movement Disorders, 30*(14), 1937-1943. Retrieved from http://onlinelibrary.wiley.com/doi/10.1002/mds.26455/abstract

Israel, Z., & Burchiel, K. (2004). *Microelectrode recording in movement disorder surgery*. New York: Thieme Medical Publishers.

Izhikevich, E. M. (2007). *Dynamical systems in neuroscience: the geometry of excitability and bursting*. Cambridge, Mass.: MIT Press.

Jacobs, J., Kahana, M. J., Ekstrom, A. D., & Fried, I. (2007). Brain oscillations control timing of single-neuron activity in humans. *J Neurosci, 27*(14), 3839-3844. doi:10.1523/JNEUROSCI.4636-06.2007

Jezernik, S., & Morari, M. (2005). Energy-optimal electrical excitation of nerve fibers. *IEEE Trans Biomed Eng, 52*(4), 740-743. doi:10.1109/TBME.2005.844050

Kirk, D. E. (2004). *Optimal control theory : an introduction*. Mineola, N.Y.: Dover Publications.

Kleiner-Fisman, G., Saint-Cyr, J. A., Miyasaki, J., Lozano, A., & Lang, A. E. (2002). Subthalamic DBS replaces levodopa in Parkinson's disease. *Neurology, 59*(8), 1293-1294; author reply 1294.

Kopell, N., & Ermentrout, G. B. (2002). Mechanisms of phase-locking and frequency control in pairs of coupled neural oscillators. In B. Fiedler (Ed.), *Handbook on dynamical systems: toward applications* (pp. 3-54). New York, NY: Elsevier.

Kravitz, A. V., Freeze, B. S., Parker, P. R., Kay, K., Thwin, M. T., Deisseroth, K., & Kreitzer, A. C. (2010). Regulation of parkinsonian motor behaviours by optogenetic control of basal ganglia circuitry. *Nature, 466*(7306), 622-626. doi:10.1038/nature09159

Kuhn, A. A., Kempf, F., Brucke, C., Gaynor Doyle, L., Martinez-Torres, I., Pogosyan, A., . . . Brown, P. (2008). High-frequency stimulation of the subthalamic nucleus suppresses oscillatory beta activity in patients with Parkinson's disease in parallel with improvement in motor performance. *The Journal of neuroscience : the official journal of the Society for Neuroscience, 28*(24), 6165-6173. doi:10.1523/JNEUROSCI.0282-08.2008

Kuhn, A. A., Kupsch, A., Schneider, G. H., & Brown, P. (2006). Reduction in subthalamic 8-35 Hz oscillatory activity correlates with clinical improvement in Parkinson's disease. *Eur J Neurosci, 23*(7), 1956-1960. doi:10.1111/j.1460-9568.2006.04717.x

Kuhn, A. A., Trottenberg, T., Kivi, A., Kupsch, A., Schneider, G. H., & Brown, P. (2005). The relationship between local field potential and neuronal discharge in the subthalamic nucleus of patients with Parkinson's disease. *Exp Neurol, 194*(1), 212-220. doi:10.1016/j.expneurol.2005.02.010

Kuramoto, Y. (1984). *Chemical oscillations, waves, and turbulence*. Berlin ; New York: Springer-Verlag.

Kühn, A. A., Tsui, A., Aziz, T., Ray, N., Brücke, C., Kupsch, A., . . . Brown, P. (2009). Pathological synchronisation in the subthalamic nucleus of patients with

Parkinson's disease relates to both bradykinesia and rigidity. *Exp Neurol, 215*(2), 380-387. doi:10.1016/j.expneurol.2008.11.008

Laitinen, L. V., Bergenheim, A. T., & Hariz, M. I. (1992). Ventroposterolateral pallidotomy can abolish all parkinsonian symptoms. *Stereotact Funct Neurosurg, 58*(1-4), 14-21.

Lakatos, P., Karmos, G., Mehta, A. D., Ulbert, I., & Schroeder, C. E. (2008). Entrainment of neuronal oscillations as a mechanism of attentional selection. *Science, 320*(5872), 110-113. doi:10.1126/science.1154735

Langston, J. W., Ballard, P., Tetrud, J. W., & Irwin, I. (1983). Chronic Parkinsonism in humans due to a product of meperidine-analog synthesis. *Science, 219*(4587), 979-980.

Leblois, A., Boraud, T., Meissner, W., Bergman, H., & Hansel, D. (2006). Competition between feedback loops underlies normal and pathological dynamics in the basal ganglia. *The Journal of neuroscience : the official journal of the Society for Neuroscience, 26*(13), 3567-3583. doi:10.1523/JNEUROSCI.5050-05.2006

Lempka, S. F., & McIntyre, C. C. (2013). Theoretical analysis of the local field potential in deep brain stimulation applications. *PLoS One, 8*(3), e59839. doi:10.1371/journal.pone.0059839

Lengyel, M., Kwag, J., Paulsen, O., & Dayan, P. (2005). Matching storage and recall: hippocampal spike timing-dependent plasticity and phase response curves. *Nat Neurosci, 8*(12), 1677-1683. doi:10.1038/nn1561

LeWitt, P., Rezai, A., Leehey, M., Ojemann, S., Flaherty, A., Eskandar, E., . . . Feigin, A. (2011). AAV2-GAD gene therapy for advanced Parkinson's disease: a double-blind, sham-surgery controlled, randomised trial. *Lancet Neurology, 10*, 309-319.

Li, Q., Qian, Z. M., Arbuthnott, G. W., Ke, Y., & Yung, W. H. (2014). Cortical effects of deep brain stimulation: implications for pathogenesis and treatment of Parkinson disease. *JAMA Neurol, 71*(1), 100-103. doi:10.1001/jamaneurol.2013.4221

Li, S., Arbuthnott, G. W., Jutras, M. J., Goldberg, J. A., & Jaeger, D. (2007). Resonant antidromic cortical circuit activation as a consequence of high-frequency subthalamic deep-brain stimulation. *J Neurophysiol, 98*(6), 3525-3537. doi:10.1152/jn.00808.2007

Lilly, J. C., Hughes, J. R., Alvord, E. C., & Galkin, T. W. (1955). Brief, noninjurious electric waveform for stimulation of the brain. *Science, 121*(3144), 468-469.

Limousin, P., Pollak, P., Benazzouz, A., Hoffmann, D., Le Bas, J. F., Broussolle, E., . . . Benabid, A. L. (1995). Effect of parkinsonian signs and symptoms of bilateral subthalamic nucleus stimulation. *Lancet, 345*(8942), 91-95.

Little, S., & Brown, P. (2014). The functional role of beta oscillations in Parkinson's disease. *Parkinsonism Relat Disord, 20 Suppl 1*, S44-48. doi:10.1016/S1353-8020(13)70013-0

Little, S., Pogosyan, A., Kuhn, A. A., & Brown, P. (2012). β band stability over time correlates with Parkinsonian rigidity and bradykinesia. *Exp Neurol, 236*(2), 383-388. doi:10.1016/j.expneurol.2012.04.024

Little, S., Pogosyan, A., Neal, S., Zavala, B., Zrinzo, L., Hariz, M., . . . Brown, P. (2013). Adaptive deep brain stimulation in advanced Parkinson disease. *Ann Neurol, 74*(3), 449-457. doi:10.1002/ana.23951

Lopes da Silva, F. H., Hoeks, A., Smits, H., & Zetterberg, L. H. (1973). Model of brain rhythmic activity. *Biological cybernetics, 15*(1), 27-37.

Lozano, A. M., Lang, A. E., Galvez-Jimenez, N., Miyasaki, J., Duff, J., Hutchinson, W. D., & Dostrovsky, J. O. (1995). Effect of GPi pallidotomy on motor function in Parkinson's disease. *Lancet, 346*(8987), 1383-1387.

Mahon, S., Deniau, J. M., Charpier, S., & Delord, B. (2000). Role of a striatal slowly inactivating potassium current in short-term facilitation of corticostriatal inputs: a computer simulation study. *Learn Mem, 7*(5), 357-362.

Malekmohammadi, M., Herron, J., Velisar, A., Blumenfeld, Z., Trager, M. H., Chizeck, H. J., & Bronte-Stewart, H. (2016). Kinematic adaptive deep brain stimulation for resting tremor in Parkinson's disease. *Movement disorders*. doi:doi: 10.1002/mds.26482

Malekmohannadi, M., Herron, J., Velisar, A., Blumenfeld, Z., Trager, M. H., Chizeck, H. J., & Bronte-Stewart, H. (2016). Kinematic adaptive deep brain stimulation for resting tremor in Parkinson's disease. *Movement disorders*. doi:doi: 10.1002/mds.26482

Mallet, N., Pogosyan, A., Marton, L. F., Bolam, J. P., Brown, P., & Magill, P. J. (2008). Parkinsonian beta oscillations in the external globus pallidus and their relationship with subthalamic nucleus activity. *J Neurosci, 28*(52), 14245-14258. doi:10.1523/jneurosci.4199-08.2008

Marreiros, A. C., Cagnan, H., Moran, R. J., Friston, K. J., & Brown, P. (2012). Basal ganglia-cortical interactions in Parkinsonian patients. *Neuroimage, 66c*, 301-310. doi:10.1016/j.neuroimage.2012.10.088

Marsden, J. F., Limousin-Dowsey, P., Ashby, P., Pollak, P., & Brown, P. (2001). Subthalamic nucleus, sensorimotor cortex and muscle interrelationships in Parkinson's disease. *Brain, 124*(Pt 2), 378-388.

Martens, H. C., Toader, E., Decre, M. M., Anderson, D. J., Vetter, R., Kipke, D. R., . . . Vitek, J. L. (2011). Spatial steering of deep brain stimulation volumes using a

novel lead design. *Clinical neurophysiology : official journal of the International Federation of Clinical Neurophysiology, 122*(3), 558-566. doi:10.1016/j.clinph.2010.07.026; 10.1016/j.clinph.2010.07.026

McCarthy, M. M., Moore-Kochlacs, C., Gu, X., Boyden, E. S., Han, X., & Kopell, N. (2011). Striatal origin of the pathologic beta oscillations in Parkinson's disease. *Proc Natl Acad Sci U S A, 108*(28), 11620-11625. doi:10.1073/pnas.1107748108

McConnell, G. C., So, R. Q., Hilliard, J. D., Lopomo, P., & Grill, W. M. (2012). Effective deep brain stimulation suppresses low-frequency network oscillations in the basal ganglia by regularizing neural firing patterns. *The Journal of neuroscience : the official journal of the Society for Neuroscience, 32*(45), 15657-15668. doi:10.1523/JNEUROSCI.2824-12.2012; 10.1523/JNEUROSCI.2824-12.2012

McIntyre, C. C., & Foutz, T. J. (2013). Computational modeling of deep brain stimulation. *Handb Clin Neurol, 116*, 55-61. doi:10.1016/B978-0-444-53497-2.00005-X

McIntyre, C. C., Grill, W. M., Sherman, D. L., & Thakor, N. V. (2004). Cellular effects of deep brain stimulation: model-based analysis of activation and inhibition. *Journal of neurophysiology, 91*(4), 1457-1469. doi:10.1152/jn.00989.2003

McIntyre, C. C., Mori, S., Sherman, D. L., Thakor, N. V., & Vitek, J. L. (2004). Electric field and stimulating influence generated by deep brain stimulation of the subthalamic nucleus. *Clin Neurophysiol, 115*(3), 589-595. doi:10.1016/j.clinph.2003.10.033

McIntyre, C. C., Savasta, M., Kerkerian-Le Goff, L., & Vitek, J. L. (2004). Uncovering the mechanism(s) of action of deep brain stimulation: activation, inhibition, or both. *Clin Neurophysiol, 115*(6), 1239-1248. doi:10.1016/j.clinph.2003.12.024

McIntyre, C. C., Savasta, M., Walter, B. L., & Vitek, J. L. (2004). How does deep brain stimulation work? Present understanding and future questions. *J Clin Neurophysiol, 21*(1), 40-50.

Meissner, W., Leblois, A., Hansel, D., Bioulac, B., Gross, C. E., Benazzouz, A., & Boraud, T. (2005). Subthalamic high frequency stimulation resets subthalamic firing and reduces abnormal oscillations. *Brain : a journal of neurology, 128*(Pt 10), 2372-2382. doi:10.1093/brain/awh616

Mera, T., Vitek, J. L., Alberts, J. L., & Giuffrida, J. P. (2011). Kinematic optimization of deep brain stimulation across multiple motor symptoms in Parkinson's disease. *Journal of neuroscience methods, 198*(2), 280-286. doi:10.1016/j.jneumeth.2011.03.019; 10.1016/j.jneumeth.2011.03.019

Merrill, D. R., Bikson, M., & Jefferys, J. G. (2005). Electrical stimulation of excitable tissue: design of efficacious and safe protocols. *J Neurosci Methods, 141*(2), 171-198. doi:10.1016/j.jneumeth.2004.10.020

Milton, J. G., Gotman, J., Remillard, G. M., & Andermann, F. (1987). Timing of seizure recurrence in adult epileptic patients: a statistical analysis. *Epilepsia, 28*(5), 471-478.

Mina, F., Benquet, P., Pasnicu, A., Biraben, A., & Wendling, F. (2013). Modulation of epileptic activity by deep brain stimulation: a model-based study of frequency-dependent effects. *Front Comput Neurosci, 7*, 94. doi:10.3389/fncom.2013.00094

Mink, J. W. (2003). The Basal Ganglia and involuntary movements: impaired inhibition of competing motor patterns. *Arch Neurol, 60*(10), 1365-1368. doi:10.1001/archneur.60.10.1365

Miocinovic, S., Noecker, A. M., Maks, C. B., Butson, C. R., & McIntyre, C. C. (2007). Cicerone: stereotactic neurophysiological recording and deep brain stimulation electrode placement software system. *Acta Neurochir Suppl, 97*(Pt 2), 561-567.

Miranda-Dominguez, O., Gonia, J., & Netoff, T. I. (2010). Firing rate control of a neuron using a linear proportional-integral controller. *Journal of neural engineering, 7*(6), 066004. doi:10.1088/1741-2560/7/6/066004

Miranda-Domínguez, Ó., & Netoff, T. I. (2013). Parameterized phase response curves for characterizing neuronal behaviors under transient conditions. *J Neurophysiol, 109*(9), 2306-2316. doi:10.1152/jn.00942.2012

Mirollo, R. E., & Strogatz, S. H. (1990). Synchronization of pulse-coupled biological oscillators. *SIAM Journal of Applied Mathematics, 50*(6), 1645-1662.

Modolo, J., Edwards, R., Campagnaud, J., Bhattacharya, B., & Beuter, A. (2010). Past, Present and Future of Brain Stimulation. *Mathematical Modelling of Natural Phenomena, 5*(2), 185-207.

Modolo, J., Henry, J., & Beuter, A. (2008). Dynamics of the subthalamo-pallidal complex in Parkinson's disease during deep brain stimulation. *J Biol Phys, 34*(3-4), 251-266. doi:10.1007/s10867-008-9095-y

Moehlis, J., Nabi, A., & Danzl, P. (2010). Charge-balanced spike timing control for phase models of spiking neurons. *Discrete and Continuous Dynamical Systems, 28*(4), 1413 <last_page> 1435. doi:10.3934/dcds.2010.28.1413

Montgomery, E. B., & Baker, K. B. (2000). Mechanisms of deep brain stimulation and future technical developments. *Neurol Res, 22*(3), 259-266.

Moran, R. J., Mallet, N., Litvak, V., Dolan, R. J., Magill, P. J., Friston, K. J., & Brown, P. (2011). Alterations in brain connectivity underlying beta oscillations in

Parkinsonism. *PLoS Comput Biol, 7*(8), e1002124. doi:10.1371/journal.pcbi.1002124

Moro, E., Esselink, R. J., Xie, J., Hommel, M., Benabid, A. L., & Pollak, P. (2002). The impact on Parkinson's disease of electrical parameter settings in STN stimulation. *Neurology, 59*(5), 706-713.

Moroney, R., Heida, C., & Geelen, J. (2008). Increased bradykinesia in Parkinson's disease with increased movement complexity: elbow flexion-extension movements. *J Comput Neurosci, 25*(3), 501-519. doi:10.1007/s10827-008-0091-9

Nabi, A., Stigen, T., Moehlis, J., & Netoff, T. (2013). Minimum energy control for in vitro neurons. *J Neural Eng, 10*(3), 036005. doi:10.1088/1741-2560/10/3/036005

Nambu, A. (2008). Seven problems on the basal ganglia. *Curr Opin Neurobiol, 18*(6), 595-604. doi:10.1016/j.conb.2008.11.001

Nambu, A., Tokuno, H., Hamada, I., Kita, H., Imanishi, M., Akazawa, T., . . . Hasegawa, N. (2000). Excitatory cortical inputs to pallidal neurons via the subthalamic nucleus in the monkey. *Journal of neurophysiology, 84*(1), 289-300.

Nambu, A., Tokuno, H., & Takada, M. (2002). Functional significance of the cortico-subthalamo-pallidal 'hyperdirect' pathway. *Neurosci Res, 43*(2), 111-117.

Netoff, T. I., Banks, M. I., Dorval, A. D., Acker, C. D., Haas, J. S., Kopell, N., & White, J. A. (2005). Synchronization in hybrid neuronal networks of the hippocampal formation. *Journal of neurophysiology, 93*(3), 1197-1208. doi:10.1152/jn.00982.2004

Nevado-Holgado, A. J., Mallet, N., Magill, P. J., & Bogacz, R. (2014). Effective connectivity of the subthalamic nucleus-globus pallidus network during Parkinsonian oscillations. *J Physiol, 592*(Pt 7), 1429-1455. doi:10.1113/jphysiol.2013.259721

Nolden, L. F., Tartavoulle, T., & Porche, D. J. (2014). Parkinson's disease: assessment, diagnosis, and management. *The Journal for Nurse Practitioners, 10*(7), 500-506.

Nunez, P. L. (1974). The brain wave equation: a model for EEG. *Math Biosci., 21*, 279.

Obeso, J. A., Marin, C., Rodriguez-Oroz, C., Blesa, J., Benitez-Temiño, B., Mena-Segovia, J., . . . Olanow, C. W. (2008). The basal ganglia in Parkinson's disease: current concepts and unexplained observations. *Ann Neurol, 64 Suppl 2*, S30-46. doi:10.1002/ana.21481

Okun, M. S., & Vitek, J. L. (2004). Lesion therapy for Parkinson's disease and other movement disorders

Update and controversies, Movement Disorders Volume 19, Issue 4. *Movement Disorders, 19*(4), 375-389. Retrieved from http://onlinelibrary.wiley.com/doi/10.1002/mds.20037/abstract

Oppenheim, A. V., Willsky, A. S., & Nawab, S. H. (1996). *Signals & systems (2nd ed.)*: Prentice-Hall, Inc.

Ota, K., Omori, T., & Aonishi, T. (2009). MAP estimation algorithm for phase response curves based on analysis of the observation process. *J Comput Neurosci, 26*(2), 185-202. doi:10.1007/s10827-008-0104-8

Parent, A., & Hazrati, L. N. (1995). Functional anatomy of the basal ganglia. I. The cortico-basal ganglia-thalamo-cortical loop. *Brain Res Brain Res Rev, 20*(1), 91-127.

Parkinson, J. (2002). An essay on the shaking palsy. 1817. *J Neuropsychiatry Clin Neurosci, 14*(2), 223-236; discussion 222. doi:10.1176/jnp.14.2.223

Pasillas-Lépine, W. (2013). Delay-induced oscillations in Wilson and Cowan's model: an analysis of the subthalamo-pallidal feedback loop in healthy and parkinsonian subjects. *Biol Cybern, 107*(3), 289-308. doi:10.1007/s00422-013-0549-3

Pavlides, A., Hogan, S. J., & Bogacz, R. (2015). Computational models describing possible mechanisms for generation of excessive beta oscillations in Parkinson's disease. *PLOS Computational Biology*. doi:10.1371/journal.pcbi.1004609

Penney, J. B., & Young, A. B. (1983). Speculations on the functional anatomy of basal ganglia disorders. *Annu Rev Neurosci, 6*, 73-94. doi:10.1146/annurev.ne.06.030183.000445

Percheron, G. r., McKenzie, J. S., Férger, J., & International Basal Ganglia Society. Symposium. (1994). *The Basal ganglia IV : new ideas and data on structure and function*. New York: Plenum Press.

Pirini, M., Rocchi, L., Sensi, M., & Chiari, L. (2009). A computational modelling approach to investigate different targets in deep brain stimulation for Parkinson's disease. *J Comput Neurosci, 26*(1), 91-107. doi:10.1007/s10827-008-0100-z

Plenz, D., & Kital, S. T. (1999). A basal ganglia pacemaker formed by the subthalamic nucleus and external globus pallidus. *Nature, 400*(6745), 677-682. doi:10.1038/23281

Polymeropoulos, M. H., Lavedan, C., Leroy, E., Ide, S. E., Dehejia, A., Dutra, A., . . . Nussbaum, R. L. (1997). Mutation in the alpha-synuclein gene identified in families with Parkinson's disease. *Science, 276*(5321), 2045-2047.

Priori, A., Foffani, G., Pesenti, A., Bianchi, A., Chiesa, V., Baselli, G., . . . Scarlato, G. (2002). Movement-related modulation of neural activity in human basal ganglia

and its L-DOPA dependency: recordings from deep brain stimulation electrodes in patients with Parkinson's disease. *Neurol Sci, 23 Suppl 2*, S101-102. doi:10.1007/s100720200089

Priori, A., Foffani, G., Pesenti, A., Tamma, F., Bianchi, A. M., Pellegrini, M., . . . Villani, R. M. (2004). Rhythm-specific pharmacological modulation of subthalamic activity in Parkinson's disease. *Experimental neurology, 189*(2), 369-379. doi:10.1016/j.expneurol.2004.06.001

Rivlin-Etzion, M., Elias, S., Heimer, G., & Bergman, H. (2010). Computational physiology of the basal ganglia in Parkinson's disease. *Prog Brain Res, 183*, 259-273. doi:10.1016/S0079-6123(10)83013-4

Rizzone, M., Lanotte, M., Bergamasco, B., Tavella, A., Torre, E., Faccani, G., . . . Lopiano, L. (2001). Deep brain stimulation of the subthalamic nucleus in Parkinson's disease: effects of variation in stimulation parameters. *J Neurol Neurosurg Psychiatry, 71*(2), 215-219.

Rosenblum, M., & Pikovsky, A. (2004). Delayed feedback control of collective synchrony: an approach to suppression of pathological brain rhythms. *Phys Rev E Stat Nonlin Soft Matter Phys, 70*(4 Pt 1), 041904. doi:10.1103/PhysRevE.70.041904

Rosenblum, M. G., & Pikovsky, A. S. (2004). Controlling synchronization in an ensemble of globally coupled oscillators. *Phys Rev Lett, 92*(11), 114102. doi:10.1103/PhysRevLett.92.114102

Rosin, B., Slovik, M., Mitelman, R., Rivlin-Etzion, M., Haber, S. N., Israel, Z., . . . Bergman, H. (2011). Closed-loop deep brain stimulation is superior in ameliorating parkinsonism. *Neuron, 72*(2), 370-384. doi:10.1016/j.neuron.2011.08.023; 10.1016/j.neuron.2011.08.023

Roulston, M. S. (1999). Estimating the errors on measured entropy and mutual information. *Physica D: Nonlinear Phenomena, 125*(3-4), 285-294.

Rouse, A. G., Stanslaski, S. R., Cong, P., Jensen, R. M., Afshar, P., Ullestad, D., . . . Denison, T. J. (2011). A chronic generalized bi-directional brain-machine interface. *Journal of neural engineering, 8*(3), 036018-032560/036018/036013/036018. Epub 032011 May 036015. doi:10.1088/1741-2560/8/3/036018; 10.1088/1741-2560/8/3/036018

Rubin, J. E., & Terman, D. (2004). High frequency stimulation of the subthalamic nucleus eliminates pathological thalamic rhythmicity in a computational model. *Journal of computational neuroscience, 16*(3), 211-235. doi:10.1023/B:JCNS.0000025686.47117.67

Ryapolova-Webb, E., Afshar, P., Stanslaski, S., Denison, T., de Hemptinne, C., Bankiewicz, K., & Starr, P. A. (2014). Chronic cortical and electromyographic recordings from a fully implantable device: preclinical experience in a nonhuman primate. *J Neural Eng, 11*(1), 016009. doi:10.1088/1741-2560/11/1/016009

Sahin, M., & Tie, Y. (2007). Non-rectangular waveforms for neural stimulation with practical electrodes. *J Neural Eng, 4*(3), 227-233. doi:10.1088/1741-2560/4/3/008

Santaniello, S., Fiengo, G., Glielmo, L., & Grill, W. M. (2011). Closed-loop control of deep brain stimulation: a simulation study. *IEEE transactions on neural systems and rehabilitation engineering : a publication of the IEEE Engineering in Medicine and Biology Society, 19*(1), 15-24. doi:10.1109/TNSRE.2010.2081377; 10.1109/TNSRE.2010.2081377

Santaniello, S., McCarthy, M. M., Montgomery, E. B., Gale, J. T., Kopell, N., & Sarma, S. V. (2015). Therapeutic mechanisms of high-frequency stimulation in Parkinson's disease and neural restoration via loop-based reinforcement. *Proc Natl Acad Sci U S A, 112*(6), E586-595. doi:10.1073/pnas.1406549111

Schiff, S. J. (2010). Towards model-based control of Parkinson's disease. *Philos Trans A Math Phys Eng Sci, 368*(1918), 2269-2308. doi:10.1098/rsta.2010.0050

Schultheiss, N. W., Edgerton, J. R., & Jaeger, D. (2010). Phase response curve analysis of a full morphological globus pallidus neuron model reveals distinct perisomatic and dendritic modes of synaptic integration. *J Neurosci, 30*(7), 2767-2782. doi:10.1523/jneurosci.3959-09.2010

Schultheiss, N. W., Prinz, A. A., & Butera, R. J. (2012). *Phase response curves in neuroscience : theory, experiment, and analysis*. New York: Springer.

Sharott, A., Magill, P. J., Harnack, D., Kupsch, A., Meissner, W., & Brown, P. (2005). Dopamine depletion increases the power and coherence of beta-oscillations in the cerebral cortex and subthalamic nucleus of the awake rat. *Eur J Neurosci, 21*(5), 1413-1422. doi:10.1111/j.1460-9568.2005.03973.x

Shepherd, R. K., & McCreery, D. B. (2006). Basis of electrical stimulation of the cochlea and the cochlear nucleus. *Adv Otorhinolaryngol, 64*, 186-205. doi:10.1159/000094652

Smeal, R. M., Ermentrout, G. B., & White, J. A. (2010). Phase-response curves and synchronized neural networks. *Philos Trans R Soc Lond B Biol Sci, 365*(1551), 2407-2422. doi:10.1098/rstb.2009.0292

Smith, Y., Wichmann, T., Factor, S. A., & DeLong, M. R. (2012). Parkinson's disease therapeutics: new developments and challenges since the introduction of levodopa. *Neuropsychopharmacology, 37*(1), 213-246. doi:10.1038/npp.2011.212

So, R. Q., Kent, A. R., & Grill, W. M. (2012). Relative contributions of local cell and passing fiber activation and silencing to changes in thalamic fidelity during deep brain stimulation and lesioning: a computational modeling study. *J Comput Neurosci, 32*(3), 499-519. doi:10.1007/s10827-011-0366-4

Stiefel, K. M., Gutkin, B. S., & Sejnowski, T. J. (2008). Cholinergic neuromodulation changes phase response curve shape and type in cortical pyramidal neurons. *PLoS One, 3*(12), e3947. doi:10.1371/journal.pone.0003947

Stigen, T., Danzl, P., Moehlis, J., & Netoff, T. (2009). Linear control of neuronal spike timing using phase response curves. *Conference proceedings : ...Annual International Conference of the IEEE Engineering in Medicine and Biology Society.IEEE Engineering in Medicine and Biology Society.Conference, 2009*, 1541-1544. doi:10.1109/IEMBS.2009.5333079

Sun, F. T., & Morrell, M. J. (2014). Closed-loop neurostimulation: the clinical experience. *Neurotherapeutics, 11*(3), 553-563. doi:10.1007/s13311-014-0280-3

Suri, R. E., & Schultz, W. (1998). Learning of sequential movements by neural network model with dopamine-like reinforcement signal. *Exp Brain Res, 121*(3), 350-354.

Tachibana, Y., Iwamuro, H., Kita, H., Takada, M., & Nambu, A. (2011). Subthalamo-pallidal interactions underlying parkinsonian neuronal oscillations in the primate basal ganglia. *The European journal of neuroscience, 34*(9), 1470-1484. doi:10.1111/j.1460-9568.2011.07865.x; 10.1111/j.1460-9568.2011.07865.x

Tass, P. A. (2001). Desynchronizing double-pulse phase resetting and application to deep brain stimulation. *Biological cybernetics, 85*(5), 343-354.

Tass, P. A. (2002). Desynchronization of brain rhythms with soft phase-resetting techniques. *Biol Cybern, 87*(2), 102-115. doi:10.1007/s00422-002-0322-5

Tass, P. A. (2003). A model of desynchronizing deep brain stimulation with a demand-controlled coordinated reset of neural subpopulations. *Biol Cybern, 89*(2), 81-88. doi:10.1007/s00422-003-0425-7

Tass, P. A. (2007). *Phase resetting in medicine and biology : stochastic modelling and data analysis*. Berlin ; New York: Springer.

Tass, P. A., Qin, L., Hauptmann, C., Dovero, S., Bezard, E., Boraud, T., & Meissner, W. G. (2012). Coordinated reset has sustained aftereffects in Parkinsonian monkeys. *Ann Neurol, 72*(5), 816-820. doi:10.1002/ana.23663

Terman, D., Rubin, J. E., Yew, A. C., & Wilson, C. J. (2002). Activity patterns in a model for the subthalamopallidal network of the basal ganglia. *The Journal of neuroscience : the official journal of the Society for Neuroscience, 22*(7), 2963-2976. doi:20026266

Thibeault, C. M., & Srinivasa, N. (2013). Using a hybrid neuron in physiologically inspired models of the basal ganglia. *Front Comput Neurosci, 7*, 88. doi:10.3389/fncom.2013.00088

Thounaojam, U. S., Cui, J., Norman, S. E., Butera, R. J., & Canavier, C. C. (2014). Slow noise in the period of a biological oscillator underlies gradual trends and abrupt transitions in phasic relationships in hybrid neural networks. *PLoS Comput Biol, 10*(5), e1003622. doi:10.1371/journal.pcbi.1003622

Timmermann, L., Wojtecki, L., Gross, J., Lehrke, R., Voges, J., Maarouf, M., . . . Schnitzler, A. (2004). Ten-Hertz stimulation of subthalamic nucleus deteriorates motor symptoms in Parkinson's disease. *Mov Disord, 19*(11), 1328-1333. doi:10.1002/mds.20198

Titcombe, M. S., Glass, L., Guehl, D., & Beuter, A. (2001). Dynamics of Parkinsonian tremor during deep brain stimulation. *Chaos, 11*(4), 766-773. doi:10.1063/1.1408257

Torben-Nielsen, B., Uusisaari, M., & Stiefel, K. M. (2010). A comparison of methods to determine neuronal phase-response curves. *Front Neuroinform, 4*, 6. doi:10.3389/fninf.2010.00006

Tsang, E. W., Hamani, C., Moro, E., Mazzella, F., Saha, U., Lozano, A. M., . . . Chen, R. (2012). Subthalamic deep brain stimulation at individualized frequencies for Parkinson disease. *Neurology, 78*(24), 1930-1938. doi:10.1212/WNL.0b013e318259e183

Turner, J. A., Loeser, J. D., Deyo, R. A., & Sanders, S. B. (2004). Spinal cord stimulation for patients with failed back surgery syndrome or complex regional pain syndrome: a systematic review of effectiveness and complications. *Pain, 108*(1-2), 137-147. doi:10.1016/j.pain.2003.12.016

Uhlhaas, P. J., & Singer, W. (2006). Neural synchrony in brain disorders: relevance for cognitive dysfunctions and pathophysiology. *Neuron, 52*(1), 155-168. doi:10.1016/j.neuron.2006.09.020

Uhlhaas, P. J., & Singer, W. (2013). High-frequency oscillations and the neurobiology of schizophrenia. *Dialogues Clin Neurosci, 15*(3), 301-313.

Urbano, F., Leznik, E., & Llinas, R. (2002). Cortical activation patterns evoked by afferent axons stimuli at different frequencies: an in vitro voltage-sensitive dye imaging study. *Thalamus & Related Systems, 1*, 371-378.

van Albada, S. J., Gray, R. T., Drysdale, P. M., & Robinson, P. A. (2009). Mean-field modeling of the basal ganglia-thalamocortical system. II Dynamics of parkinsonian oscillations. *Journal of theoretical biology, 257*(4), 664-688. doi:10.1016/j.jtbi.2008.12.013

van Albada, S. J., & Robinson, P. A. (2009). Mean-field modeling of the basal ganglia-thalamocortical system. I Firing rates in healthy and parkinsonian states. *Journal of theoretical biology, 257*(4), 642-663. doi:10.1016/j.jtbi.2008.12.018

Vitek, J. L. (2002). Mechanisms of deep brain stimulation: excitation or inhibition. *Mov Disord, 17 Suppl 3*, S69-72.

Vitek, J. L., Hashimoto, T., Peoples, J., DeLong, M. R., & Bakay, R. A. (2004). Acute stimulation in the external segment of the globus pallidus improves parkinsonian motor signs. *Movement disorders : official journal of the Movement Disorder Society, 19*(8), 907-915. doi:10.1002/mds.20137

Volkmann, J., Herzog, J., Kopper, F., & Deuschl, G. (2002). Introduction to the programming of deep brain stimulators. *Movement disorders : official journal of the Movement Disorder Society, 17 Suppl 3*, S181-187.

Volkmann, J., Moro, E., & Pahwa, R. (2006). Basic algorithms for the programming of deep brain stimulation in Parkinson's disease. *Mov Disord, 21 Suppl 14*, S284-289. doi:10.1002/mds.20961

Wang, Y., & Manis, P. B. (2006). Temporal coding by cochlear nucleus bushy cells in DBA/2J mice with early onset hearing loss. *J Assoc Res Otolaryngol, 7*(4), 412-424. doi:10.1007/s10162-006-0052-9

Westman, R. S. (1975). *The Copernican achievement* (Vol. 7). Berkeley: University of California Press.

Wichmann, T., & Soares, J. (2006). Neuronal firing before and after burst discharges in the monkey basal ganglia is predictably patterned in the normal state and altered in parkinsonism. *J Neurophysiol, 95*(4), 2120-2133. doi:10.1152/jn.01013.2005

Williams, D., Tijssen, M., Van Bruggen, G., Bosch, A., Insola, A., Di Lazzaro, V., . . . Brown, P. (2002). Dopamine-dependent changes in the functional connectivity between basal ganglia and cerebral cortex in humans. *Brain, 125*(Pt 7), 1558-1569.

Willsie, A. C., & Dorval, A. D. (2015). Computational Field Shaping for Deep Brain Stimulation With Thousands of Contacts in a Novel Electrode Geometry. *Neuromodulation, 18*(7), 542-550; discussion 550-541. doi:10.1111/ner.12330

Wilson, C. J. (2014). Oscillators and Oscillations in the Basal Ganglia. *Neuroscientist*. doi:10.1177/1073858414560826

Wilson, C. J., Beverlin, B., 2nd, & Netoff, T. (2011). Chaotic desynchronization as the therapeutic mechanism of deep brain stimulation. *Frontiers in systems neuroscience, 5*, 50. doi:10.3389/fnsys.2011.00050

Wilson, D., Holt, A. B., Netoff, T. I., & Moehlis, J. (2015). Optimal entrainment of heterogeneous noisy neurons. *Front Neurosci, 9*, 192. doi:10.3389/fnins.2015.00192

Wilson, D., & Moehlis, J. (2014a). An energy-optimal approach for entrainment of uncertain circadian oscillators. *Biophys J, 107*(7), 1744-1755. doi:10.1016/j.bpj.2014.08.013

Wilson, D., & Moehlis, J. (2014b). Locally optimal extracellular stimulation for chaotic desynchronization of neural populations. *J Comput Neurosci, 37*(2), 243-257. doi:10.1007/s10827-014-0499-3

Wilson, H. R., & Cowan, J. D. (1972). Excitatory and inhibitory interactions in localized populations of model neurons. *Biophysical journal, 12*(1), 1-24. doi:10.1016/S0006-3495(72)86068-5

Winfree, A. T. (2001). *The Geometry of Biological Time* (W. S. Marsden JE, Sirovich L Ed. 2nd ed. Vol. 12). New York: Springer.

Wongsarnpigoon, A., & Grill, W. M. (2010). Energy-efficient waveform shapes for neural stimulation revealed with a genetic algorithm. *J Neural Eng, 7*(4), 046009. doi:10.1088/1741-2560/7/4/046009

Wu, W., Liu, B., & Chen, T. (2010). Analysis of firing behaviors in networks of pulse-coupled oscillators with delayed excitatory coupling. *Neural Netw, 23*(7), 783-788. doi:10.1016/j.neunet.2010.02.005

Xiao, Y., Pena, E., & Johnson, M. D. (2016). Theoretical Optimization of Stimulation Strategies for a Directionally Segmented Deep Brain Stimulation Electrode Array. *IEEE Trans Biomed Eng, 63*(2), 359-371. doi:10.1109/TBME.2015.2457873

Zijlmans, M., Jiruska, P., Zelmann, R., Leijten, F. S., Jefferys, J. G., & Gotman, J. (2012). High-frequency oscillations as a new biomarker in epilepsy. *Ann Neurol, 71*(2), 169-178. doi:10.1002/ana.22548

Zitella, L. M., Teplitzky, B. A., Yager, P., Hudson, H. M., Brintz, K., Duchin, Y., . . . Johnson, M. D. (2015). Subject-specific computational modeling of DBS in the PPTg area. *Front Comput Neurosci, 9*, 93. doi:10.3389/fncom.2015.00093